Studies in Mycology 106: 41–94 (2023).

Diversity of colacosome-interacting mycoparasites expands the understanding of the evolution and ecology of *Microbotryomycetes*

N. Schoutteten[1*], A. Yurkov[2], O. Leroux[3], D. Haelewaters[1,4,5], D. Van Der Straeten[3], O. Miettinen[6], T. Boekhout[7], D. Begerow[8], A. Verbeken[1]

[1]*Research Group Mycology, Department of Biology, Ghent University, K.L. Ledeganckstraat 35, 9000 Gent, Belgium;* [2]*Leibniz Institute DSMZ - German Collection of Microorganisms and Cell Cultures GmbH, Inhoffenstraße 7B, 38124 Braunschweig, Germany;* [3]*Laboratory of Functional Plant Biology, Ghent University, K.L. Ledeganckstraat 35, 9000 Gent, Belgium;* [4]*Faculty of Science, University of South Bohemia, Branišovská 31, 370 05 České Budějovice, Czech Republic;* [5]*Department of Ecology and Evolutionary Biology, University of Colorado Boulder, 1900 Pleasant Street, 334 UCB, Boulder, Colorado 80309, USA;* [6]*Botanical Museum, Finnish Museum of Natural History, University of Helsinki, P.O. Box 7, Helsinki, FI-00014, Finland;* [7]*College of Science, King Saud university, Riyadh, Saudi Arabia;* [8]*Organismic Botany and Mycology, Institute of Plant Science and Microbiology, Ohnhorststraße 18, 22609 Hamburg, Germany*

**Corresponding author*: N. Schoutteten, Nathan.schoutteten@ugent.be | nathan.schoutteten@gmail.com

Abstract: Mycoparasites in *Basidiomycota* comprise a diverse group of fungi, both morphologically and phylogenetically. They interact with their hosts through either fusion-interaction or colacosome-interaction. Colacosomes are subcellular structures formed by the mycoparasite at the host–parasite interface, which penetrate the parasite and host cell walls. Previously, these structures were detected in 19 fungal species, usually by means of transmission electron microscopy. Most colacosome-forming species have been assigned to *Microbotryomycetes* (*Pucciniomycotina*, *Basidiomycota*), a highly diverse class, comprising saprobic yeasts, mycoparasites, and phytoparasites. In general, these myco- and phytoparasites are dimorphic organisms, with a parasitic filamentous morph and saprobic yeast morph. We investigated colacosome-forming mycoparasites based on fungarium material, freshly collected specimens, and cultures of yeast morphs. We characterised the micromorphology of filamentous morphs, the physiological characteristics of yeast morphs, and inferred phylogenetic relationships based on DNA sequence data from seven loci. We outline and employ an epifluorescence-based microscopic method to assess the presence and organisation of colacosomes. We describe five new species in the genus *Colacogloea*, the novel dimorphic mycoparasite *Mycogloiocolax gerardii*, and provide the first report of a sexual, mycoparasitic morph in *Colacogloea philyla* and in the genus *Slooffia*. We detected colacosomes in eight fungal species, which brings the total number of known colacosome-forming fungi to 27. Finally, we revealed three distinct types of colacosome organisation in *Microbotryomycetes*.

Key words: *Basidiomycota*, epifluorescence microscopy, molecular phylogeny, new taxa, Transmission Electron Microscopy, *Pucciniomycotina*, systematics, yeasts.

Taxonomic novelties and typifications: New family: *Mycogloiocolacaeae* Schoutteten & Yurkov; **New genus:** *Mycogloiocolax* Schoutteten & Rödel; **New species:** *Colacogloea bettinae* Schoutteten & Begerow, *C. biconidiata* Schoutteten, *C. fennica* Schoutteten & Miettinen, *C. microspora* Schoutteten, *C. universitatis-gandavensis* Schoutteten & Verbeken, *Mycogloiocolax gerardii* Schoutteten & Rödel; **New combinations:** *Slooffia micra* (Bourdot & Galzin) Schoutteten, *Fellozyma cerberi* (A.M. Yurkov *et al.*) Schoutteten & Yurkov, *Fellozyma telluris* (A.M. Yurkov *et al.*) Schoutteten & Yurkov; **Epitypifications (basionyms):** *Achroomyces insignis* Hauerslev, *Platygloea micra* Bourdot & Galzin, *Platygloea peniophorae* Bourdot & Galzin; **Lectotypification (basionym):** *Platygloea peniophorae* Bourdot & Galzin

Citation: Schoutteten N, Yurkov A, Leroux O, Haelewaters D, Van Der Straeten D, Miettinen O, Boekhout T, Begerow D, Verbeken A (2023). Diversity of colacosome-interacting mycoparasites expands the understanding of the evolution and ecology of *Microbotryomycetes*. *Studies in Mycology* **106**: 41–94. doi: 10.3114/sim.2022.106.02

Received: 31 December 2022; **Accepted:** 12 June 2023; **Effectively published online:** 19 July 2023

Corresponding editor: Robert A. Samson

INTRODUCTION

Fungi are heterotrophic eukaryotes, relying on other living organisms or organic substrates to meet their nutritional needs (Willis 2018). Based on the specific nutrient substrate and type of interaction they engage in, fungi are generally assigned to the following ecological guilds: (i) saprotrophs decomposing dead organic material; (ii) mutualistic symbionts engaging in trophic interactions that are beneficial for both partners and (iii) parasites deriving nutrients from other living organisms. Recently, the scientific community started considering fungal ecological strategies rather as a continuum, in which fungal species have mixtures of ecological capabilities ranging from saprotrophic to symbiotic to parasitic (*e.g.*, Selosse *et al.* 2018). Moreover, fungi with complex lifecycles may have changing ecological strategies when alternating the different stages of their life histories (Bandoni 1995, Boekhout *et al.* 2011, Begerow *et al.* 2017). Parasitic stages of fungi interact with a huge diversity of host organisms, comprising both prokaryotes as well as organisms in all major groups of eukaryotes: *e.g.*, *Amoebozoa*, *Alveolates*, *Heterokontae*, *Metazoa*, *Viridiplantae* and *Fungi* (Begerow *et al.* 2017, 2018, Naranjo-Ortiz & Gabaldón 2019). Fungal species that engage in parasitic interactions with other fungi as host are denoted as mycoparasites (Kirk *et al.* 2008).

Mycoparasitism is phylogenetically widespread within the kingdom *Fungi*, and has been reported in eight phyla thus far. These are *Rozellomycota*, *Blastocladiomycota*, *Zoopagomycota*, *Mortierellomycota*, *Kickxellomycota*, *Mucoromycota*, *Ascomycota*, and *Basidiomycota* (Begerow *et al.* 2017, 2018, Naranjo-Ortiz &

Studies in Mycology

Gabaldón 2019). The prevalence of mycoparasitism in multiple early-diverging lineages has led to the hypothesis that this strategy arose early in fungal evolution, which is supported by 400 million-year-old year Devonian fossil data (Hass *et al.* 1994). Among *Basidiomycota*, roughly 200 species of mycoparasites are currently known, making up less than 0.5 % of the currently described species diversity (according to He *et al.* 2019). Although this number seems to be rather modest based on current knowledge, basidiomycetous mycoparasitic fungi exhibit a high level of phylogenetic, macro- and micromorphological, and ecological diversity.

Molecular phylogenies have revealed that mycoparasitism mainly occurs in two subphyla of *Basidiomycota*: *Agaricomycotina* and *Pucciniomycotina* (Fig. 1) (Weiß *et al.* 2004, Bauer *et al.* 2006, Begerow *et al.* 2017). In *Agaricomycotina*, the majority of mycoparasites are members of *Tremellomycetes*, whereas only few belong to *Agaricomycetes*, *e.g.*, species of *Asterophora*, *Pseudoboletus*, and *Squamanita* (Redhead *et al.* 1994, Oberwinkler 2012, Weiß *et al.* 2014, Koch & Herr 2021, Caiafa & Smith 2022). In *Pucciniomycotina*, mycoparasitism is phylogenetically widespread, occurring in at least six out of ten currently recognised classes: *Agaricostilbomycetes*, *Classiculomycetes*, *Cryptomycocolacomycetes*, *Cystobasidiomycetes*, *Microbotryomycetes*, and *Spiculogloeomycetes* (Bauer *et al.* 2006, Aime *et al.* 2006, 2014, Oberwinkler 2017, Begerow *et al.* 2017, 2018). The occurrence of mycoparasitism in *Tritirachiomycetes* (*Pucciniomycotina*) was suggested by Aime *et al.* (2014), although no cellular interaction structures or specific mechanisms for nutrient transfer were reported (Beguin 2010).

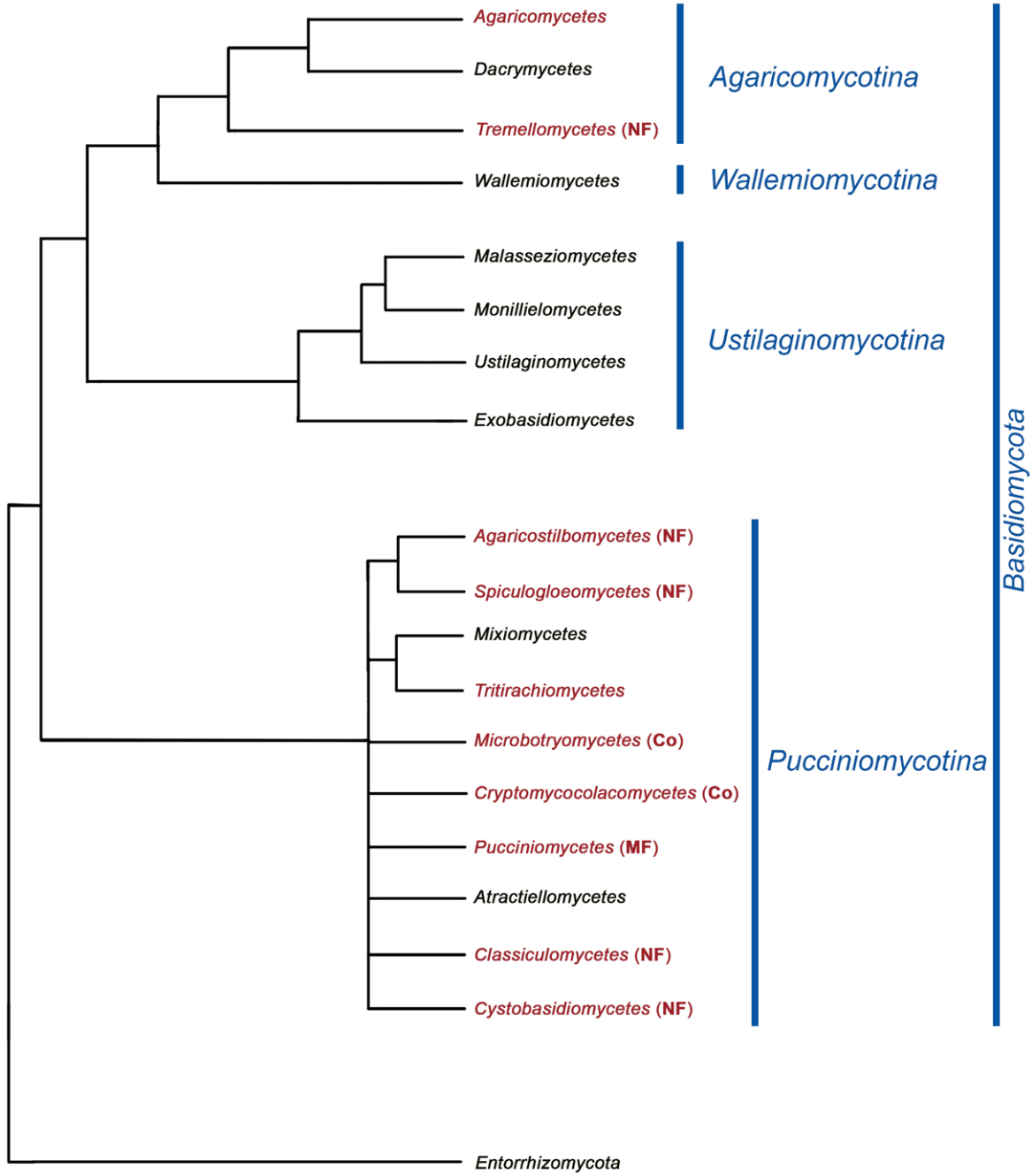

Fig. 1. Phylogram of *Basidiomycota*, interpretation based on of different previously published phylogenetic reconstructions of this phylum (Aime *et al.* 2006, Bauer *et al.* 2006, Schell *et al.* 2011, Wang *et al.* 2015a, Zhao *et al.* 2017, He *et al.* 2019). Names of classes indicated in red represent those comprising mycoparasitic species. Colacosome-interacting (Co) mycoparasites belong to *Cryptomycocolacomycetes* and *Microbotryomycetes*. Nanopore fusion-interacting (NF) mycoparasites belong to *Agaricostilbomycetes*, *Classiculomycetes*, *Cystobasidiomycetes*, *Spiculogloeomycetes* and *Tremellomycetes*. Micropore fusion-interacting (MF) mycoparasites belong to *Pucciniomycetes*.

Basidiomycetous mycoparasites show remarkable variation in the production of basidiomata. Within *Agaricomycetes*, they typically produce mushroom-like basidiomata, whereas various *Tremellomycetes* normally produce gelatinous basidiomata. Moreover, many mycoparasites do not produce basidiomata, but grow in or between the tissues of their host. This characteristic growth type was referred to as *intrahymenial growth* by Oberwinkler (1964) and occurs in multiple genera of *Tremellomycetes* (*e.g.*, *Phragmoxenidium*, *Syzygospora,* and *Tremella*) and *Pucciniomycotina* (*Achroomyces*, *Colacogloea*, *Kryptastrina*, *Naohidea*, *Occultifur*, *Spiculogloea*, and *Zygogloea*). However, not all intrahymenial species are mycoparasites, *e.g.*, species in *Tulasnella* and *Serendipita* are regarded as species with saprobic and symbiotic capabilities (Weiß *et al.* 2016, Oberwinkler *et al.* 2017). Host species of basidiomycetous mycoparasites generally belong to *Agaricomycetes*, primarily corticioid fungi and jelly fungi, although some ascomycetous hosts are also known. Despite the hosts usually being widespread in nature, these mycoparasites are rarely reported. Due to their inconspicuousness, they are frequently overlooked and difficult to discern. Observations often happen accidentally, *e.g.*, during microscopic investigation of the host fungus. This results in a limited availability of cultures and DNA sequence data for these mycoparasites, impeding their phylogenetic placement as well as their species delimitation (Kachalkin *et al.* 2019).

The majority of basidiomycetous mycoparasites in *Pucciniomycotina* and *Tremellomycetes* are characterised by dimorphic lifecycles. Generally, dimorphic fungi alternate between an ontogenetic haploid yeast stage, and an infectious dikaryotic hyphal stage (Brefeld 1888, Bandoni 1995, Boekhout et al. 2011, Begerow *et al.* 2017). These different stages of the lifecycle coincide with distinct types of growth, reproduction, karyological situation, and ecological strategies for nutrient acquisition (Begerow *et al.* 2017). Due to a certain degree of variation in these life histories, it is difficult to establish a uniform terminology that applies for all species. In literature considering dimorphic basidiomycetes, the two different stages are generally referred to as 'yeast stage' and 'filamentous stage'. In this manuscript, we apply the terms 'yeast morph' and 'filamentous morph' to describe the different stages of the life cycle, based on how these stages can be observed and recognised. The yeast morph is a unicellular stage, characterised by budding of basidiospores. It is considered to be saprobic, and in most cases to represent the haploid stage. Following conjugation (mating) of compatible yeast cells, a dikaryotic hyphal stage is initiated, which generally leads to sexual reproduction. In the case of dimorphic mycoparasites, this stage has adaptations for host–parasite interaction and is here referred to as the filamentous morph. To complete the lifecycle, basidia develop from dikaryotic hyphae, in which meiosis takes place and eventually basidiospores are formed. In some species, mono- or dikaryotic conidia may be formed along with sexual structures. It is important to mention that not for all dimorphic species in *Basidiomycota* the entire lifecycle has been observed in natural or laboratory conditions. For example, many mycoparasites are only known from their filamentous morph. It is assumed that a yeast morph exists for these species, although it was never isolated in culture.

The functional interaction between a mycoparasite and its host fungus differs among various lineages of *Basidiomycota*. Two major interaction mechanisms have been described: (i) *fusion-interaction* and (ii) *colacosome-interaction* (Oberwinkler & Bauer 2018). A large variation at the ultrastructural level exists within each of these interaction types (Bauer 2004, Bauer *et al.* 2006, Oberwinkler & Bauer 2018).

The first interaction mechanism is the fusion-interaction. Most basidiomycetous mycoparasites interact with their host by means of haustoria, which are often referred to as 'tremelloid haustoria' or 'nanopore fusion haustoria' (Bauer 2004). Haustoria are produced by the parasite and can be recognised by light microscopy as structures with often three discernible regions: a swollen base, a tapered middle region and an apex. Haustoria either attach to host hyphae or invaginate host cells. Depending on the species, one or more nanopore channels, with a diameter of 14–19 nm, are formed at the contact interface of the haustorium apex and host hypha (Bauer 2004). These channels are formed by fusion of the host and parasite's plasma membranes and establish cytoplasmic connection between host and parasite. This is in sharp contrast to basidiomycetous haustorial phytoparasites where no membrane fusion occurs and the cytoplasm of both interaction partners remains separated. As such, this phenomenon of cytoplasmic continuity between host and parasite is unique among fungal mycoparasites. Bauer (2004) hypothesised that cytoplasmic continuity facilitates nutrient transfer, but this remains to be investigated. The fusion-interaction is phylogenetically widespread in *Tremellomycetes* and *Pucciniomycotina*. Nevertheless, there is a large degree of difference in ultrastructure of these nanopore fusion haustoria among different lineages (Bauer 2004). The micropore fusion-interaction, in which fusion channels have a diameter of 1–2 µm, was so far only reported in *Tuberculina* species (*Helicobasidiales*) (Bauer *et al.* 2004, Lutz *et al.* 2004).

The second host–parasite interaction mechanism is the colacosome-interaction. Colacosomes are subcellular structures of 0.5–1 µm in diameter and are comprised of an electron-dense core surrounded by a membrane and an electron-transparent sheath (Kreger-van Rij & Veenhuis 1971b, Bauer & Oberwinkler 1991). They are formed in hyphae of the mycoparasite along the host–parasite interface (Fig. 2). Colacosomes, initially named lenticular bodies, were first reported from axenic cultures of *Rhodosporidiobolus ruineniae, Rhodotorula toruloides*, *R. sphaerocarpa*, and *Sporobolomyces johnsonii* (Kreger-van Rij & Veenhuis 1971b). These species, traditionally referred to as 'red yeast', are dimorphic fungi completing their lifecycle in culture, and colacosomes are formed along the contact surface of touching hyphae of the same species. Later, colacosomes were reported in hyphae of seven more dimorphic *Microbotryomycetes* growing in axenic culture (Table 1) (Kreger-van Rij & Veenhuis 1971a, De Hoog & Boekhout 1982, Boekhout *et al.* 1992, Sampaio *et al.* 2003). Bauer & Oberwinkler (1991) introduced the term 'colacosomes' when they discovered these structures for the first time along the host–parasite interface of the basidiomycetous mycoparasite *Colacogloea effusa* [as *Platygloea peniophorae*] and its host *Peniophorella praetermissa*. Since the term colacosomes has been in wider use than lenticular bodies, and several taxon names have their etymology based on this term, we prefer to adopt this term throughout the manuscript.

Bauer & Oberwinkler (1991) studied the ultrastructure of colacosomes and provided a schematic hypothesis of their development, which remains largely hypothetical [figs 8–13 in Bauer & Oberwinkler (1991)]. During colacosome development, the plasmalemma of the mycoparasite invaginates internally, creating an entirely membrane-enclosed globular space. This enclosed compartment becomes filled with electron-dense components, and a secondary cell wall around the invagination is produced by the mycoparasite, visible as an electron-transparent sheath. Next, the electron-dense components extrude through a tubular projection,

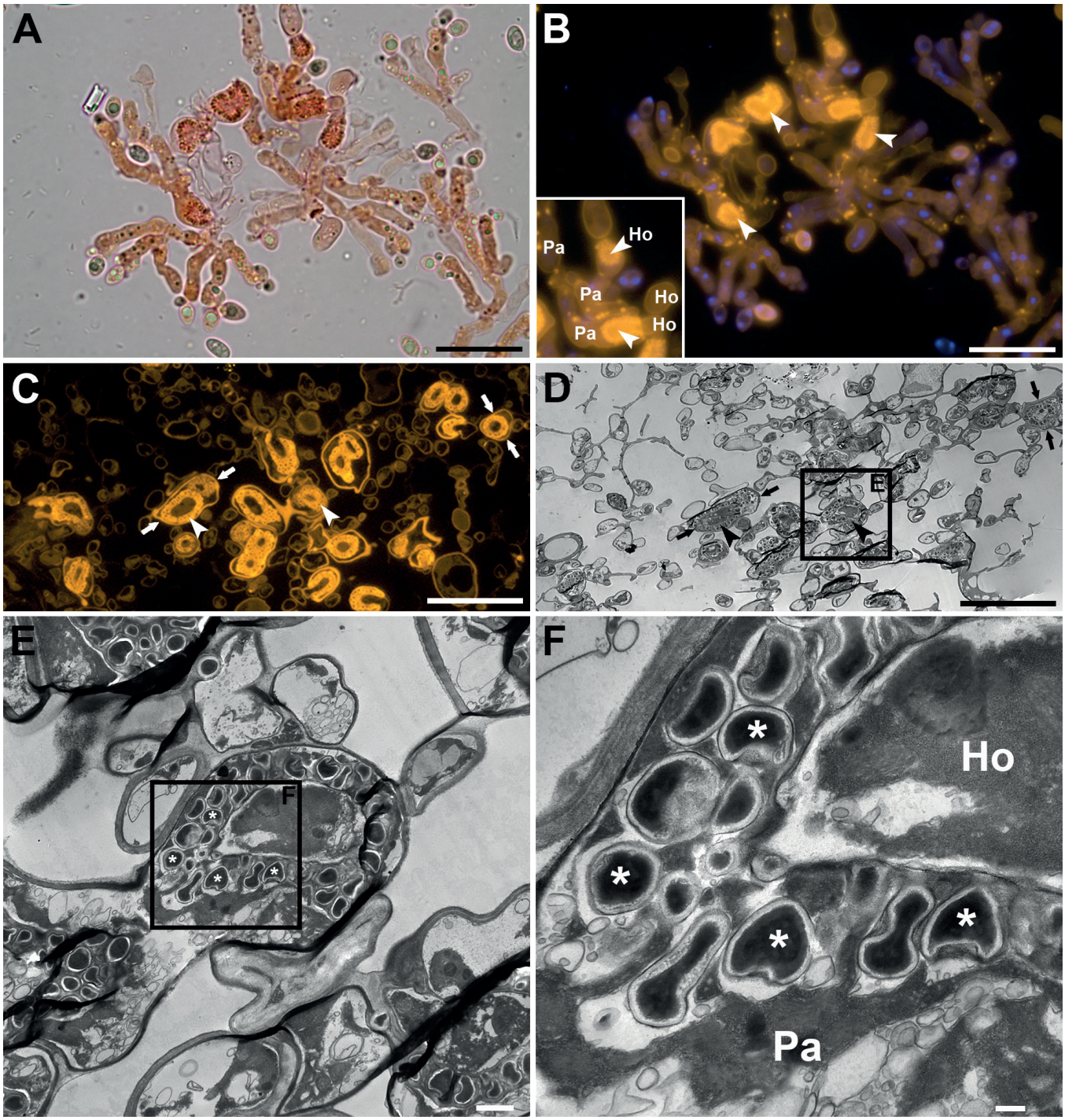

Fig. 2. Brightfield, epifluorescence and transmission electron microscopy (TEM) of *Colacogloea universitatis-gandavensis sp. nov*. **A, B.** Whole-mount preparation, stained with Congo red and DAPI, visualised using brightfield (A) and epifluorescence (B) microscopy. Epifluorescence microscopy facilitates fast detection of colacosomes as they exhibit bright fluorescence signals. Inset shows the intricate host–parasite (Ho-Pa) interface. Arrowheads indicate regions of colacosome clustering. Note the occurrence of individual colacosomes in parasite tissue (bright spots). **C, D.** Serial sections of a Spurr-embedded sample, showing the same region. Corresponding structures are indicated with arrows. (C) Section stained with Congo red and visualised using epifluorescence microscopy. (D) Equivalent serial section of the same region as in (C), visualised using TEM. **E, F.** High-magnification details of colacosome clusters (arrowheads), composed of many individual colacosomes (asterisks), arranged in parasitic hyphae (Pa) along the host–parasite interface (Ho-Pa), showing their typical electron dense cores. Scale bars: A–D = 20 µm, E = 10 µm, F = 200 nm.

penetrating the outer cell wall of the parasite and eventually the cell wall of the host fungus.

To date, the function of colacosomes remains unclear. Bauer & Oberwinkler (1991) provided the first hypothesis on the function of colacosomes, suggesting they are involved in the mycoparasitic interaction, possibly facilitating transfer of nutrients from host to parasite. Also a structural role was proposed, in which colacosomes can anchor parasite hyphae to host cells (Bauer & Oberwinkler 1991, Bauer 2004, Bauer *et al.* 2006, Begerow *et al.* 2017, Oberwinkler & Bauer 2018). Using X-ray diffraction, Kreger-van Rij & Veenhuis (1971b) determined that the electron-transparent sheath envelopping the colacosome is a chitin-rich structure. However, the biochemical composition of the electron-dense part of the colacosomes remains unknown.

Colacosomes have currently been reported from 19 fungal species, distributed over 11 genera in two classes

Table 1. Summary of species in which colacosomes have been detected, including data on the applied methodology for colacosome detection, organisation type of colacosomes, life cycle, host species, availability of cultures, and references.

Species	Method colacosome detection	Colacosome organisation	Observed morphs	Sexual stage observed	Source of colacosome detection	Host species	Culture available	Selected references
Microbotryomycetes								
Atractocolax pulvinatus R. Kirschner, R. Bauer & Oberw.	TEM	Scattered in mycoparasite hyphae	Dimorphic	Yes	Axenic culture	Unknown, possibly member of *Ascomycota*	Yes	Kirschner *et al.* (1999)
Bannozyma yamatoana (Nakase, M. Suzuki & Itoh) Q.M. Wang, F.Y. Bai, M. Groenew. & Boekhout	TEM	n/d	Dimorphic	No	Axenic culture	Unknown - colacosomes formed in own mycelium	Yes	Boekhout *et al.* (1992)
Colacogloea bettinae Schoutteten & Begerow *sp. nov.*	Fluorescence microscopy	Vesicular gall-like cells	Dimorphic	Yes	Host basidiome	*Peniophorella pubera* (Fr.) P. Karst.	Yes	This publication
Colacogloea biconidiata Schoutteten *sp. nov.*	Fluorescence microscopy	Scattered in mycoparasite hyphae	Dimorphic	Yes	Host basidiome	*Peniophorella praetermissa* (P. Karst.) K.H. Larss. *s.l.*	Yes	This publication
Colacogloea effusa (J. Schröt.) V. Malysheva, Schoutteten & Spirin	TEM	Scattered in mycoparasite hyphae	Dimorphic	Yes	Host basidiome	*Peniophorella praetermissa* (P. Karst.) K.H. Larss. *s.l.*	Yes	Bauer & Oberwinkler (1991); This publication
Colacogloea fennica Schoutteten & Miettinen *sp. nov.*	Fluorescence microscopy	Scattered in mycoparasite hyphae	Dimorphic	Yes	Host basidiome	*Peniophorella praetermissa* (P. Karst.) K.H. Larss. *s.l.*	Yes	This publication
Colacogloea microspora Schoutteten *sp. nov.*	Fluorescence microscopy	Scattered in mycoparasite hyphae	Dimorphic	Yes	Host basidiome	*Peniophorella praetermissa* (P. Karst.) K.H. Larss. *s.l.*	Yes	This publication
Colacogloea papilionacea R. Kirschner & Oberw.	TEM	Coiling of mycoparasite hyphae	Dimorphic	Yes	Co-culture with host	Unknown, possibly member of *Ascomycota*	Yes	Kirschner & Oberwinkler (2000)
Colacogloea philyla (Van der Walt, Klift & D.B. Scott) Q.M. Wang, F.Y. Bai, M. Groenew. & Boekhout	Fluorescence microscopy	Scattered in mycoparasite hyphae	Dimorphic	Yes	Host basidiome	*Peniophorella pubera* (Fr.) P. Karst.	no	This publication
Colacogloea universitatis-gandavensis Schoutteten & Verbeken *sp. nov.*	Fluorescence microscopy	Vesicular gall-like cells	Only filamentous morph known	Yes	Host basidiome	*Peniophorella praetermissa* (P. Karst.) K.H. Larss. *s.l.*	no	This publication
Hyalopycnis hyalina Höhn. (syn. *Heterogastridium pycnidioideum* Oberw. & R. Bauer)	TEM	Vesicular gall-like cells	Only filamentous morph known	Yes	Axenic culture and host basidiome	Unknown, possibly member of *Ascomycota*	Yes	Bauer 2004
Leucosporidium fellii Gim.-Jurado & Uden	TEM	n/d	Dimorphic	Yes	Axenic culture	Unknown - colacosomes formed in own mycelium	Yes	Sampaio *et al.* (2003)

Table 1. (Continued).

Species	Method colacosome detection	Colacosome organisation	Observed morphs	Sexual stage observed	Source of colacosome detection	Host species	Culture available	Selected references
Leucosporidium golubevii Gadanho, J.P. Samp. & R. Bauer	TEM	n/d	Dimorphic	Yes	Axenic culture	Unknown - colacosomes formed in own mycelium	Yes	Sampaio *et al.* (2003)
Leucosporidium intermedium (Nakase & M. Suzuki) M. Groenew. & Q.M. Wang	TEM	n/d	Dimorphic	Yes	Axenic culture	Unknown - colacosomes formed in own mycelium	Yes	Sampaio *et al.* (2003)
Leucosporidium scottii Fell, Statzell, I.L. Hunter & Phaff	TEM	n/d	Dimorphic	Yes	Axenic culture	Unknown - colacosomes formed in own mycelium	Yes	Kreger-van Rij & Veenhuis (1971a); Moore (1972)
Mycogloiocolax gerardii Schoutteten & Rödel *sp. nov.*	Fluorescence microscopy	Scattered in mycoparasite hyphae	Dimorphic	Yes	Host basidiome	*Xenasmatella tulasnelloidea* (Höhn. & Litsch.) Oberw.	Yes	This publication
Rhodosporidiobolus ruineniae (Holzschu, Tredick & Phaff) Q.M. Wang, F.Y. Bai, M. Groenew. & Boekhout	TEM	n/d	Dimorphic	Yes	Axenic culture	Unknown - colacosomes formed in own mycelium	Yes	Kreger-van Rij & Veenhuis (1971b); Moore (1972)
Rhodotorula sphaerocarpa (S.Y. Newell & Fell) Q.M. Wang, F.Y. Bai, M. Groenew. & Boekhout	TEM	n/d	Dimorphic	Yes	Axenic culture	Unknown - colacosomes formed in own mycelium	Yes	Kreger-van Rij & Veenhuis (1971b); Moore (1972)
Rhodotorula toruloides (Banno) Q.M. Wang, F.Y. Bai, M. Groenew. & Boekhout	TEM	n/d	Dimorphic	Yes	Axenic culture	Unknown - colacosomes formed in own mycelium	Yes	Kreger-van Rij & Veenhuis (1971b); De Hoog & Boekhout (1982)
Slooffia micra (Bourdot & Galzin) Schoutteten *comb. nov.*	Fluorescence microscopy	Coiling of mycoparasite hyphae	Dimorphic	Yes	Host basidiome	*Myxarium podlachicum* (Bres.) Raitv.	Yes	This publication
Sporobolomyces johnsonii (Nyland) Q.M. Wang, F.Y. Bai, M. Groenew. & Boekhout	TEM	n/d	Dimorphic	Yes	Axenic culture	Unknown - colacosomes formed in own mycelium	Yes	Kreger-van Rij & Veenhuis (1971a); Moore (1972)
Sporobolomyces salmonicolor (B. Fisch. & Brebeck) Kluyver & C.B. Niel	TEM	n/d	Dimorphic	Yes	Axenic culture	Unknown - colacosomes formed in own mycelium	Yes	Moore (1972)
Cryptomycocolacomycetes								
Colacosiphon filiformis R. Kirschner, R. Bauer & Oberw.	TEM	Vesicular gall-like cells	Only filamentous morph known	Uncertain	Co-culture with host	Unknown, possibly member of *Ascomycota*	No	Kirschner *et al.* (2001)
Cryptomycocolax abnormis Oberw. & R. Bauer	TEM	Vesicular gall-like cells	Dimorphic	Yes	Host basidiome	Unknown, possibly member of *Ascomycota*	No	Oberwinkler & Bauer (1990)

Table 1. (Continued).

Species	Method colacosome detection	Colacosome organisation	Observed morphs	Sexual stage observed	Source of colacosome detection	Host species	Culture available	Selected references
Basidiomycota incertae sedis								
Colacogloea allantospora Ginns & Bandoni	Brightfield microscopy	n/d	Unknown	Yes	Host basidiome	*Tubulicrinis calothrix* (Pat.) Donk	No	Bandoni *et al.*(2002)
Colacogloea bispora (Hauerslev) Oberw. & R. Bauer	TEM	Vesicular gall-like cells	Unknown	Yes	Host basidiome	*Tubulicrinis angustus* (D.P. Rogers & Weresub) Donk	No	Oberwinkler *et al.* (1999)
Krieglsteinera lasiosphaeriae Pouzar	TEM	Vesicular gall-like cells	Unknown	Yes	Host basidiome	*Lasiosphaeria ovina* (Pers.) Ces. & De Not.	No	Bauer (2004)

of *Pucciniomycotina*: *Cryptomycocolacomycetes* and *Microbotryomycetes* (Table 1). For four species, *i.e.*, *Atractocolax pulvinatus*, *Colacogloea allantospora*, *C. bispora*, and *Krieglsteinera lasiosphaeriae*, no living cultures and/or DNA sequence data are currently available, and their placement in *Microbotryomycetes* is tentative (Kirschner *et al.* 1999, Oberwinkler *et al.* 1999, Oberwinkler 2017). Filamentous morphs of colacosome-forming fungi which are associated with a host fungus are considered to represent a mycoparasitic stage. However, the ecology of fungi in which colacosomes were only observed in pure culture conditions is less clear, since no host–parasite interaction was observed. These species were often isolated as yeasts from a variety of substrates such as phylloplanes, soils, and (decaying) organic substrates, and are generally believed to be saprobes. However, because of their ability to produce colacosomes, these species are discussed to also have mycoparasitic capabilities (Sampaio *et al.* 2003, Boekhout *et al.* 2011, Begerow *et al.* 2017, 2018).

Most likely, the diversity of colacosome-forming mycoparasites is much broader than currently known, a statement for which at least three reasons can be put forward. A first argument is that for all currently known colacosome-forming species, only one or a few collections or isolates were investigated. This leaves room for unexplored diversity in species complexes and (pseudo-) cryptic diversity. Secondly, due to the rather recent discovery of colacosomes and the lack of specialised tools to visualise and detect them, it is likely that for various currently known fungicolous fungi the presence of colacosomes is yet to be assessed. Currently, more than 20 species assigned to the heterogenous morphogenera *Achroomyces* and *Platygloea* are presumed mycoparasites, for which no detailed information on the host–parasite interaction is available (Bandoni 1956, Oberwinkler *et al.* 1990a). Such mycoparasites, for which no haustoria have been observed, are potential colacosome-interacting species and should be investigated more carefully. Thirdly, many colacosome-forming fungi remain undescribed due to their inconspicuous nature. These species either have minute basidiomata, or only grow intrahymenially. It has also been noted that many yeasts in *Cystobasidiomycetes* and *Microbotryomycetes* are slow-growing fastidious or extremophilic species and are known from a few isolates only (Buzzini *et al.* 2018). Therefore, many groups in these two classes remain largely undersampled (Kachalkin *et al.* 2019).

Most studies that reported the presence of colacosomes in fungi made use of transmission electron microscopy (TEM) (Table 1). Sample preparation for TEM is a labour-intensive process requiring knowledge and equipment for embedding, sectioning, staining, and imaging (Oberwinkler & Bauer 2018). Therefore, it is currently challenging to perform a large-scale screening for the presence of colacosomes in fungal specimens. One study reported on the presumed presence of colacosomes based on Congo red stained samples visualised with brightfield microscopy (Bandoni *et al.* 2002). A reliable light microscopy-based method would be more efficient and accessible to detect the presence of colacosomes compared to TEM. Further, it could allow for a wide screening for colacosome-forming fungi towards improving our knowledge of the diversity of these mycoparasites.

In this paper, we aim to investigate the taxonomy and phylogenetic relationships of colacosome-forming mycoparasites. To do so, we developed an accessible and easy light microscopy-based method for colacosome detection, which we validated using correlative light microscopy and TEM. This helped us to find out how the colacosomes are organised along the host–parasite interface. Using this microscopy technique, freshly collected

samples of mycoparasites from various host species were investigated for the presence of colacosomes. Positively assessed colacosome-interacting mycoparasites were isolated in pure culture. These samples were used for phenotypic characterisation of their filamentous- and yeast morphs, and DNA sequencing of seven genetic loci. To assess the phylogenetic relationships of these mycoparasites, we compiled an extensive dataset of *Microbotryomycetes* based on the seven loci commonly used in this class. We also generated DNA sequences of additional loci for certain species to obtain a better phylogenetic resolution (Table 3). This allowed to determine the phylogenetic diversity, -relationships, and -distribution of colacosome-forming mycoparasites, and to explore how they influence the current classification of *Microbotryomycetes*. We translated obtained results into a taxonomic arrangement of colacosome-forming mycoparasites, and an updated classification of *Microbotryomycetes*. Integration of these different types of information allows to formulate an evolutionary hypothesis on colacosome-interacting mycoparasites.

MATERIALS AND METHODS

Material examined

Samples of colacosome-forming fungi were collected from different places in Europe (Belgium, Denmark, Finland, France, Germany, Norway, The Netherlands) in recent years. Herbarium collections from C, GENT, H, LIP, and PC (*sensu* Thiers 2022) were investigated. Examined collections are listed under the species descriptions in the taxonomic part of this paper. Collections indicated with an asterisk (*) were isolated in pure culture and used for DNA sequencing. GenBank accession numbers are listed in Table 3. Specimens indicated with (°) were investigated using epifluorescence microscopy and/or TEM. Some additional ex-type yeast cultures were obtained from the fungal collection of the Leibniz Institute DSMZ – German Collection of Microorganisms and Cell Cultures (Braunschweig, Germany). These cultures were used to sequence additional loci for phylogenetic analysis.

Light microscopy and morphology

Whole-mount preparations from fresh and dried host basidiomes were mounted in a Congo red staining solution in ddH_2O according to Clémençon (2009). In some cases, the Congo red staining solution was supplemented with DAPI (4'6-diamidino-2-phenylindole, with a final concentration of 1 µg/mL) for staining of nuclei. Some species were additionally studied using Cotton Blue staining solution (0.025 % w/v in Lactic acid). Specimens were investigated for micromorphological characters using phase-contrast optics (Leica DM 1000 Led), brightfield and epifluorescence microscopy using a Nikon Plan Fluor 100× objective with 1.3 numeric aperture on a Nikon Eclipse Ni-U microscope, using a TRITC (excitation: 543/22 nm; dichroic mirror 652 nm; emission: 593/40 nm) and/or DAPI filters (excitation: 387/11 nm; dichroic mirror 409 nm; emission: 447/60 nm). The presence of colacosomes was evaluated using epifluorescence microscopy of Congo red stained samples. Photographs of microscopic structures were taken with a Nikon DS-Fi3 camera and Nikon NIS-Elements software, including the Extended Depth of Field module. Pictures were edited and compiled in Photoshop CS6. The basidiospores and conidia represented in the composite plates are a compilation from different pictures. For each collection, at least 30 basidiospores and 15 basidia and conidia were measured. The measurements are presented following Parmasto & Parmasto (1987), with 5 % tails excluded and given in parentheses. The following abbreviations are used in the species descriptions: L – mean basidiospore length, W – mean basidiospore width, Q' – L/W ratio, Q – mean L/W ratio, and n – number of measurements per specimens measured. The basidiospore length measurements include the apiculus since it is often impossible to unequivocally determine its exact border with the main spore body. Basidia were measured using Nikon software, by drawing a polygonal line from the basal clamp of the basidium, over the middle of each transversal septum, to the distal end of the top cell (not including the upper sterigma if inserted apically). Structure and terminology of morphological diagnoses follow Spirin *et al.* (2018) and Savchenko *et al.* (2021).

Correlative light and Transmission Electron Microscopy

The sample fixation protocol is based on Bauer *et al.* (2006), with slight modifications. Samples were fixed in 2 % v/v glutaraldehyde in 0.1 M sodium cacodylate buffer (pH 7.2) at room temperature for 12 h in a rotating device. Following six 10 min incubations in 0.1 M sodium cacodylate buffer, samples were post fixed in 1 % v/v osmium tetroxide in cacodylate buffer for 1.5 h in darkness. Samples were dehydrated in acetone, using 15 min changes at 10, 20, 30, 50, 70, 95 % v/v and three times in 100 % acetone. Samples were infiltrated by Spurr's resin in acetone using 15 min changes at 25, 50, 75 % v/v and three times in 100 % Spurr's resin. Samples were polymerised overnight in Spurr's resin at 60 °C. Serial sections were made to perform correlative light- and transmission electron microscopy. First, semi-thin sections of 300 nm thick, made using an ultramicrotome (UC6; Leica microsystems, Vienna) equipped with a diamond ultra-knife (DiATOME), were collected on polysine coated slides. Immediately after, ultrathin sections of 80 nm thick were made and collected on copper slot grids. Semi-thin sections were mounted in Congo red and viewed using an epifluorescence microscope equipped with a TRITC filter. Ultra-thin sections were stained for 27 min in 1 % uranyl acetate at 37 °C and 10 min in 3 % lead citrate at 20 °C. Grids were examined with a JEM-1010 TEM (Jeol Inc., Peabody, MA, USA) using a 60 keV electron beam. Images were recorded with a CCD side-mounted Veleta camera. Same areas were imaged.

Isolation procedure

Isolates of the different species were obtained by a spore drop method (Clémençon 2009) on MYP medium plates (0.4 g peptone 0.8 g yeast extract, 5.6 g malt extract and 16 g agar kobe-1 in 800 ml ddH_2O). A small piece of infected host tissue was dissected and attached to the lid of a Petri plate. Plates were left at room temperature and the lid was rotated clockwise 1 h, 2 h, 4 h, 6 h, and 8 h after initial inoculation to allow sporulation on different places of the medium. Subsequently, the fungal sample was removed, and germinating spores were isolated on new MYP plates to obtain pure isolates. Cultures of all isolated collections were deposited at DSMZ.

Phenotypic characterisation of yeast morphs

Physiological tests were performed in liquid media according to the methods described in Kurtzman *et al.* (2011), in custom-made microplates (Nunc 96-Well Flat Bottom plate, Thermo Fisher

Scientific) and tubes (Passer *et al.* 2019) using the same standard set of substrates. Tests were incubated at room temperature and controlled every 3–4 d until for in total 3 wk. Culture growth in microplates was measured on Varioskan LUX (Thermo Fisher Scientific) plate reader at 600 nm wavelength. Maximal growth temperature was determined on potato-dextrose agar (PDA, Difco BD) and micromorphological features were examined on PDA, CMA (DSMZ medium 191, https://mediadive.dsmz.de/medium/191), and YM agars (DSMZ medium 186, https://mediadive.dsmz.de/medium/186). A summary of the obtained results from the growth tests is given in Supplementary Table 1.

DNA extraction, PCR amplification, and sequencing

DNA from cultures was extracted using a CTAB-based protocol. From each culture, a loop of yeast cells was harvested and stored in 500 µL CTAB buffer. After addition of 0.3 % mercaptoethanol, the samples were homogenised in a thermoshaker at 65 °C and 600 rpm for 1.5 h. Subsequently, 500 µL chloroform-iso-amylalcohol was added and the samples were vortexed. Next, samples were centrifuged for 10 min at 12 000 rpm, after which the upper phase was transferred to another tube. After repeating this step one more time, 500 µL cold iso-propanol was added to the upper phase, samples were shaken and left at -20 °C for 20 min to precipitate the DNA. Subsequently, the samples were centrifuged at 12 000 rpm for 10 min at 4 °C and the pellet was washed twice with 70 % EtOH. Finally, the DNA pellet was diluted in 50 µL Milli-Q water. PCR reactions were performed for the following seven loci: the small subunit (SSU), the internal transcribed spacers, including the 5.8S locus (ITS), and the large subunit (LSU) of the nuclear ribosomal DNA, the largest subunit of RNA polymerase II (*RPB1*), the second largest subunit of RNA polymerase II (*RPB2*), the translation elongation factor (*TEF1-α*) and mitochondrial cytochrome-b (*CYT-B*). Conditions for the amplification of seven genetic markers are given in Table 2. PCR products were purified using ThermoFisher FastAP Thermosensitive Alkaline Phosphatase and Exonuclease I (Thermo Fisher Scientific Inc., Massachusetts, USA). Purified products were sent to Macrogen (Amsterdam, The Netherlands) for Sanger sequencing using the same primers on an automated ABI 3730 XL capillary sequencer. Forward and reverse sequence reads were assembled into contigs in the BioloMICS software (BioAware SA NV, Hannut, Belgium). DNA extraction and amplification of *Colacogloea universitatis-gandavensis sp. nov.* was performed using a Multiple Displacement Amplification (MDA) procedure, using the Repli-g Whole Genome Amplification kit (QIAGEN, Hilden, Germany). Collection NS 20-022 was used for the dissection of two small pieces of parasite tissue (2 mm³ each) under a dissecting microscope. Subsequently, PCR reactions of the SSU, ITS, and LSU region were performed using conditions listed in Table 2. DSMZ cultures were cultivated on PDA (Difco BD) for 7 d at room temperature. Their DNA was isolated with the MasterPure Yeast DNA Purification Kit (Epicentre, San Diego, USA) following the manufacturer's instructions. PCR products were purified with innuPREP PCRpure Kit (Analytik Jena, Jena, Germany) and sequenced on ABI 3500 XL capillary sequencer. Assembly and editing of sequence reads were performed with Sequencher v. 5.4.5 (Gene Codes Corporation, Michigan, USA).

Phylogenetic analyses

DNA sequences were downloaded from GenBank and are listed in Table 3. To compile the dataset, we used DNA sequence data from Wang *et al.* (2015a, b), which were complemented with sequence data of remaining taxa within *Microbotryomycetes* (Table 3). The phytoparasitic *Microbotryales* are represented by a limited set of taxa as in Wang *et al.* (2015a) and Li *et al.* (2020). To exclude possible contaminant sequences from public databases, we blasted all downloaded sequences against the NCBI nucleotide database. Contaminant sequences were removed from the dataset. Sequences of each region were aligned with the online version of MAFFT (Katoh *et al.* 2019) using the L-INS-i algorithm for the ITS dataset and the Iterative FFT-NS-i algorithm for the LSU, SSU, *RPB1, RPB2, TEF1-α,* and *CYT-B* datasets. Trailing ends of the alignments were trimmed and manually curated in MEGA v. 7 (Kumar *et al.* 2016). The ITS locus was partitioned in the ITS1, 5.8S and ITS2 regions. The ITS1 and ITS2 regions of the alignment were trimmed using TrimAL v. 1.1, with the following settings: 0.6 as gap threshold and 50 as minimum percentage of positions to conserve (Capella-Gutiérrez *et al.* 2009). Alignments of all regions were manually inspected and refined, and intronic regions manually removed. Final alignments are deposited in TreeBASE (http://purl.org/phylo/treebase/phylows/study/TB2:S30327). ModelFinder as implemented in IQ-TREE v. 1.6.12 was used to infer the best model of evolution for each partition using the Akaike Information Criterion (AIC) (Kalyaanamoorthy *et al.* 2017). Maximum Likelihood analyses were performed using IQ-TREE v. 1.6.12 for single partitions and the concatenated dataset (Nguyen *et al.* 2015, Chernomor *et al.* 2016). The concatenated dataset was partitioned as follows: SSU, ITS1, 5.8S, ITS2, LSU, *RPB1, RPB2, TEF1-α*, and *CYT-B*. All analyses were performed using ultrafast bootstrapping procedure with 2 000 bootstrap replicates (Hoang *et al.* 2018).

RESULTS

Epifluorescence-based colacosome visualisation

Because the assessment of the presence of colacosomes using TEM of fungal samples is a labour-intensive and time-consuming task, we developed a more efficient and affordable, light microscopy-based method for the detection of these structures. We compared the detectability of colacosomes in Congo red-stained samples of mycoparasites using brightfield and epifluorescence microscopy. Epifluorescence microscopy proved to be superior to brightfield imaging as colacosomes exhibit intense fluorescence signals and are visible as bright circular structures (compare Fig. 2A, B). As is evident from Fig. 2B, this approach allows to distinguish between host and parasite cells, as well as to detect individual and clustered colacosomes (Fig. 2B inset). Colacosomes are easy to distinguish due to the strong contrast between the bright signal emitted by the stained secondary cell wall enveloping them and the black background. To verify whether the bright signals originate from the colacosomes, we performed correlative light microscopy and TEM of *Colacogloea universitatis-gandavensis sp. nov.* (Fig. 2C, F). The host–parasite interface encompasses parasite gall-like cells enveloping host hyphae. Colacosomes are positioned in the parasite cells along the host–parasite interface. When the same area in the sections is imaged using epifluorescence microscopy and TEM (Fig. 2C, D), it becomes apparent that the bright fluorescent signals correspond to colacosomes. Contrary to the whole-mount prepared sample (Fig. 2A, B), individual colacosomes are visible as bright circles with a dark core in semithin sections (Fig. 2C). This core does not stain with Congo red and becomes visible because the 300 nm section is less thin than the diameter of colacosomes. Magnification of this area using TEM further shows the ultrastructure of individual

Table 2. PCR conditions and primers used for DNA amplification.

Locus	Initial denaturation	Number of cycles	Denaturation	Annealing	Elongation	Final extension	Primers	Sense	Sequence (5' → 3')	Reference
ITS	95 °C for 5 min	35	95 °C for 30 s	55 °C for 45 s	72 °C for 45 s	72 °C for 5 min	ITS1-F	Forward	CTTGGTCATTTAGAGGAAGTAA	Gardes & Bruns (1993)
							ITS4	Reverse	TCCTCCGCTTATTGATATGC	White *et al.* (1990)
LSU	94 °C for 1 min	35	94 °C for 1 min	52 °C for 45 s	72 °C for 45 s	72 °C for 5 min	NL1	Forward	GCATATCAATAAGCGGAGGAAAAG	O'Donnel (1993)
							NL4	Reverse	GGTCCGTGTTTCAAGACGG	O'Donnel (1993)
	95 °C for 5 min	35	94 °C for 1 min	55 °C for 45 s	72 °C for 45 s	72 °C for 5 min	LR0R	Forward	GTACCCGCTGAAGTTAAGC	Cubeta *et al.* (1991)
							LR5	Reverse	ATCCTGAGGGAAACTTC	Vilgalys & Hester (1990)
SSU	95 °C for 5 min	35	95 °C for 35 s	55 °C for 45 s	72 °C for 1 min	72 °C for 5 min	NS1	Forward	GTAGTCATATGCTTGTCTC	White *et al.* (1990)
							NS4	Reverse	CTTCCGTCAATTCCTTTAAG	White *et al.* (1990)
RPB1	94 °C for 4 min	36	94 °C for 1 min	52 °C for 1 min	72 °C for 1 min	72 °C for 8 min	RPB1-Af	Forward	GARTGYCCDGGDCAYTTYGG	Matheny *et al.* (2002)
							RPB1-Cr	Reverse	CCNGCDATNTCRTTRTCCATRTA	Matheny *et al.* (2002)
RPB2	94 °C for 4 min	36	94 °C for 1 min	52 °C for 1 min	72 °C for 1 min	72 °C for 8 min	fRPB2-5F	Forward	GAYGAYMGWGATCAYTTYGG	Liu *et al.* (1999)
							fRPB2-7cR	Reverse	CCCATRGCTTGYTTRCCCAT	Matheny (2005)
TEF-1α	95 °C for 5 min	35	94 °C for 1 min	55 °C for 45 s	72 °C for 45 s	72 °C for 5 min	EF1-983F	Forward	GCYCCYGGHCAYCGTGAYTTYAT	Rehner & Buckley (2005)
							EF1-2218R	Reverse	ATGAACCRACRGRACRGTYTG	Rehner & Buckley (2005)
							EF1-1567R	Reverse	ACHGTRCCRATACCACCRATCTT	Rehner & Buckley (2005)
CYT-B	94 °C for 4 min	36	94 °C for 1 min	46 °C for 1 min	72 °C for 1 min	72 °C for 5 min	E1M4	Forward	TGRGGWGCWACWGTTATTACTA	Biswas *et al.* (2001)
							E2mr3	Reverse	GGWATAGCACGTARAAYWGCRTA	Biswas *et al.* (2001)

colacosomes, which consist of an electron dense core surrounded by a membrane and a secondary cell wall (Fig. 2E, F). Colacosomes are also clearly visible using a 40× objective and could be detected and discriminated from other structures (data not shown). Although other chitin-containing structures such as thick-walled conidia also emit bright fluorescent signals, they cannot be mistaken for colacosomes due to their size, shape and/or organisation.

We applied this method to assess the presence of colacosomes in nine mycoparasitic species (Figs 5F, G, 7H, 9G, H, 11G, H, 13F, G, 15G, 17G, 19F, G, 21G). Samples for which the presence of colacosomes was positively assessed were isolated in pure culture and further studied for their phylogenetic relationships and phenotypic characteristics (*i.e.*, micromorphology of the filamentous morph in the specimen, and characterisation of the yeast morph in axenic culture).

Phylogenetic reconstruction

To visualise the placement of colacosome-forming species in the *Microbotryomycetes* and their evolutionary relationships, we performed a phylogenetic analysis using the commonly used seven loci, incorporating a broad representation of all known lineages within this class. The final dataset included 238 isolates and 5 855 characters, of which 2 815 were parsimony-informative and 2 281 were invariant. A summary of the partitions, number of sequences, number of parsimony-informative- and constant sites, and selected models is presented in Table 4. The full partition model AIC score is 381 436.460 (LnL = -190 078,230 df:640). Figure 3 shows the retrieved tree topology. This seven-locus ML tree is used as basis for clade recognition, an updated classification of *Microbotryomycetes*, and one of the criteria used for species delimitation.

All currently described families and orders of *Microbotryomycetes* are recovered as monophyletic clades, with support values given in Table 5. Deeper nodes, depicting the relationships among higher taxa, are not resolved. Clades containing isolates and specimens that were newly sequenced are indicated in boxes in the phylogenetic reconstruction (Fig. 3). The inclusion of colacosome-forming mycoparasites allows to recognise several new phylogenetic lineages in *Microbotryomycetes*. A first new lineage comprises four isolates of *Atractocolax pulvinatus*, which forms a distinct lineage within *Microbotryomycetes*. A second new lineage comprises the clade of *Mycogloiocolax gerardii sp. nov.* and the currently undescribed yeast isolate KBP Y-6479, for which the family *Mycogloiocolacaceae fam. nov.* is proposed (see taxonomy section). Within the genus *Colacogloea*, five new lineages can be recognised, each representing a new species in the *Colacogloea effusa* species complex (see taxonomy section). A separate ML phylogenetic reconstruction of the genus *Colacogloea* based on the three rDNA loci SSU, ITS and LSU (results not shown) rendered the same topology as retrieved in our seven-locus class-wide reconstruction. Seven isolates identified as *Platygloea micra* cluster within the genus *Slooffia* with high support. These isolates are clearly conspecific, but are distant from the other described species within the genus, prompting a recombination (see taxonomy section).

Taxonomy

Based on the combined results from comparison of micromorphological characters of filamentous morphs, assimilation growth essays of yeast morphs, and the seven-locus phylogenetic reconstruction, we draw the following taxonomic conclusions as outlined below.

Order *Heterogastridiales* Oberw. & R. Bauer, Mycologia 82: 57. 1990.

Slooffia Q.M. Wang *et al.*, Stud. Mycol. 81: 186. 2015. ***emend.***

Generic description: Genus of dimorphic fungi. Basidiomata are absent. Filamentous morph develops intrahymenial in the host, sometimes producing a whitish layer overgrowing the host basidiome. Hyphal system monomytic, hyaline, thin-walled, smooth, clamped at all septa. Hyphidia absent. Cystidia absent. Basidia cylindrical to slightly clavate, often strongly curved to a 90° angle, transversally septate, mature basidia four-celled, clamped, thin-walled, originating from a distinct probasidium which collapses after maturation of the basidium. Sterigmata originating laterally or apically from basidial cells, rarely bifurcating. Basidiospores of irregular shape, smooth, hyaline, inamyloid. Germination of basidiospores occurs by either hyphae, budding or secondary spore production. Conidiophores stalked, basally clamped, with apically numerous appendages. Conidia irregularly shaped, thick-walled, cyanophilous.

Habitat, substrate, and ecology: *Slooffia* species have been isolated as yeasts from soils, litter, insect faeces and basidiomata of *Myxarium podlachicum*. Yeast morphs are presumed to have a saprobic ecology. A filamentous morph has only been observed for *Slooffia micra comb. nov.*, which represents a colacosome-interacting mycoparasitic stage, developing intrahymenially in the host *Myxarium podlachicum*.

Distribution: *Slooffia* species have been recorded from various European countries, Brazil, India and the USA (Hamamoto *et al.* 2011, Sampaio 2011, Bezerra *et al.* 2013, Buzzini *et al.* 2017).

Type: *Slooffia tsugae* (Phaff & Carmo Souza) Q.M. Wang, F.Y. Bai, M. Groenew. & Boekhout

Slooffia micra (Bourdot & Galzin) Schoutteten, ***comb. nov.*** MycoBank MB 848660. Figs 4, 5.
Basionym: *Platygloea micra* Bourdot & Galzin, Bull. Trimestriel Soc. Mycol. France 39: 261. 1924.

Typus: **France**, Aveyron, on rotten wood of *Populus*, 23 Oct. 1915, *A. Galzin* (**holotype**, PC Bourdot 19438°). As only one specimen of this species is available in the collection of Bourdot and Galzin in the Paris herbarium (PC), this specimen is to be interpreted as the holotype, although it was not mentioned as such by the original authors (ICNafp Art. 9.1). **Belgium**, Prov. West-Vlaanderen, Ieper, Palingbeek, on piece of wood of an unidentified deciduous tree, growing in the hymenium of *Myxarium podlachicum*, 16 Oct. 2019, *M. Detollenaere* (**epitype** GENT NS 19-337*°, designated here, MycoBank MBT 10013261, culture ex-epitype DSM 112421).

Synonym: *Achroomyces insignis* Hauerslev, Mycotaxon 49: 218. 1993.

Typus: **Denmark**, Zealand, Copenhaguen, Hareskoven, on decorticated branch of an unidentified tree, growing in the hymenium of *Myxarium podlachicum*, 21 Sep. 1991, *K. Hauerslev* (**holotype**, C C19753 = KH7222°). **The Netherlands**, Prov. Groningen, Tjuchem, Huisweersterbos, on decorticated branch of an unidentified deciduous tree, growing in the hymenium of *Myxarium podlachicum*, 14 Feb. 2020, *I. Somhorst* (**epitype** GENT IS 20-006*°, designated here, MycoBank MBT 10013262, culture ex-epitype DSM 112423).

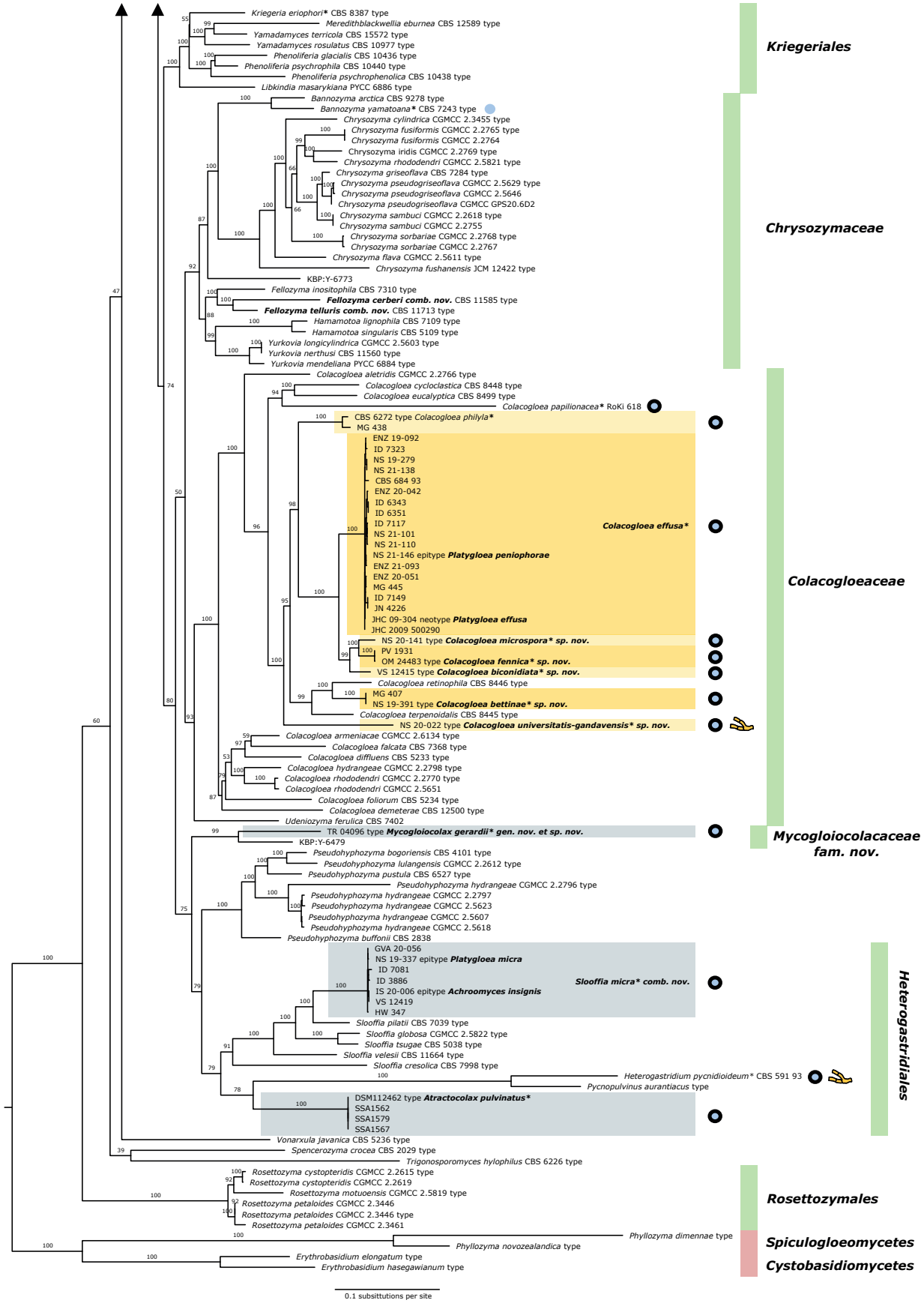

Fig. 3. Phylogenetic relationships of colacosome-forming species in *Microbotryomycetes* based on a seven-locus ML tree inference. Species names in bold indicate taxonomic novelties. Species which were explicitly investigated for the presence of colacosomes are indicated with a * symbol behind the species name. Species for which the presence of colacosomes was positively assessed are indicated by blue-filled circles. Blue circles with black outline indicate species which have been isolated as a mycoparasite and for which an interaction with a host was reported. Blue circles without outline indicate species which were only reported to form colacosomes in pure culture. Species for which currently only a filamentous morph was observed are indicated by a branching hyphae icon, for all other species in the tree, at least a yeast morph is known. Clades investigated in detail in this study are indicated with boxes. Boxes in yellow tones represent the *Colacogloea effusa* complex. Green vertical lines represent the highest described taxon available for species in the tree (family or order). Numbers on branches indicate ultrafast bootstrap values. *Cystobasidiomycetes* and *Spiculogloeomycetes* are used as outgroup.

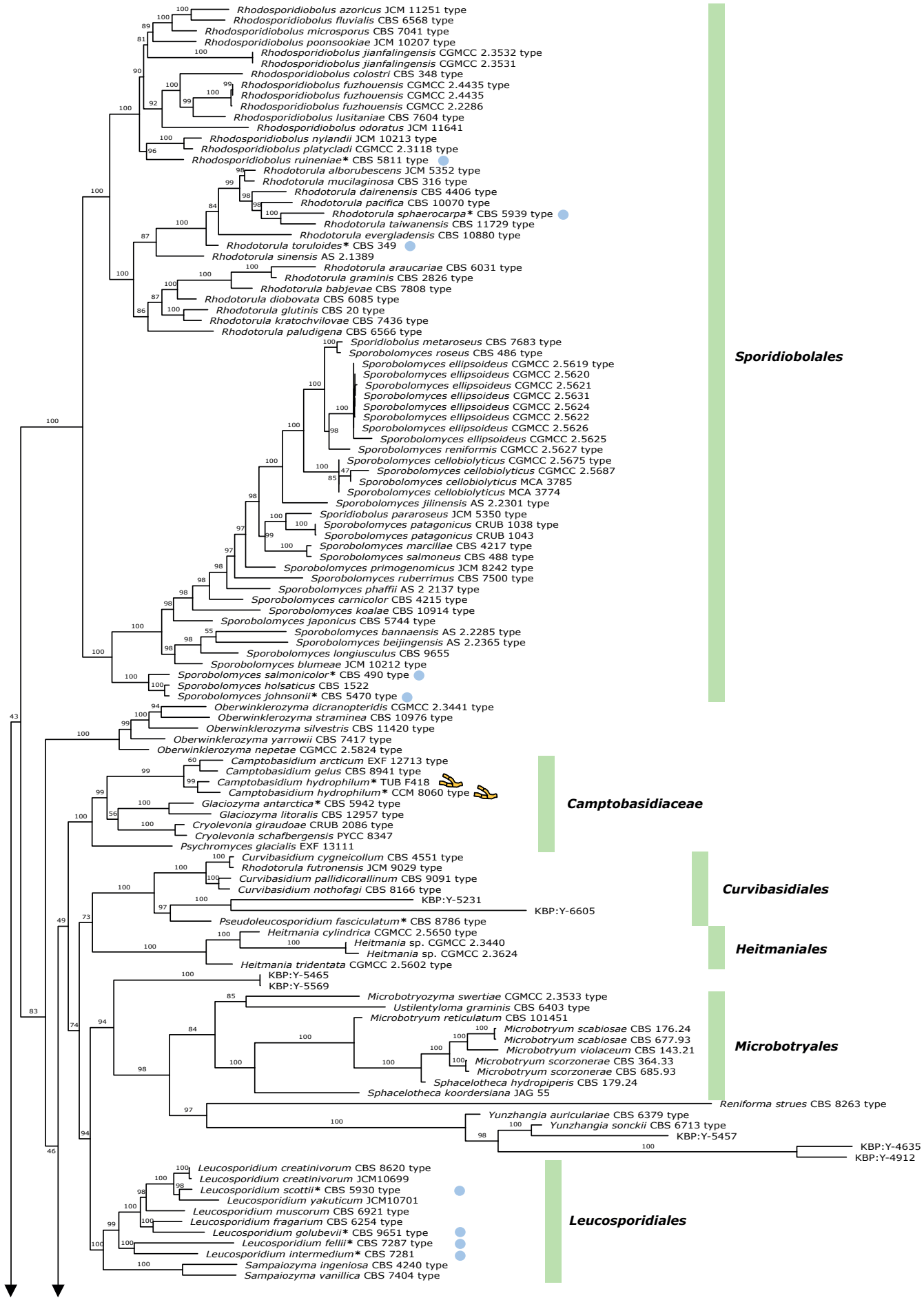

Fig. 3. (Continued).

Table 3. Summary of isolates and GenBank accession numbers of the seven genetic loci incorporated in the phylogenetic reconstruction. Accession numbers of sequences generated for this study are indicated in bold.

Order	Family	Species	Strain or specimen[1]	GenBank accession numbers[2]							Reference
				ITS	LSU	SSU	*RPB1*	*RPB2*	*TEF1-α*	*CYT-B*	
Curvibasidiales	*Curvibasidiaceae*	*Curvibasidium cygneicollum*	CBS 4551^{T}	AF444490	AF189928	KJ708423	KJ708001	KJ708169	KJ707768	KJ707678	Wang *et al.* (2015a)
		Cu. nothofagi	CBS 8166^{T}	AF444537	AF189950	KJ708447	KJ708002	KJ708248	KJ707765	AB040639	Wang *et al.* (2015a)
		Cu. pallidicorallinum	CBS 9091^{T}	AF444641	AF444736	KJ708420	KJ708000	KJ708167	KJ707767	KJ707665	Wang *et al.* (2015a)
		Rhodotorula futronensis	JCM 9029^{T}	AB038090	KP216511	KJ708444	KJ708062	KJ708232	KJ707836	AB040625	Wang *et al.* (2015a)
	—	*Pseudoleucosporidium fasciculatum*	CBS 8786^{T}	KJ778628	AY212993	KJ708387	KJ707998	KJ708183	KJ707769	—	Wang *et al.* (2015a)
	—	—	**KBP Y-5231**	**MK265709**	MK265709	**ON106835**	—	**OW409726**	**OW409725**	—	Kachalkin *et al.* (2019); This publication
	—	—	**KBP Y-6605**	MT013025	MT013025	MZ666891	—	—	**OU466849**	—	This publication
Heitmaniales	*Heitmaniaceae*	*Heitmania cylindrica*	CGMCC 2.5650^{T} = CBS 15568	MK050421	—	—	MK849237	MK849376	MK849101	MK848972	Li *et al.* (2020)
		He. tridentata	CGMCC 2.5602^{T} = CBS 15549	MK050420	—	—	MK849217	MK849356	MK849083	MK848951	Li *et al.* (2020)
		Heitmania. sp.	CGMCC 2.3440	MK050422	—	—	MK849161	MK849299	MK849031	MK848900	Li *et al.* (2020)
			CGMCC 2.3624	MK050423	—	—	MK849189	MK849327	MK849057	MK848925	Li *et al.* (2020)
Heterogastridiales	*Heterogastridiaceae*	*Heterogastridium pycnidioideum*	CBS 591.93	GU291276	GU291290	KJ708412	KJ708009	KJ708170	KJ707770	KJ707630	Wang *et al.* (2015a)
		Pycnopulvinus aurantiacus	PUL-F2679^{T} (specimen)	NR_138394	KJ676979	—	—	—	—	—	Toome & Aime (2014)
	—	***Atractocolax pulvinatus***	**DSM 112462^{T}**	**OQ870202**	**OQ875034**	**OP890260**	**OR105880**	**OQ930200**	**OR105889**	—	This publication
	—	*At. pulvinatus*	SSA1567	—	KX752071	—	—	—	—	—	Ali *et al.* (2017)
	—	*At. pulvinatus*	SSA1579	—	KX791364	—	—	—	—	—	Ali *et al.* (2017)
	—	*At. pulvinatus*	SSA1562	—	KX907647	—	—	—	—	—	Ali *et al.* (2017)
	—	*Slooffia cresolica*	CBS 7998^{T}	AF444570	AF189926	KJ708365	KJ708135	KJ708222	KJ707942	—	Wang *et al.* (2015a)
	—	*Sl. globosa*	CGMCC 2.5822^{T} = CBS 15573	MK050449	—	—	MK849255	MK849392	MK849116	MK848989	Li *et al.* (2020)
	—	***Sl. micra comb. nov.***	**NS 19-337 = DSM 112421^{ET}**	**OQ870194**	**OQ875027**	**OQ878238**	—	—	**OQ930223**	—	This publication
	—	***Sl. micra comb. nov.***	**GVA 20-056**	**OQ870195**	**OQ875028**	**OQ878239**	**OQ930175**	—	**OQ930224**	—	This publication
	—	***Sl. micra comb. nov.***	**ID 3886 (DSM)**	**OQ870196**	**OQ875029**	—	—	**OQ930197**	—	—	This publication
	—	***Sl. micra comb. nov.***	**IS 20-006 = DSM 112423^{ET}**	**OQ870197**	**OQ875030**	**OQ878240**	—	—	**OQ930225**	—	This publication
	—	***Sl. micra comb. nov.***	**HW 347 (DSM)**	**OQ870198**	**OQ875031**	**OQ878241**	**OQ930176**	**OQ930198**	**OQ930226**	**OR053646**	This publication
	—	***Sl. micra comb. nov.***	**ID 7081 (DSM)**	**OQ870199**	**OQ875032**	**OQ878242**	**OQ930177**	**OQ930199**	**OQ930227**	**OR053647**	This publication
	—	***Sl. micra comb. nov.***	**VS 12419** (specimen)	**OQ870200**	—	—	—	—	—	—	This publication
	—	*Sl. pilati*	CBS 7039^{T}	AF444598	AF189963	KJ708364	KJ708137	KJ708256	KJ707947	AB040641	Wang *et al.* (2015a)
	—	*Sl. tsugae*	CBS 5038^{T}	AF444580	AF189998	AB021692	—	KJ708340	KJ707945	KJ707628	Wang *et al.* (2015a)
	—	***Sl. velesii***	**CBS 11664^{T}**	—	FN428962	**OP910241**	**OR105881**	**OR105887**	—	—	Yurkov *et al.* (2016); This publication

Table 3. (Continued).

Order	Family	Species	Strain or specimen[1]	GenBank accession numbers[2]							Reference
				ITS	LSU	SSU	*RPB1*	*RPB2*	*TEF1-α*	*CYT-B*	
Kriegeriales	*Kriegeriaceae*	*Kriegeria eriophori*	CBS 8387^{T}	AF444602	NR_119455	DQ419918	—	—	—	—	Wang *et al.* (2015a)
		Libkindia masarykiana	**PYCC 6886^{T}**	KU187885	KU187889	**OP883947**	**OQ676583**	**OQ676584**	**OQ676580**	—	Mašínová *et al.* (2017); This publication
		Meredithblackwellia eburnea	CBS 12589^{T}	JX508799	JX508798	JX508797	—	—	—	—	Wang *et al.* (2015a)
		Phenolipheria glacialis	CBS 10436^{T}	EF151249	EF151258	KJ708381	KJ708067	KJ708233	KJ707831	KJ707597	Wang *et al.* (2015a)
		Ph. psychrophenolica	CBS 10438^{T}	EF151246	EF151255	KJ708382	KJ708071	KJ708259	KJ707859	KJ707598	Wang *et al.* (2015a)
		Ph. psychrophila	CBS 10440^{T}	EF151243	EF151252	KJ708383	—	KJ708260	KJ707833	KJ707599	Wang *et al.* (2015a)
		Yamadamyces rosulatus	CBS 10977^{T}	EU872492	EU872490	KJ708384	KJ708083	KJ708263	KJ707854	KJ707607	Wang *et al.* (2015a)
		Ya. terricola	CBS 15572^{T}	MK050425	—	—	MK849127	MK849268	MK848999	MK848874	Li *et al.* (2020)
Leucosporidiales	*Leucosporidiaceae*	*Leucosporidium creatinivorum*	JCM 10699	KJ778627	KJ708455	KJ708385	KJ708064	KJ708221	KJ707857	KJ707687	Wang *et al.* (2015a)
		Le. creatinivorum	CBS 8620^{T}	AF444629	AF189925	KJ708418	KJ708036	KJ708178	KJ707789	KJ707658	Wang *et al.* (2015a)
		Le. fellii	JCM 9887^{T}	AF444508	AF189907	KJ708449	KJ708030	KJ708184	KJ707784	KJ707748	Wang *et al.* (2015a)
		Le. fragarium	CBS 6254^{T}	AF444530	AF070428	KJ708413	KJ708031	KJ708179	KJ707791	AB040623	Wang *et al.* (2015a)
		Le. golubevii	CBS 9651^{T}	AY212987	AY212999	KJ708386	KJ708037	KJ708185	KJ707787	—	Wang *et al.* (2015a)
		Le. intermedium	JCM 5291^{T}	AF444630	AF189889	D38235	KJ708132	KJ708188	KJ707785	KJ707711	Wang *et al.* (2015a)
		Le. muscorum	CBS 6921^{T}	AF444527	AF070433	KJ708414	KJ708038	KJ708180	KJ707793	AB040638	Wang *et al.* (2015a)
		Le. scottii	JCM 9052^{T}	AF444495	AF070419	X53499	KJ708033	KJ708186	KJ707788	AB040658	Wang *et al.* (2015a)
		Le. yakuticum	JCM 10701	AY212989	AF189971	KJ708426	KJ708032	KJ708274	KJ707794	KJ707688	Wang *et al.* (2015a)
		Le. yakuticum	CBS 8621^{T}	AY212989	AY213001	KJ708419	—	KJ708181	—	KJ707659	Wang *et al.* (2015a)
		Sampaiozyma ingeniosa	CBS 4240^{T}	AF444534	AF189934	KJ708445	KJ708004	KJ708237	KJ707803	AB040631	Wang *et al.* (2015a)
		Sa. vanillica	CBS 7404^{T}	AF444575	AF189970	KJ708448	KJ708005	KJ708273	KJ707809	KJ707747	Wang *et al.* (2015a)
Microbotryales	*Microbotryaceae*	*Microbotryozyma swertiae*	CGMCC 2.3533^{T} = CBS 15495	MK050424	—	—	MK849180	MK849318	MK849049	—	Li *et al.* (2020)
		Microbotryum reticulatum	CBS 101451	KJ778630	KJ708457	KJ708389	KJ708040	KJ708189	KJ707806	KJ707596	Wang *et al.* (2015a)
		Mi. scabiosae	CBS 677.93	KJ708459	KJ708459	KJ708390	—	KJ708195	KJ707808	KJ707633	Wang *et al.* (2015a)
		Mi. scabiosae	CBS 176.24	KJ708458	KJ708458	KJ708391	KJ708039	KJ708190	KJ707810	KJ707615	Wang *et al.* (2015a)
		Mi. scorzonerae	CBS 685.93	KJ708461	KJ708461	KJ708392	—	KJ708191	KJ707804	KJ707635	Wang *et al.* (2015a)
		Mi. scorzonerae	CBS 364.33	KJ708460	KJ708460	KJ708393	KJ708043	KJ708196	KJ707805	KJ707624	Wang *et al.* (2015a)
		Mi. violaceum	CBS 143.21	KJ708462	KJ708462	KJ708388	KJ708042	KJ708192	KJ707811	KJ707613	Wang *et al.* (2015a)
	Ustilentylomataceae	*Sphacelotheca hydropiperis*	CBS 179.24	KJ708463	KJ708463	KJ708394	KJ708041	KJ708281	KJ707807	KJ707616	Wang *et al.* (2015a)
		Sp. koordersiana	JAG 55	DQ832221	DQ832219	DQ832220	DQ832223	DQ832222	DQ832224	—	Wang *et al.* (2015a)
		Ustilentyloma graminis	JCM 3932^{T}	AF444524	AF189933	AY657013	—	KJ708235	KJ707802	—	Wang *et al.* (2015a)
Rosettozymales	*Rosettozymaceae*	*Rosettozyma cystopteridis*	CGMCC 2.2615^{T}= CBS 15448	MK050398	—	—	MK849131	MK849272	MK849002	MK848876	Li *et al.* (2020)
v		*Ro. cystopteridis*	CGMCC 2.2619 = CBS 15451	MK050399	—	—	—	—	—	MK848877	Li *et al.* (2020)

Table 3. (Continued).

Order	Family	Species	Strain or specimen[1]	GenBank accession numbers[2]							Reference
				ITS	LSU	SSU	*RPB1*	*RPB2*	*TEF1-α*	*CYT-B*	
Rosettozymales	*Rosettozymaceae*	*Ro. motuoensis*	CGMCC 2.5819^T = CBS 15588	MK050400	—	—	MK849260	MK849397	—	MK848991	Li *et al.* (2020)
		Ro. petaloides	CGMCC 2.3446^T = CBS 15480	MK050395	—	—	MK849165	MK849303	MK849034	MK848904	Li *et al.* (2020)
		Ro. petaloides	CGMCC 2.3466 = CBS 15488	MK050396	—	—	MK849174	—	—	—	Li *et al.* (2020)
		Ro. petaloides	CGMCC 2.3461	MK050397	—	—	—	—	—	—	Li *et al.* (2020)
Sporidiobolales	*Sporidiobolaceae*	*Rhodosporidiobolus azoricus*	JCM 11251^T	AB073229	AF321977	AB073269	KJ708053	KJ708202	KJ707813	KJ707693	Wang *et al.* (2015a)
		Rho. colostri	CBS 348^T	JN246563	AY372177	KJ708399	KJ708051	KJ708220	KJ707818	KJ707622	Wang *et al.* (2015a)
		Rho. fluvialis	CBS 6568^T	AY015432	AF189915	AB073272	KJ708046	KJ708204	KJ707816	KJ707679	Wang *et al.* (2015a)
		Rho. fuzhouensis	CGMCC 2.4435^T = CBS 12492	MK050404	—	—	MK849201	MK849340	MK849067	MK848936	Li *et al.* (2020)
		Rho. fuzhouensis	CGMCC 2.2286 = CBS 9205	KY105509	—	KY109744	MN180194	MN180195	MN180197	MN180196	Li *et al.* (2020)
		Rho. jianfalingensis	CGMCC 2.3532^T = CBS 15494	MK050402	—	—	MK849179	MK849317	MK849048	MK848917	Li *et al.* (2020)
		Rho. jianfalingensis	CGMCC 2.3531	MK050403	—	—	MK849178	MK849316	MK849047	MK848916	Li *et al.* (2020)
		Rho. lusitaniae	JCM 8547^T	AY015430	AF070423	AB073274	KJ708047	—	KJ707812	KJ707737	Wang *et al.* (2015a)
		Rho. microsporus	CBS 7041^T	AF444535	AF070436	KJ708441	KJ708054	KJ708284	KJ707817	KJ707724	Wang *et al.* (2015a)
		Rho. nylandii	JCM 10213^T	AB030323	AF387123	AB030319	KJ708050	KJ708321	KJ707822	KJ707674	Wang *et al.* (2015a)
		Rho. odoratus	JCM 11641^T	KJ778638	AF387125	KJ708427	KJ708045	KJ708322	KJ707819	KJ707694	Wang *et al.* (2015a)
		Rho. platycladi	CGMCC 2.3118^T = CBS 15469	MK050401	—	—	MK849153	MK849293	MK849023	MK848895	Li *et al.* (2020)
		Rho. poonsookiae	JCM 10207^T	AB030327	AF387124	AB030320	KJ708048	KJ708329	KJ707821	KJ707672	Wang *et al.* (2015a)
		Rho. ruineniae	CBS 5811^T	AF444491	AF070434	AB021693	KJ708052	KJ708286	KJ707820	KJ707700	Wang *et al.* (2015a)
		Rhodotorula alborubescens	JCM 5352^T	AB030342	AF207886	KJ708440	KJ708089	KJ708289	KJ707864	KJ707714	Wang *et al.* (2015a)
		Rh. araucariae	CBS 6031^T	AF444510	AF070427	KJ708435	KJ708096	KJ708209	KJ707862	AB041048	Wang *et al.* (2015a)
		Rh. babjevae	CBS 7808^T	AF444542	AF070420	AB073270	—	—	KJ707874	KJ707746	Wang *et al.* (2015a)
		Rh. dairenensis	CBS 4406^T	AF444501	AY033552	KJ708411	—	KJ708276	KJ707866	KJ707625	Wang *et al.* (2015a)
		Rh. diobovata	CBS 6085^T	AF444502	AF070421	AB073271	KJ708091	KJ708277	KJ707865	KJ707708	Wang *et al.* (2015a)
		Rh. evergladiensis	CBS 10880^T	FJ008054	FJ008048	KJ708398	—	KJ708228	KJ707834	—	Wang *et al.* (2015a)
		Rh. glutinis	CBS 20^T	AF444539	AF070429	X69853	—	—	KJ707869	AB040626	Wang *et al.* (2015a)
		Rh. graminis	CBS 2826^T	AF444505	AF070431	X83827	KJ708093	KJ708234	KJ707868	AB040628	Wang *et al.* (2015a)
		Rh. kratochvilovae	CBS 7436^T	AF444520	AF071436	AB073273	KJ708095	KJ708205	KJ707863	KJ707733	Wang *et al.* (2015a)
		Rh. mucilaginosa	CBS 316^T	AF444541	AF070432	AB021668	—	KJ708247	KJ707861	KJ707731	Wang *et al.* (2015a)

Table 3. (Continued).

Order	Family	Species	Strain or specimen[1]	GenBank accession numbers[2]							Reference
				ITS	LSU	SSU	*RPB1*	*RPB2*	*TEF1-α*	*CYT-B*	
Sporidiobolales	*Sporidiobolaceae*	*Rh. pacifica*	CBS 10070^{T}	AB026006	AB026006	KJ708397	KJ708087	KJ708252	KJ707860	KJ707595	Wang *et al.* (2015a)
		Rh. paludigena	CBS 6566^{T}	AF444492	AF070424	KJ708422	KJ708094	KJ708206	KJ707870	KJ707676	Wang *et al.* (2015a)
		Rh. sinensis	AS 2.1389 (CGMCC)	KJ778637	KP216510	KJ708403	KJ708072	KJ708265	KJ707846	KJ707561	Wang *et al.* (2015a)
		Rh. sphaerocarpa	CBS 5969^{T}	AF444499	AF070425	AB073275	KJ708086	KJ708207	KJ707867	KJ707734	Wang *et al.* (2015a)
		Rh. taiwanensis	CBS 11729^{T}	GU646862	GU646863	KJ708409	KJ708066	KJ708271	KJ707838	KJ707611	Wang *et al.* (2015a)
		Rh. toruloides	CBS 349	AF444489	AF070426	X60180	KJ708090	KJ708278	—	KJ707623	Wang *et al.* (2015a)
		Sporobolomyces bannaensis	AS 2.2285^{T} (CGMCC)	AY274824	AY274823	KJ708405	KJ708120	KJ708290	KJ707934	KJ707581	Wang *et al.* (2015a)
		Sp. beijingensis	AS 2.2365^{T} (CGMCC)	AY364837	AY364837	KJ708407	KJ708116	KJ708291	KJ707919	KJ707588	Wang *et al.* (2015a)
		Sp. blumeae	JCM 10212^{T}	AB030331	AY213010	AB030321	—	KJ708293	KJ707926	KJ707673	Wang *et al.* (2015a)
		Sp. carnicolor	CBS 4215^{T}	AY069991	AY070008	KJ708434	KJ708117	KJ708294	KJ707912	KJ707707	Wang *et al.* (2015a)
		Sp. cellobiolyticus	CGMCC 2.5675^{T} = CBS 13964	MK050406	—	—	MK849246	MK849383	MK849110	MK848982	Li *et al.* (2020)
		Sp. cellobiolyticus	CGMCC 2.5687 = CBS 13963	MK050407	—	—	MK849249	MK849386	MK849113	MK848985	Li *et al.* (2020)
		Sp. cellobiolyticus	MCA 3774	JN942193	—	JN940715	—	—	—	—	Li *et al.* (2020)
		Sp. cellobiolyticus	MCA 3785	JN942199	—	JN940720	—	—	—	—	Li *et al.* (2020)
		Sp. ellipsoideus	CGMCC 2.5619^{T} = CBS 15590	MK050409	—	—	MK849225	MK849364	MK849088	MK848957	Li *et al.* (2020)
		Sp. ellipsoideus	CGMCC 2.5620	MK050410	—	—	—	—	—	—	Li *et al.* (2020)
		Sp. ellipsoideus	CGMCC 2.5621	MK050411	—	—	MK849227	—	MK849090	MK848959	Li *et al.* (2020)
		Sp. ellipsoideus	CGMCC 2.5622	MK050412	—	—	MK849228	MK849366	MK849091	MK848960	Li *et al.* (2020)
		Sp. ellipsoideus	CGMCC 2.5624	MK050413	—	—	—	—	MK849093	MK848962	Li *et al.* (2020)
		Sp. ellipsoideus	CGMCC 2.5625	MK050414	—	—	MK849229	MK849368	MK849094	MK848963	Li *et al.* (2020)
		Sp. ellipsoideus	CGMCC 2.5626	MK050415	—	—	—	MK849369	MK849095	MK848964	Li *et al.* (2020)
		Sp. ellipsoideus	CGMCC 2.5631	MK050416	—	—	MK849233	—	MK849099	MK848969	Li *et al.* (2020)
		Sp. holsaticus	CBS 1522	AF444509	AF189975	AB021672	KJ708106	—	KJ707916	KJ707614	Wang *et al.* (2015a)
		Sp. japonicus	CBS 5744^{T}	AY069992	AY158640	—	KJ708123	KJ708307	KJ707932	KJ707578	Wang *et al.* (2015a)
		Sp. jilinensis	AS 2.2301^{T} (CGMCC)	AY364838	AY364838	KJ708450	KJ708111	KJ708308	KJ707913	KJ707583	Wang *et al.* (2015a)
		Sp. johnsonii	CBS 5470^{T}	AY015431	AF070435	L22261	KJ708105	—	KJ707914	KJ707564	Wang *et al.* (2015a)
		Sp. koalae	CBS 10914^{T}	EU276008	EU276011	KP216519	KJ708063	KJ708311	KJ707850	KJ707604	Wang *et al.* (2015a)
		Sp. longiusculus	CBS 9655^{T}	JN246566	KJ708464	KJ708400	KJ708109	KJ708282	KJ707929	KJ707668	Wang *et al.* (2015a)
		Sp. marcillae	CBS 4217^{T}	AY015437	AF070440	KJ708442	KJ708112	KJ708318	KJ707933	KJ707725	Wang *et al.* (2015a)
		Sp. metaroseus	CBS 7683^{T}	EU003482	EU003461	KJ708415	KJ708068	KJ708283	KJ707841	KJ707644	Wang *et al.* (2015a)
		Sp. pararoseus	JCM 5350^{T}	AF417115	AF070437	AB021694	KJ708115	KJ708279	KJ707924	KJ707713	Wang *et al.* (2015a)

Table 3. (Continued).

Order	Family	Species	Strain or specimen[1]	GenBank accession numbers[2]							Reference
				ITS	LSU	SSU	*RPB1*	*RPB2*	*TEF1-α*	*CYT-B*	
Sporidiobolales	*Sporidiobolaceae*	*Sp. patagonicus*	CRUB 1043	AY552329	AY158656	KP216518	KJ708108	KJ708326	KJ707930	KJ707669	Wang *et al.* (2015a)
		Sp. patagonicus	CRUB 1038^{T}	AY552328	AY158655	KJ708421	KJ708110	KJ708325	KJ707928	KP216520	Wang *et al.* (2015a)
		Sp. phaffii	AS 2.2137^{T} (CGMCC)	AY069995	AY070011	KJ708404	KJ708113	KJ708327	KJ707918	KJ707577	Wang *et al.* (2015a)
		Sp. primogenomicus	JCM 8242^{T} = CBS 15935	MK050417	MK050419	MK050418	MK849124	MK849266	MK848998	MK848872	Li *et al.* (2020)
		Sp. reniformis	CGMCC 2.5627^{T} = CBS 15562	MK050408	—	—	MK849230	MK849370	MK849096	MK848965	Li *et al.* (2020)
		Sp. roseus	CBS 486^{T}	AY015438	AF070441	X60181	KJ708119	KJ708331	KJ707917	KJ707569	Wang *et al.* (2015a)
		Sp. ruberrimus	CBS 7500^{T}	AY015439	AF070442	KJ708402	KJ708121	KJ708332	KJ707915	KJ707643	Wang *et al.* (2015a)
		Sp. salmoneus	CBS 488^{T}	AY070005	AY070017	KJ708401	KJ708107	KJ708334	KJ707920	KJ707580	Wang *et al.* (2015a)
		Sp. salmonicolor	CBS 490^{T}	AY015434	AF070439	AB021697	KJ708114	KJ708287	KJ707923	KJ707701	Wang *et al.* (2015a)
Incertae sedis	*Camptobasidiaceae*	*Camptobasidium arcticum*	EXF 12713	MN983248	MK454798	MT304813	—	MT260386	MT260390	MT260394	Perini *et al.* (2021)
		Ca. gelus	CBS 8941^{T}	AY040665	AY040647	—	—	—	—	—	Garcia *et al.* (2020)
		Ca. hydrophilum	TUB F418	—	AY512837	DQ198783	—	—	—	—	Bauer *et al.* (2006)
		Ca. hydrophilum	CCM 8060^{T}	MN626358	AY212991	—	—	—	—	—	Bauer *et al.* (2006)
		Cryolevonia giraudoae	CRUB 2086^{T}	MN622687	MN626546	—	—	—	—	—	Garcia *et al.* (2020)
		Cr. schafbergensis	PYCC 8347	MN058074	MN058075	—	—	—	—	—	Pontes *et al.* (2020)
		Glaciozyma antarctica	CBS 5942^{T}	AF444529	AF189906	DQ785788	KJ708131	KJ708182	—	KJ707745	Wang *et al.* (2015a)
		Gl. litoralis	**CBS 12957^{T}**	HF934009	HF934009	**OP883915**	**OR105876**	**OR105884**	**OR105890**	—	Kachalkin *et al.* (2014); This publication
		Psychromyces glacialis	EXF 13111	MK671633	MT301949	MT248408	—	MW036268	MT260389	MT260392	Perini *et al.* 2021
	Chrysozymaceae	*Bannozyma arctica*	CBS 9278^{T}	AB478857	AB478858	KJ708371	KJ708070	KJ708210	KJ707856	KJ707666	Wang *et al.* (2015a)
		Ba.yamatoana	CBS 7243^{T}	AF444634	AF189896	D38239	KJ708141	KJ708160	KJ707948	KJ707572	Wang *et al.* (2015a)
		Chrysozyma cylindrica	CGMCC 2.3455^{T} = CBS 15482	MK050439	—	—	MK849168	MK849306	MK849036	MK848906	Li *et al.* (2020)
		Chr. flava	CGMCC 2.5611^{T}= CBS 15552	MK050440	—	—	MK849221	MK849360	MK849086	MK848955	Li *et al.* (2020)
		Chr. fushanensis	JCM 12422^{T}	KP216522	AB176591	AB176530	KJ708142	KJ708303	KJ707944	KJ707698	Wang *et al.* (2015a)
		Chr. fusiformis	CGMCC 2.2765^{T} = CBS 15458	MK050437	—	—	MK849140	MK849281	MK849010	MK848883	Li *et al.* (2020)
		Chr. fusiformis	CGMCC 2.2764	MK050438	—	—	—	—	—	—	Li *et al.* (2020)
		Chr. griseoflava	CBS 7284^{T}	AF444557	AF189986	D66884	KJ708143	KJ708305	KJ707950	KJ707717	Wang *et al.* (2015a)
		Chr. iridis	CGMCC 2.2769^{T} = CBS 15461	MK050434	—	—	MK849144	MK849285	MK849013	MK848886	Li *et al.* (2020)

Table 3. (Continued).

Order	Family	Species	Strain or specimen[1]	GenBank accession numbers[2]							Reference
				ITS	LSU	SSU	*RPB1*	*RPB2*	*TEF1-α*	*CYT-B*	
Incertae sedis	*Chrysozymaceae*	*Chr. pseudogriseoflava*	CGMCC 2.5629^{T} = CBS 15564	MK050428	—	—	MK849232	MK849372	MK849098	MK848967	Li *et al.* (2020)
		Chr. pseudogriseoflava	CGMCC 2.5646	MK050430	—	—	MK849234	MK849373	—	—	Li *et al.* (2020)
		Chr. pseudogriseoflava	GPS20.6D2 (CGMCC)	MK050429	—	—	—	—	—	—	Li *et al.* (2020)
		Chr. rhododendri	CGMCC 2.5821^{T} = CBS 15583	MK050433	—	—	MK849263	MK849400	MK849121	MK848995	Li *et al.* (2020)
		Chr. sambuci	CGMCC 2.2618^{T} = CBS 15450	MK050431	—	—	MK849133	MK849273	MK849004	—	Li *et al.* (2020)
		Chr. sambuci	CGMCC 2.2755	MK050432	—	—	MK849137	MK849277	—	—	Li *et al.* (2020)
		Chr. sorbariae	CGMCC 2.2768^{T} = CBS 15460	MK050435	—	—	MK849143	MK849284	MK849012	MK848885	Li *et al.* (2020)
		Chr. sorbariae	CGMCC 2.2767	MK050436	—	—	MK849142	MK849283	—	MK848884	Li *et al.* (2020)
		Hamamotoa lignophila	CBS 7109^{T}	AF444513	AF189943	KJ708372	KJ708139	KJ708241	KJ707953	KJ707637	Wang *et al.* (2015a)
		Ha. singularis	CBS 5109^{T}	AF444600	AF189996	AB021690	KJ708140	KJ708336	KJ707957	KJ707716	Wang *et al.* (2015a)
		Fellozyma cerberi comb. nov.	**CBS 11585^{T}**	—	FN428972	**OP884087**	**OR105878**	**OQ676585**	**OQ676581**	—	Yurkov *et al.* (2016); This publication
		Fe. Inositophila	CBS 7310^{T}	AF444559	AF189987	AB021673	KJ708136	KJ708306	KJ707951	KJ707718	Wang *et al.* (2015a)
		Fe. telluris comb. nov.	**CBS 11713^{T}**	—	FN428971	**OP884088**	**OR105879**	**OR105886**	**OQ676582**	—	Yurkov *et al.* (2016); This publication
		Yurkovia longicylindrica	CGMCC 2.5603^{T} = CBS 15550	MK050441	—	—	MK849218	MK849357	MK849084	MK848952	Li *et al.* (2020)
		Yu. mendeliana	**PYCC 6884^{T}**	KU187884	KU187888	**OP883946**	**OR105877**	**OR105885**	**OQ676579**	—	Mašínová *et al.* (2017); This publication
		Yu.nerthusi	CBS 11560^{T}	—	FN428970	—	—	—	—	—	Kachalkin *et al.* (2019)
		—	**KBP Y-6773**	MZ666406	MZ666406	—	**OR105883**	—	**OR105892**	—	This publication
	Colacogloeaceae	*Colacogloea aletridis*	CGMCC 2.2766^{T} = CBS 15459	MK050450	—	—	MK849141	MK849282	MK849011	—	Li *et al.* (2020)
		Co. armeniacae	CGMCC 2.6134^{T}	MT252007	MT252007	MT252007	—	MT268686	MT268691	MT268700	Wang *et al.* (2021)
		Co. bettinae sp. nov.	**NS 19-391 = DSM 112418^{T}**	**OQ870173**	**OQ875008**	**OQ878235**	—	—	**OQ930214**	**OR053644**	This publication
		Co. bettinae sp. nov.	**MG 407^{PT} (DSM)**	**OQ870174**	**OQ875009**	**OQ878236**	—	—	**OQ930215**	**OR053645**	This publication
		Co. biconidiata sp. nov.	**VS 12415 = DSM 112405^{T}**	**OQ870175**	**OQ875010**	**OQ878223**	**OQ930163**	**OQ930183**	**OQ930201**	**OR053636**	This publication
		Co. cycloclastica	CBS 8448^{T}	AF444732	AF444631	KJ708376	KJ707997	KJ708224	KJ707775	KJ707652	Wang *et al.* (2015a)
		Co. demeterae	**CBS 12500^{T} (DSM)**	—	FN428967	**OP884091**	**OR105882**	**OR105888**	**OR105891**	—	Yurkov *et al.* (2016); This publication

Table 3. (Continued).

Order	Family	Species	Strain or specimen[1]	GenBank accession numbers[2]							Reference
				ITS	LSU	SSU	*RPB1*	*RPB2*	*TEF1-α*	*CYT-B*	
Incertae sedis	*Colacogloeaceae*	*Co. diffluens*	CBS 5233^{T}	AF444533	AF075485	KJ708380	KJ708125	KJ708226	KJ707939	AB040621	Wang *et al.* (2015a)
		Co. effusa	CBS 684.93	DQ202270	AY629313	—	DQ234569	DQ234550	DQ234566	—	Wang *et al.* (2015a)
		Co. effusa	**ENZ 19-092 (DSM)**	**OQ870176**	**OQ875011**	**OQ878227**	**OQ930167**	**OQ930187**	**OQ930205**	**OR053638**	This publication
		Co. effusa	**ENZ 20-042 (DSM)**	**OQ870177**	**OQ875012**	**OQ878229**	**OQ930169**	**OQ930189**	**OQ930207**	**OR053640**	This publication
		Co. effusa	**ENZ 21-093 (DSM)**	**OQ870178**	**OQ875013**	—	—	**OQ930180**	**OQ930220**	—	This publication
		Co. effusa	**ENZ 20-051 (DSM)**	**OQ870179**	**OQ875014**	**OQ878230**	**OQ930170**	**OQ930190**	**OQ930208**	**OR053641**	This publication
		Co. effusa	**NS 19-279 (DSM)**	**OQ870180**	**OQ875015**	**OQ878224**	**OQ930164**	**OQ930184**	**OQ930202**	**OR053637**	This publication
		Co. effusa	**NS 21-138 (DSM)**	**OQ870181**	**OQ875016**	**OQ878221**	—	**OQ930179**	**OQ930218**	—	This publication
		Co. effusa	**NS 21-101 (DSM)**	**OQ870182**	—	—	—	**OQ930181**	**OQ930221**	—	This publication
		Co. effusa	**NS 21-110 (DSM)**	**OQ870183**		—	—	**OQ930182**	**OQ930222**	—	This publication
		Co. effusa	**NS 21-146 = DSM 113583^{ET}**	**OQ870184**	**OQ875017**	**OQ878222**	—	—	**OQ930219**	—	This publication
		Co. effusa	**ID 7323 (DSM)**	**OQ870185**	**OQ875018**	**OQ878234**	**OQ930173**	**OQ930194**	**OQ930212**	**OR053643**	This publication
		Co. effusa	**ID 6343 (DSM)**	MW303962	MW310243	**OQ878226**	**OQ930166**	**OQ930186**	**OQ930204**	—	Malysheva *et al.* (2021); This publication
		Co. effusa	**ID 6351 (DSM)**	**OQ870186**	**OQ875019**	**OQ878225**	**OQ930165**	**OQ930185**	**OQ930203**	—	This publication
		Co. effusa	**ID 7117 (DSM)**	**OQ870187**	**OQ875020**	**OQ878228**	**OQ930168**	**OQ930188**	**OQ930206**	**OR053639**	This publication
		Co. effusa	**JHC 2009 500290** (specimen)	**OQ870188**	**OQ875021**	—	—	—	—	—	This publication
		Co. effusa	**MG 445 (DSM)**	**OQ870189**	**OQ875022**	**OQ878233**	—	**OQ930193**	**OQ930211**	**OR053642**	This publication
		Co. effusa	**ID 7149 (DSM)**	**OQ935347**	**OQ927087**	**OQ878232**	**OQ930172**	**OQ930192**	**OQ930210**	—	This publication
		Co. effusa	JN 4226 (specimen)	MW293722	MW293726	—	—	—	MW298152	—	Malysheva *et al.* (2021)
		Co. effusa	JHC 09-304^{NT} (specimen)	MW293723	MW293727	—	—	—	—	—	Malysheva *et al.* (2021)
		Co. eucalyptica	CBS 8499^{T}	EU075185	EU075183	KJ708377	KJ708061	KJ708227	KJ707839	KJ707655	Wang *et al.* (2015a)
		Co. falcata	CBS 7368^{T}	AF444543	AF075490	AB021670	KJ708124	KJ708301	KJ707943	KJ707723	Wang *et al.* (2015a)
		Co. fennica sp. nov.	**PV 1931^{PT} (DSM)**	**OQ870190**	**OQ875023**	**OQ878220**	—	**OQ930178**	**OQ930217**	—	This publication
		Co. fennica sp. nov.	**OM 24483 = DSM 112417^{T}**	**OQ870191**	**OQ875024**	—	—	**OQ930195**	**OQ930213**	—	This publication
		Co. foliorum	CBS 5234^{T}	AF444633	AF317804	KJ708378	KJ708126	KJ708230	KJ707941	AB040622	Wang *et al.* (2015a)
		Co. hydrangeae	CGMCC 2.2798^{T} = CBS 15463	MK050451	—	—	MK849147	—	MK849017	—	Li *et al.* (2020)
		Co. microspora sp. nov.	**NS 20-141 = DSM 112413^{T}**	**OQ870193**	**OQ875026**	**OQ878231**	**OQ930171**	**OQ930191**	**OQ930209**	—	This publication
		Co. papilionacea	RoKi 618	—	EF450545	—	—	—	—	—	Kirschner & Oberwinkler (2000)
		Co. philyla	**MG 438**	**OQ870192**	**OQ875025**	**OQ878237**	**OQ930174**	**OQ930196**	**OQ930216**	—	This publication
		Co. philyla	CBS 6272^{T}	AF444506	AF075471	KJ708438	KJ707995	KJ708254	KJ707772	KJ707631	Wang *et al.* (2015a)
		Co. retinophila	CBS 8446^{T}	AF444624	AF444730	KJ708373	KJ707994	KJ708262	KJ707771	KJ707651	Wang *et al.* (2015a)

Table 3. (Continued).

Order	Family	Species	Strain or specimen[1]	GenBank accession numbers[2]							Reference
				ITS	LSU	SSU	*RPB1*	*RPB2*	*TEF1-α*	*CYT-B*	
Incertae sedis	*Colacogloeaceae*	*Co. rhododendri*	CGMCC 2.2770^{T} = CBS 15652	MK050452	—	—	MK849145	MK849286	MK849014	MK848887	Li *et al.* (2020)
		Co. rhododendri	CGMCC 2.5651	MK050457	—	—	MK849238	—	MK849102	MK848973	Li *et al.* (2020)
		Co. terpenoidalis	CBS 8445^{T}	AF444623	AF444729	KJ708374	KJ707999	KJ708272	KJ707774	KJ707650	Wang *et al.* (2015a)
		Co. universitatis-gandavensis sp. nov.	**NS 20-022^{PT}** (specimen)	—	**OQ875007**	—	—	—	—	—	This publication
		Udeniozyma ferulica	CBS 7402	AF444528	AF363653	KJ708379	KJ708129	KJ708229	KJ707940	—	Wang *et al.* (2015a)
	Mycogloiocolacaceae	***Mycogloiocolax gerardii sp. nov.***	**TR 04096 = DSM 112426^{T}**	**OQ870201**	**OQ875033**	**OQ878243**	—	—	**OQ930228**	**OR053648**	This publication
		—	**KBP Y-6479**	MN128419	MN128419	—	—	**OU562599**	**OU466850**	—	This publication
	—	*Oberwinklerozyma dicranopteridis*	CGMCC 2.3441^{T} = CBS 15476	MK050426	—	—	MK849162	MK849300	—	MK848901	Li *et al.* (2020)
	—	*Ob. nepetae*	CGMCC 2.5824^{T} = CBS 15579	MK050427	—	—	MK849254	MK849391	—	MK848992	Li *et al.* (2020)
	—	*Ob. silvestris*	CBS 11420^{T}	GQ121045	GQ121044	KJ708366	KJ708069	KJ708264	KJ707849	KJ707610	Wang *et al.* (2015a)
	—	*Ob. straminea*	CBS 10976^{T}	EU872491	EU872489	KJ708367	KJ708065	KJ708269	KJ707844	KJ707606	Wang *et al.* (2015a)
	—	*Ob. yarrowii*	CBS 7417^{T}	AF444628	AF189971	AB032658	—	KJ708275	KJ707938	KJ707735	Wang *et al.* (2015a)
	—	*Pseudohyphozyma bogoriensis*	CBS 4101^{T}	AF444536	AF189923	KJ708363	KJ708130	KJ708216	KJ707949	AB040619	Wang *et al.* (2015a)
	—	*Pse. buffonii*	CBS 2838	AF444526	AF189924	KJ708362	KJ708127	KJ708217	KJ707946	AB040620	Wang *et al.* (2015a)
	—	*Pse. hydrangeae*	CGMCC 2.2796^{T} = CBS 15462	MK050443	—	—	MK849126	MK849287	MK849015	MK848888	Li *et al.* (2020)
	—	*Pse. hydrangeae*	CGMCC 2.27975	MK050444	—	—	MK849146	MK849288	MK849016	—	Li *et al.* (2020)
	—	*Pse. hydrangeae*	CGMCC 2.5607	MK050445	—	—	MK849219	MK849358	—	MK848953	Li *et al.* (2020)
	—	*Pse. hydrangeae*	CGMCC 2.5618	MK050446	—	—	MK849224	MK849363	—	—	Li *et al.* (2020)
	—	*Pse. hydrangeae*	CGMCC 2.5623	MK050447	—	—	—	MK849367	MK849092	MK848961	Li *et al.* (2020)
	—	*Pse. lulangensis*	CGMCC 2.2612^{T} = CBS 15446	MK050442	—	—	MK849129	MK849270	—	MK848875	Li *et al.* (2020)
	—	*Pse. pustula*	CBS 6527^{T}	AF444531	AF189964	KJ708361	KJ708128	KJ708261	KJ707937	AB040642	Wang *et al.* (2015a)
	—	*Reniforma strues*	CBS 8263^{T}	AF444573	AF189912	KP216517	KJ708122	KJ708200	KJ707927	KJ707648	Wang *et al.* (2015a)
	—	*Spencerozyma crocea*	CBS 2029^{T}	FM957565	AY372179	KJ708410	KJ708007	KJ708223	KP216513	KJ707618	Wang *et al.* (2015a)
	—	*Trigonosporomyces hylophilus*	CBS 6226^{T}	AF444622	AF363645	KJ708431	KJ708008	KJ708236	KJ707764	AB040630	Wang *et al.* (2015a)
	—	*Vonarxula javanica*	CBS 5236^{T}	AF444532	AF189935	KJ708446	KJ708006	KJ708238	KJ707766	AB040632	Wang *et al.* (2015a)
	—	*Yunzhangia auriculariae*	CBS 6379^{T}	AF444507	AF189922	KJ708429	KJ708134	KJ708213	KJ707935	AB040617	Wang *et al.* (2015a)
	—	*Yun. sonckii*	CBS 6713^{T}	AF444601	AF189969	KJ708439	KJ708118	KJ708267	KJ707911	AB040643	Wang *et al.* (2015a)
	—	—	**KBP Y-4635**	**MK265707**	MK265707	—	—	**OW409723**	—	—	Kachalkin *et al.* (2019); This publication

Table 3. (Continued).

Order	Family	Species	Strain or specimen[1]	GenBank accession numbers[2]							Reference
				ITS	LSU	SSU	*RPB1*	*RPB2*	*TEF1-α*	*CYT-B*	
Incertae sedis	—	—	**KBP Y-4912**	**MK265706**	MK265706	—	—	**OW409724**	—	—	Kachalkin *et al.* (2019); This publication
	—	—	**KBP Y-5457**	**MK265708**	MK265708	—	**OW409728**	**OW409729**	**OW409727**	—	Kachalkin *et al.* (2019); This publication
	—	—	**KBP Y-5465**	**MK265710**	MK265710	**ON106836**	**OW409731**	**OW409733**	—	—	Kachalkin *et al.* (2019); This publication
	—	—	**KBP Y-5569**	**MK265711**	MK265711	**ON106837**	**OW409730**	**OW409732**	**OW409734**	—	Kachalkin *et al.* (2019); This publication
Cystobasidiomycetes	*Erythrobasidiaceae*	*Erythrobasidium elongatus*	AS 2.1949^{T} (CGMCC)	AF444561	AF189983	AB021669	KJ708012	KJ708300	KJ707782	KJ707570	Wang *et al.* (2015a)
		Ery. hasegawianum	AS 2.1923^{T} (CGMCC)	AF444522	AF189899	D12803	KF706506	KF706534	KJ707776	KJ707563	Wang *et al.* (2015a)
Spiculogloeomycetes	*Spiculogloeaceae*	*Phyllozyma dimmenae*	JCM 8762^{T}	AB038046	AB644404	D66881	KJ707991	KJ708297	KJ707907	KJ707739	Wang *et al.* (2015a)
		Phy. novozealandica	JCM 8756^{T}	AB038048	KJ708467	KJ708443	KJ708073	KJ708319	KJ707851	KJ707738	Wang *et al.* (2015a)

[1]Acronyms of culture collections in alphabetic order: **CBS**, Westerdijk Fungal Biodiversity Institute, Utrecht, the Netherlands; **CGMCC**, Chinese General Microbiological Culture Collection Center, Beijing, China; **CRUB**, Culture Collection of Yeasts from Centro Regional Universitario Bariloche, Bariloche, Argentinia; **DSM**, German Collection of Microorganisms and Cell Cultures GmbH, Braunschweig, Germany; **EXF**, Microbial Culture Collection Ex of the Infrastructural Centre Mycosmo, Ljubljana, Slovenia; **JCM**, Japan Collection of Microorganisms, RIKEN BioResource Center, Saitama, Japan; **KBP Y**, Yeast collection of the Lomonosov Moscow State University, Moscow, Russia; **PYCC**, Portuguese Yeast Culture Collection, Caparica, Portugal; **TUB**, Former Fungal Culture Collection of the university of Tübingen, now in laboratory of prof. D. Begerow, Hamburg, Germany. Other acronyms represent personal collections. T = ex-type strain or type specimen, ET = ex-epitype strain or epitype specimen, NT = ex-neotype strain or neotype specimen, PT = ex-paratype strain or paratype specimen.

[2]Genetic loci are abbreviated as follows: partial small subunit (SSU), internal transcribed spacers including the 5.8S locus (ITS), and partial large subunit (LSU) of the nuclear ribosomal DNA, partial largest subunit of RNA polymerase II (*RPB1*), partial second largest subunit of RNA polymerase II (*RPB2*), partial translation elongation factor (*TEF1-α*) and partial mitochondrial cytochrome-b (*CYT-B*).

Table 4. Summary of the seven genetic loci included in the phylogenetic ML analysis, with for every partition the number of incorporated sequences, total number of sites, number of parsimony informative sites, number of invariable sites, and the selected model of nucleotide substitution as selected by ModelFinder.

Partition	Locus	Sequences	Sites	Informative sites	Invariable sites	Model
1	SSU	192	1 848	408	1 108	TIM+F+R8
2	ITS1	226	153	146	3	GTR+F+R5
3	5.8S	226	168	117	45	K2P+R7
4	ITS2	226	207	185	12	TVM+F+R5
5	LSU	229	646	313	277	GTR+F+R10
6	*RPB1*	174	616	447	107	GTR+F+R6
7	*RPB2*	192	866	476	297	SYM+R4
8	*TEF1-α*	196	950	469	347	GTR+F+R10
9	*CYT-B*	163	401	254	85	TVM+F+R5
Concatenated	9 loci	238	5 855	2 815	2 281	—

Table 5. Summary of support values for higher taxa in *Microbotryomycetes* recovered in the seven-locus ML phylogenetic reconstruction.

Taxon	Ultrafast Bootstrap value	Reference
Camptobasidiaceae	100	Moore (1996)
Chrysozymaceae	92	Wang *et al.* (2015b)
Colacogloeaceae	100	Wang *et al.* (2015b)
Curvibasidiales	100	Doweld (2014)
Heitmaniales	100	Li *et al.* (2020)
Heterogastridiales	79	Oberwinkler *et al.* (1990b)
Kriegeriales	100	Toome *et al.* (2013)
Leucosporidiales	100	Sampaio *et al.* (2003)
Microbotryales	84	Bauer *et al.* (1997)
Rosettozymales	100	Li *et al.* (2020)
Sporidiobolales	100	Doweld (2001)

Description of filamentous morph: Intrahymenial, often invisible but sometimes producing a whitish pruinose layer on the host species. Monomitic; hyphae hyaline, thin-walled, smooth, clamped at all septa, 1.1–2.7 µm in diam. Hyphidia absent. Cystidia absent. Probasidia variable in shape, often pyriform, thin walled, collapsing after maturation of the basidium, 8.1–17.8 × 2.3–8.6 µm. Basidia narrowly clavate, often strongly curved, (21.6–)22.2–29.8(–31.4) × (4.5–)4.8–6.4 µm (n=20/1), transversally septate, mature basidia four-celled, often somewhat constricted at each septum, clamped at the base, thin-walled. Sterigmata simple or more rarely bifurcate, up to 18 µm long. Basidiospores of irregular shape, ellipsoid-angular to drop- or comma-shaped, (2.9–)3.0–4.5(–4.8) × 1.5–2.9(–3.0), L = 3.69, W = 2.19, Q' = (1.35–)1.36–2.21(–2.25), Q = 1.72 (n = 30/1), germinating by hyphae, budding or secondary spores. Conidiophores stalked, stalk often somewhat widened, basally clamped, with numerous apical appendages (where conidia are formed), (9.1–)10.5–22.3(–30.6) × (1.4–)2.0–3.9(–4.3) µm. Conidia irregularly shaped, ellipsoid to curved, often with one flattened side, thick-walled (wall up to 1 µm), cyanophilous, (4.0–)4.1–5.7(–5.8) × (2.8–)3.1–3.9(–4.3) µm. Colacosomes scattered, no vesicular gall-like cells observed.

Description of yeast morph: After growth on YM agar plates for 1 mo at 22 °C, the streak culture is white to cream-coloured, glistening, mucoid and smooth. The margin is entire. Cells are subglobose to ovoid, occurring singly or in pairs, and proliferating by polar budding. Good growth on D-glucose, L-sorbose, D-glucosamine, D-arabinose, sucrose (delayed), a,a-trehalose, me a-D-glucoside, cellobiose, raffinose, melezitose, ribitol, D-glucitol, D-mannitol, 5-keto-D-gluconate, D-gluconate, and D-glucuronate. Weak growth on maltose, lactose, glycerol, L-arabinitol, galactitol, ethanol, D-glucarate, and L-tartaric acid. No growth on D-galactose, D-ribose, D-xylose, L-arabinose, L-rhamnose, salicin, melibiose, inulin, starch, erythritol, myo-inositol, D-galacturonate, DL-lactate, succinate, citrate, D-tartaric acid, and L-malic acid. No growth in the presence of 5 %, 8 %, and 10 % NaCl. No growth on MEA with 50 % and 60 % glucose. No starch-like substance is produced. Urea hydrolysis and the Diazonium blue B reaction is positive. Maximum growth temperature: 35 °C.

Habitat and distribution: Growing in the hymenium of *Myxarium podlachicum* (= *M. subhyalinum*), for further synonymy see Spirin *et al.* (2019). This species has been recorded from various European countries: Belgium, Denmark, Germany, France, Norway and The Netherlands.

Materials examined: **Denmark**, Zealand, Enghave Skov ved Dragsholm, on decorticated branch of *Fraxinus*, growing in the hymenium of *Myxarium podlachicum*, 28 Jun. 2009, *J. Heilmann-Clausen*, JHC 09-049 (H, duplicate in GENT). **Belgium**, Prov. Antwerpen, Mechelen, Kauwdaalbos, on fallen log op *Populus*, growing in the hymenium of *Myxarium podlachicum*, 28 Feb. 2020, *G. Van Autgaerden*, GVA 20-056* (GENT). **Netherlands**, Prov. Utrecht, Houten, Nieuw Wulven, on piece of wood of an unidentified deciduous tree, growing in the hymenium of *Myxarium podlachicum*, 8 Mar. 2019, *I. Nannenga-Bruggeman*, ID 3883* (GENT);

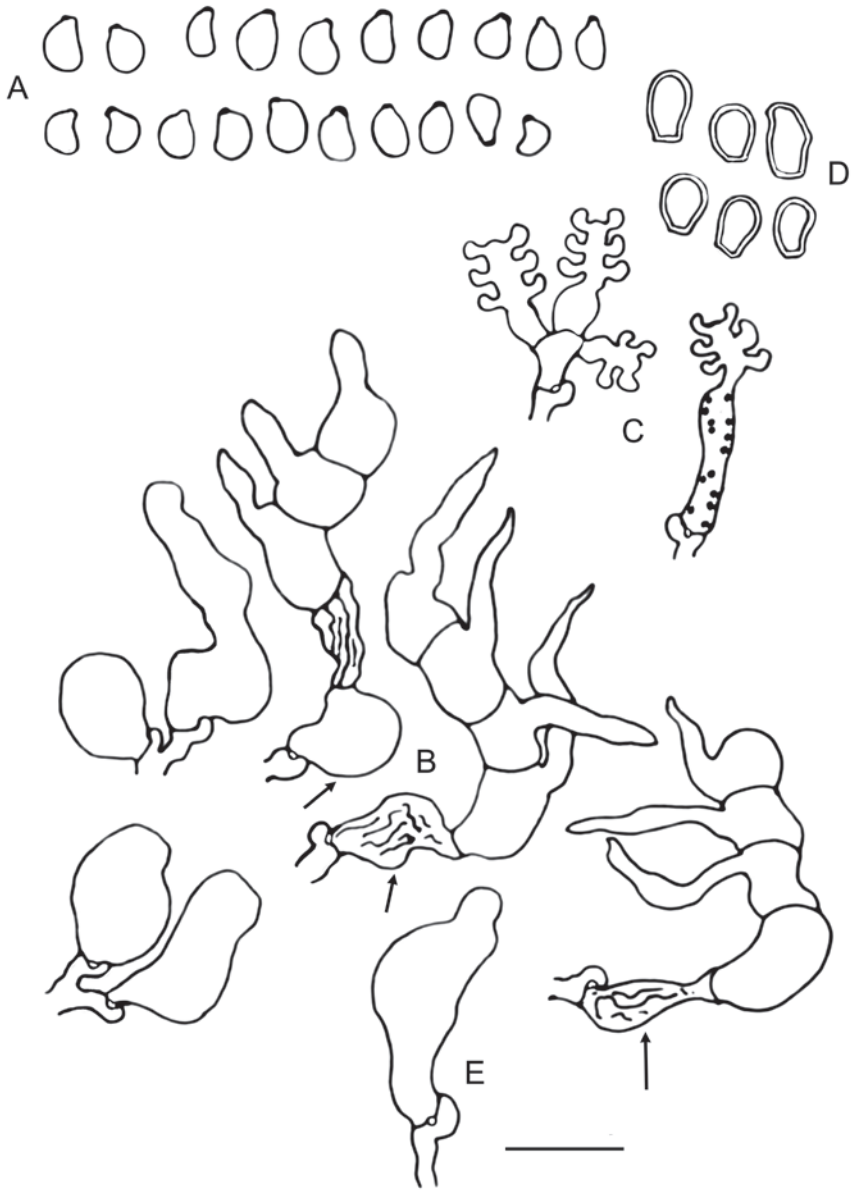

Fig. 4. *Slooffia micra comb. nov.* (KH7222) line drawings. **A.** Basidiospores. **B.** Basidia. **C.** Cluster of conidiophores. **D.** Conidia. **E.** Basidioles, arrows indicate probasidia. Black dots represent colacosomes. Scale bar = 10 µm.

Prov. Utrecht, Zeist-West, De Brink, on piece of wood of an unidentified deciduous tree, growing in the hymenium of *Myxarium podlachicum*, 2 Oct. 2020, *I. Nannenga-Bruggeman*, ID 7081* (GENT); Prov. Gelderland, Ruurlo, Morsdijk, on fallen decorticated branch of *Alnus*, growing in the hymenium of *Myxarium podlachicum*, 27 Jul. 2020, *H. Wassink*, HW 347* (GENT). **Norway**, Hedmark, Stange, Rotlia, rotten stem of *Corylus avellana*, growing on *Myxarium podlachicum*, 26 Sep. 2018, *V. Spirin*, VS 12419* (O, H).

Notes: Colacosomes in this species are formed in mycoparasite hyphae in places where physical contact with other hyphae occurs (mostly host hyphae). Colacosomes can also be found in conidiophores and probasidia. In certain places at the host–parasite interface, hyphae of the mycoparasite coil around hyphae of the host, resulting in rosette-like structures when viewed in epifluorescence microscopy. In these structures, colacosomes are formed abundantly at the contact surface (see Fig. 5F, G). Colacosomes have also been observed attaching to hyphae of the mycoparasite, which may be interpreted as self-parasitism. During fluorescence microscopical investigation of the holotypes of *A. insignis* (1991) and *P. micra* (1915), colacosomes could easily be observed. This may indicate a high durability of these structures.

Microbotryomycetes incertae sedis

Family *Chrysozymaceae* Q.M. Wang *et al.*, Stud. Mycol. 81: 183. 2015.

Fellozyma cerberi (A.M. Yurkov *et al.*) Schoutteten & Yurkov, ***comb. nov.*** MycoBank MB 848664.
Basionym: *Hamamotoa cerberi* A.M. Yurkov *et al.*, Mycol. Prog. 15: 854. 2016.

Fellozyma telluris (A.M. Yurkov *et al.*) Schoutteten & Yurkov, ***comb. nov.*** MycoBank MB 848665.
Basionym: *Hamamotoa telluris* A.M. Yurkov *et al.*, Mycol. Prog. 15: 855. 2016.

Family *Colacogloeaceae* Q.M. Wang *et al.*, Stud. Mycol. 81: 182. 2015.

Colacogloea Oberw. & Bandoni, Canad. J. Bot. 68: 2532. 1991. ***emend.***

Generic description: Genus of dimorphic fungi. Basidiomata pulvinate or absent. Filamentous morphs mostly develop

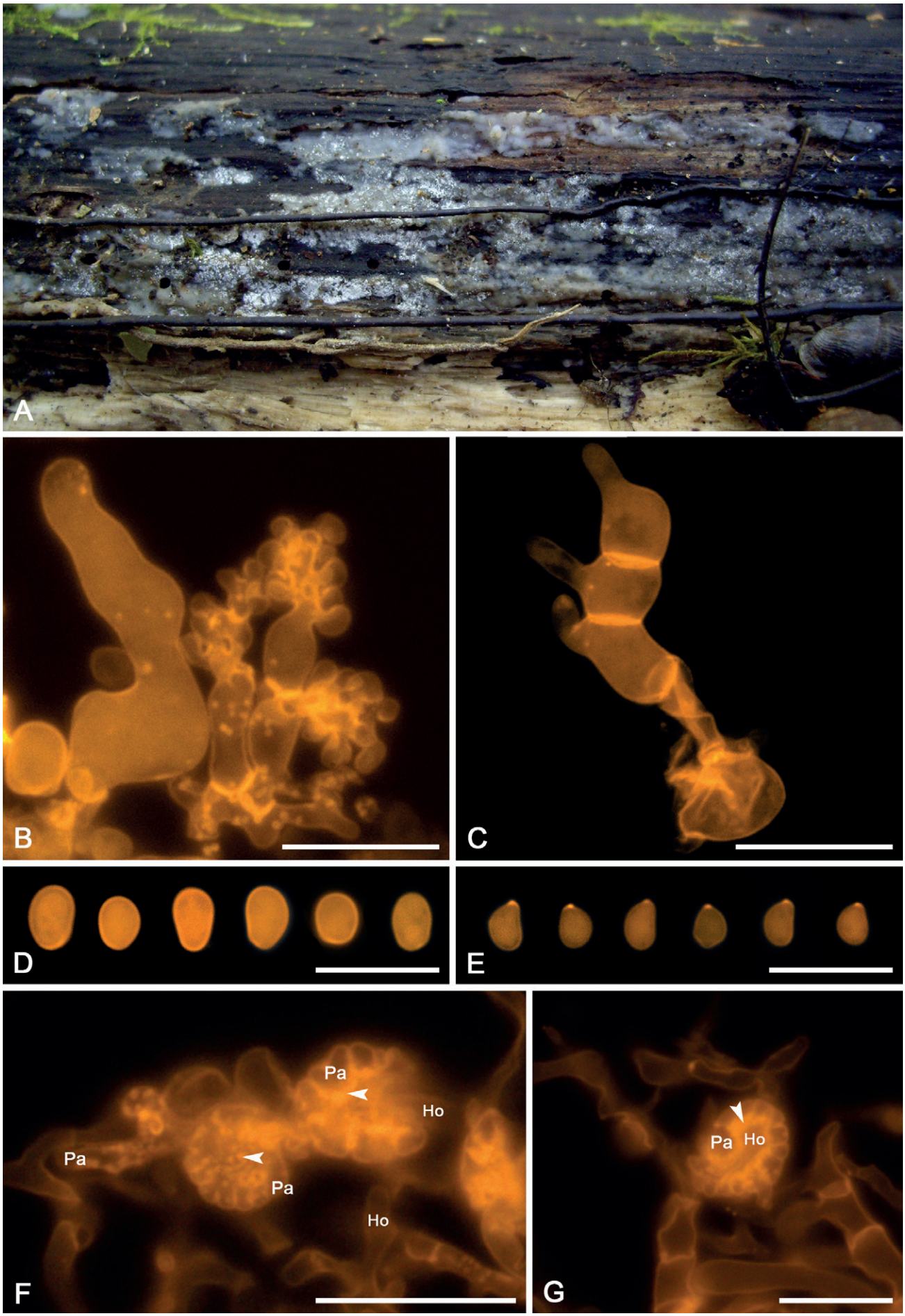

Fig. 5. *Slooffia micra comb. nov.* (KH7222). **A.** Basidiome (VS 12419). **B.** Basidiole (left) and cluster of conidiophores (right), note colacosomes in hyphae and conidiophores. **C.** Three-septate basidium with three sterigmata, the first cell of the basidium and the probasidium are collapsed. **D.** Conidia. **E.** Basidiospores. **F.** Host–parasite interface, Pa = parasite hyphae, Ho = host hyphae, arrowheads indicate some positions of colacosomes. Scale bars = 10 µm.

intrahymenially in the hymenium of their host species, producing a yellow to orange, slimy to arid layer overgrowing the host basidiome. Hyphal system monomytic, hyaline, thin-walled, smooth, clamped at all septa. Hyphidia present in some species. Cystidia absent. Basidia cylindrical to clavate, straight to sinuous to curved in some species, transversally septate, two- to four-celled, clamped at basal cell, thin-walled, without distinct probasidium. Sterigmata originating laterally or apically from basidial cells. Basidiospores ellipsoid to curved, smooth, hyaline, thin-walled, often with a prominent apiculus. Germination of basidiospores either occurs by hyphae, budding or secondary spore production. Conidia present in most species, usually thick-walled and cyanophilous, globose, ellipsoid to ovoid or irregularly shaped, monokaryotic or dikaryotic, zygoconidia present in some species. Yeast colonies are usually cream-coloured, mucoid to butyrous. Yeast cells proliferate by polar budding, no ballistoconidia are formed. Major CoQ system Q-10.

Habitat, substrate, and ecology: Filamentous morphs of *Colacogloea* species which have been observed to engage in mycoparasitic interactions were mainly isolated from the hymenia of corticioid fungi, especially from the genera *Peniophorella* and *Tubulicrinis*. *Colacogloea papilionacea* was isolated from bark beetle galleries of *Pinus sylvestris* and is characterised by a dikaryotic yeast morph. *Colacogloea* species of which currently only the yeast morph has been observed were isolated from marine and terrestrial environments, including soils and phylloplanes. Yeast morphs are presumed to have a saprobic ecology.

Distribution: *Colacogloea* species have been recorded from various countries, including Austria, Belgium, Brazil, Canada, China, Denmark, Finland, France, Germany, India, Italy, Japan, The Netherlands, Norway, Poland, Portugal, Russian Federation, Spain, Sweden, Switzerland, and the Unites States of America (Sampaio *et al.* 2011, Bezerra *et al.* 2013, Buzzini *et al.* 2017, Menolli & Sánchez-García 2020).

Type: *Colacogloea effusa* (J. Schröt.) V. Malysheva *et al*.

Colacogloea bettinae Schoutteten & Begerow, ***sp. nov.*** MycoBank MB 848655. Figs 6, 7.

Etymology: Named after Bettina Greschner-Aschenbrenner, who conducted an extensive study of the *Colacogloea effusa* species complex for her master dissertation (Diplomarbeit) at the former

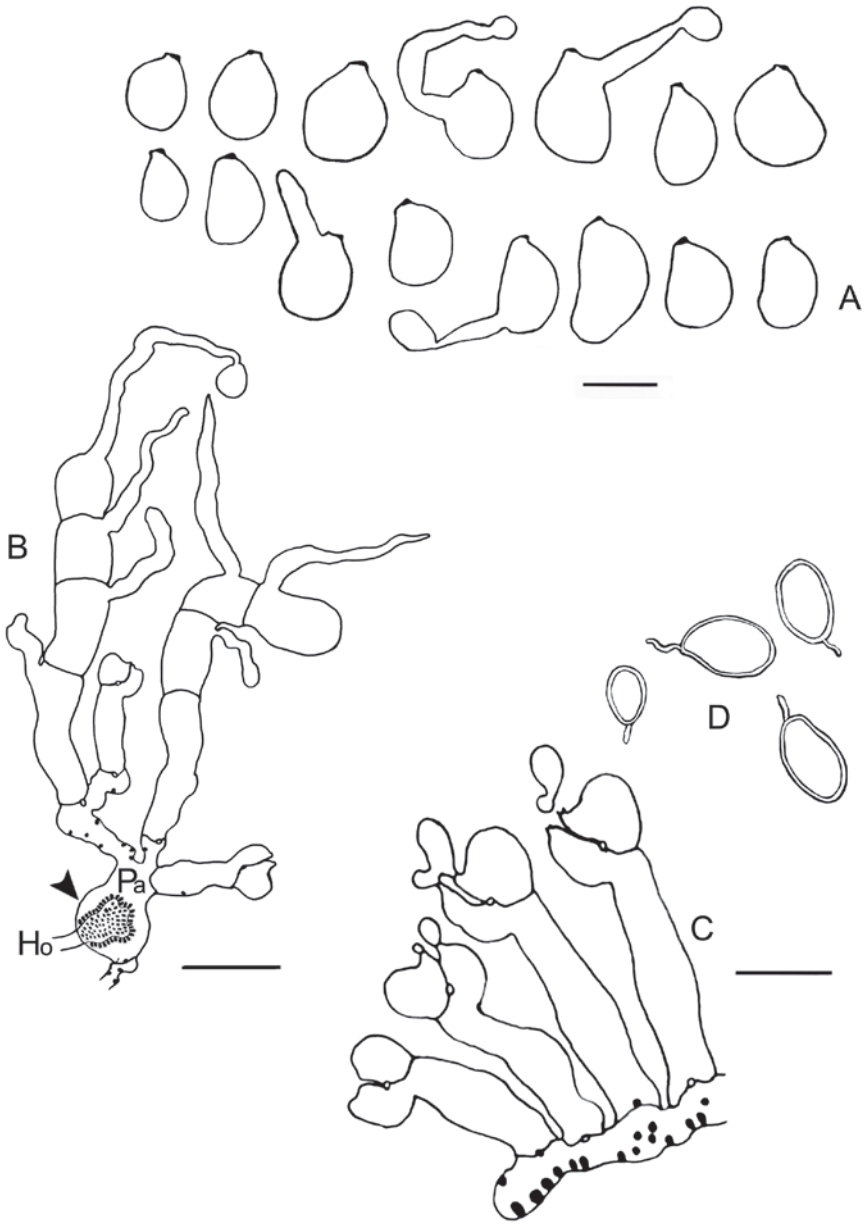

Fig. 6. *Colacogloea bettinae sp. nov.* (NS 19-391) line drawings. **A.** Basidiospores and germinating basidiospores with secondary spores. **B.** Cluster of basidia and conidiophores. **C.** Cluster of conidiophores, showing subsequent stages of conidiogenesis. Each conidiophore consists of two conidiogenous cells. Each cell produces a conidium, of which one grows larger than the other. Subsequently the two daughter conidia fuse, and the cellular content of the smaller conidium is transferred to the larger conidium, after which the zygoconidium is abscised. The cell wall of the smeller conidium remains attached to the larger conidium. **D.** Conidia. **E.** Gall-like cell of the parasite (Pa) enveloping a host hyphae (Ho). Black dots represent colacosomes. Note the different distribution of colacosomes in the gall-like cell and the hyphae. Scale bars = 10 µm.

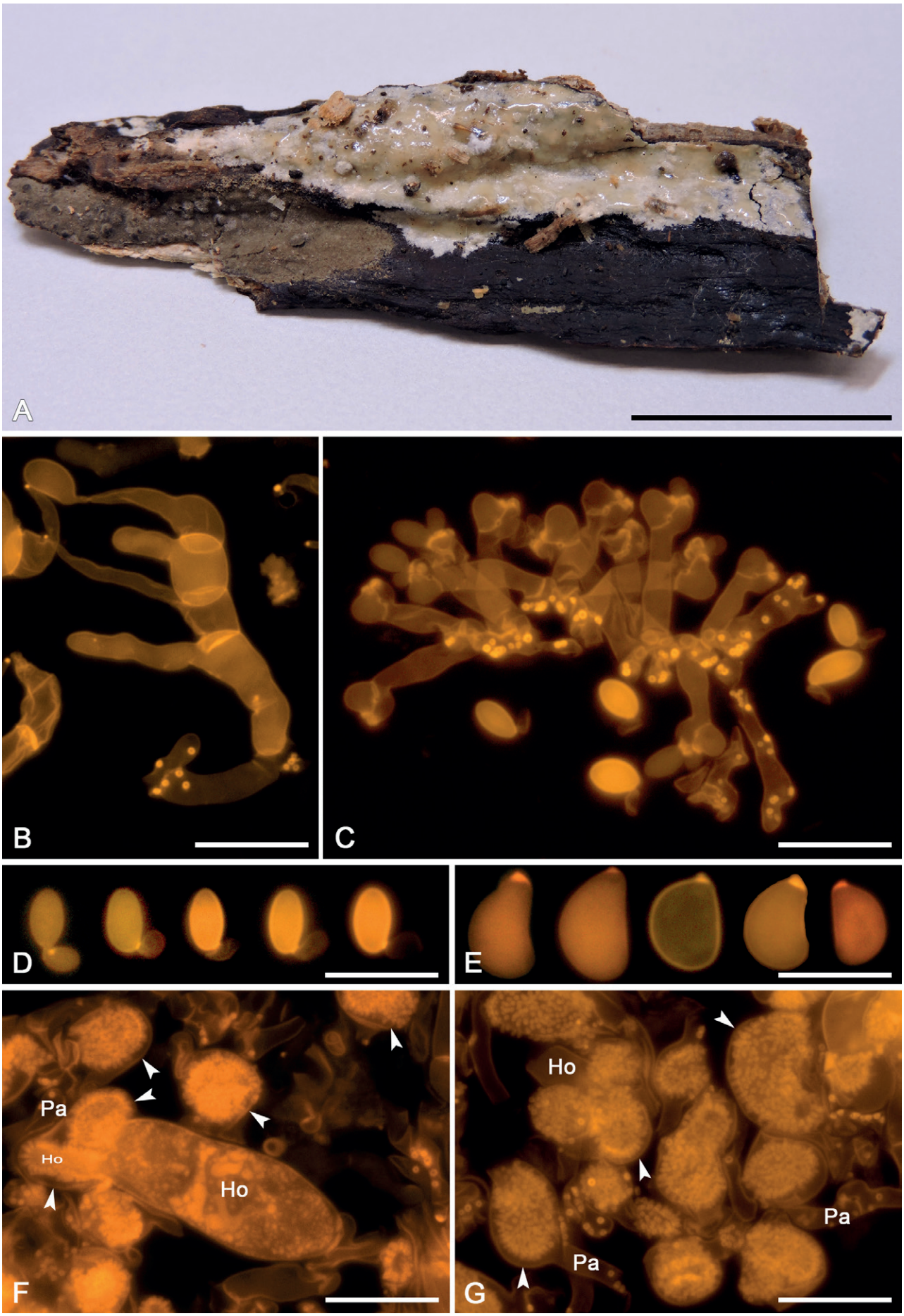

Fig. 7. *Colacogloea bettinae sp. nov.* (NS 19-391). **A.** Basidiome. **B.** Three-septate basidium with four sterigmata, note one attached basidiospore. **C.** Cluster of conidiophores and conidia. **D.** Conidia. **E.** Basidiospores. **F, G.** Host–parasite interface, Pa = parasite cell, Ho = host cell, arrowheads indicate gall-like cells of the parasite enveloping host hyphae, colacosomes are formed along the contact interface within these galls. Scale bars: A = 1 cm; B–G = 10 µm.

Lehrstuhl für Spezielle Botanik und Mykologie (University of Tübingen), supervised by the late dr. Robert Bauer and prof. Franz Oberwinkler.

Typus: **Netherlands**, Prov. Gelderland, Veluwe region, Brummen, Leusveld, on a decorticated branch of an unidentified deciduous tree, growing in the hymenium of *Peniophorella pubera*, 15 Nov. 2019, *N. Schoutteten* (**holotype** GENT NS 19-391*°, culture ex-type DSM 112418).

Description of filamentous morph: Intrahymenial, producing a whitish to yellowish slimy layer on the hymenial surface of the host basidiome. Monomitic; hyphae hyaline, thin-walled, smooth, clamped at all septa, 2.7–4.4 µm in diam. Hyphidia absent. Cystidia absent. Basidia tubular-clavate, sinuous to strongly curved, (25.5–)31–50(–51) × 4.6–7.2(–7.4) µm (n = 20/1), transversally septate, four-celled when mature, clamped at the base, thin-walled, often arranged in clusters of 2–5. Sterigmata up to 46 µm long. Basidiospores ellipsoid, with ventral side often flattened to concave, (6.7–)6.8–8.8(–9.0) × 4–5.9(–6.7) µm, L = 7.60 µm, W = 4.96 µm, Q' = (1.1–)1.2–1.8, Q = 1.54 (n = 60/2), often with prominent apiculus up to 1.8 × 1.2 µm, germinating by hyphae, budding or secondary spore production. Conidiophores comprised of two cells being separated by a septum, each cell apically giving rise to a conidium, basally clamped, often arranged in clusters, intermixed with basidia, 12.5–24.5 × 3–4.8 µm. Mature conidia ellipsoid to ovoid, more rarely subfusiform, sometimes asymmetrical or becoming oblong, rarely with a small lateral outgrowth, always with an appendage (cell wall remnant of the smaller twin-conidium), thick-walled (wall up to 1 µm), cyanophilous, dikaryotic, 6–8.1(–8.3) × (2.9–)3.0–4.6(–4.8) µm (n = 30). Colacosomes arranged both scattered in parasite hyphae and in vesicular gall-like cells produced by this species.

Description of yeast morph: After growth on YM agar plates for 1 mo at 22 °C, the streak culture is white to cream-coloured, glistening, mucoid and smooth. The margin is entire. Cells are subglobose to ovoid, occurring singly or in pairs, and proliferating by polar budding. Good growth on D-glucose, D-glucosamine, D-ribose, D-arabinose, sucrose, me a-D-glucoside, glycerol, ribitol, D-glucitol, D-mannitol, 5-keto-D-gluconate, D-gluconate, and succinate. Weak growth on L-sorbose, D-xylose, L-arabinose, L-rhamnose, lactose, raffinose, galactitol, ethanol, D-glucarate, and L-tartaric acid. No growth on D-galactose, maltose, a,a-trehalose, cellobiose, salicin, melibiose, melezitose, inulin, starch, erythritol, L-arabinitol, myo-inositol, D-glucuronate, D-galacturonate, DL-lactate, citrate, D-tartaric acid, and L-malic acid. Growth in the presence of 5 % and 8 % but not 10 % NaCl. Weak growth on MEA with 50 % and 60 % glucose. No starch-like substance is produced. Urea hydrolysis and the Diazonium blue B reaction is positive. Maximum growth temperature: 35 °C.

Habitat and distribution: This species has up to now only been found in the Netherlands, in mixed forests, always associated with the host species *Peniophorella pubera*.

Materials examined: **The Netherlands**, Drenthe, Gasteren, Gasterensche Holt, on a rotten branch of an unidentified deciduous tree, growing in the hymenium of *Peniophorella pubera*, 5 Sep. 2020, *R. Enzlin*, ENZ 20-043 (GENT); Gelderland, Bronckhorst, Hekenbroek, Hoog Keppel, on a fallen branch of an unidentified tree, growing in the hymenium of *Peniophorella pubera*, 19 Jul. 2020, *M. Gotink*, MG 407* (GENT).

Notes: This is one of the two *Colacogloea* species described in this study which agrees with the morphotype illustrated by Martin (1940) (see also *C. universitatis-gandavensis sp. nov.* and in discussion). Conidiogenesis in this species is of the same type as in *C. universitatis-gandavensis*, where more elaborate observations are provided. The colacosome organisation is similar to the one observed in *C. universitatis-gandavensis*. Colacosomes are mainly arranged in vesicular gall-like cells produced by the mycoparasite. To a lesser extent, colacosomes are also scattered in mycoparasite hyphae. The cell wall of these vesicular gall-like cells invaginates at places where a host hypha makes physical contact. The latter continues to grow into the invagination. As a result, the host hypha is surrounded by the gall-like cell of the mycoparasite. Along the contact surface, colacosomes are formed in the gall-like cell at regular distance from each other.

Colacogloea biconidiata Schoutteten, ***sp. nov.*** MycoBank MB 848656. Figs 8, 9.

Etymology: Referring to two different types of conidia in this species.

Typus: **Norway**, Hedmark, Gitvola, on decorticated branch of *Picea abies*, growing in the hymenium of *Peniophorella praetermissa s.l.*, 26 Sep. 2018, *V. Spirin* (**holotype** O VS12415*°, **isotype** GENT GENTFT00143, culture ex-type DSM 112405).

Description of filamentous morph: Intrahymenial, producing a yellow to orange, gelatinous layer on the host, remaining visible as yellow or orange patches when dried. Monomitic; hyphae hyaline, thin-walled, smooth, clamped at all septa, 1.3–4.5 µm in diam. Hyphidia present, simple, 1–2 µm in diam. Cystidia absent. Basidia tubular-clavate, straight to sinuous or slightly curved, (31.1–)31.8–50.2(–50.6) × 4.1–5.3(–6.9) µm (n = 17/1), transversally septate, four-celled when mature, clamped at the base, thin-walled. Sterigmata up to 54 µm long. Basidiospores ellipsoid to broadly ellipsoid, 6.7–12.2(–12.5) × 4.4–8.8(–10.2) µm, L = 8.06, W = 5.22, Q' = 1.2–1.8(–1.9), Q = 1.49 (n = 67/1), with distinct apiculus up to 2.5 × 2.3 µm, germinating by hyphae, budding or secondary spores. Conidia of two types: (1) irregularly shaped - ellipsoid, subfusiform to oblong or barrel-shaped, sometimes angular, thick-walled (wall up to 1.2 µm), strongly cyanophilous, 6.1–13.2(–15.4) × 3.2–7.1(–7.2) (n = 20/1); (2) predominantly (sub)globose, thick-walled, cyanophilous, (3.1–)3.5–4.5(–4.6) × (2.7–)2.8–3.7(–3.8) (n = 20/1). Colacosomes scattered, no vesicular gall-like cells observed.

Description of yeast morph: After growth on YM agar plates for 1 mo at 22 °C, the streak culture is white to cream-coloured, glistening, mucoid and smooth. The margin is entire. Cells are subglobose to ovoid, occurring singly or in pairs, and proliferating by polar budding. Growth on D-glucose, D-glucosamine, D-ribose, D-arabinose, me a-D-glucoside, glycerol, D-glucitol, D-gluconate, succinate and L-malic acid. Weak growth on maltose (delayed), salicin, inulin, galactitol, and D-tartaric acid. No growth on D-galactose, L-sorbose, D-xylose, L-arabinose, L-rhamnose, sucrose, a,a-trehalose, cellobiose, melibiose, lactose, raffinose, melezitose, starch, erythritol, ribitol, L-arabinitol, D-mannitol, myo-inositol, 5-keto-D-gluconate, D-glucuronate, D-galacturonate, DL-lactate, citrate, ethanol, D-glucarate, and L-tartaric acid. Growth in the presence of 5 % but not 8 % and 10 % NaCl. Weak growth on MEA with 50 % but not 60 % glucose. No starch-like substance is produced. Urea hydrolysis and the Diazonium blue B reaction is positive. Maximum growth temperature: 35 °C.

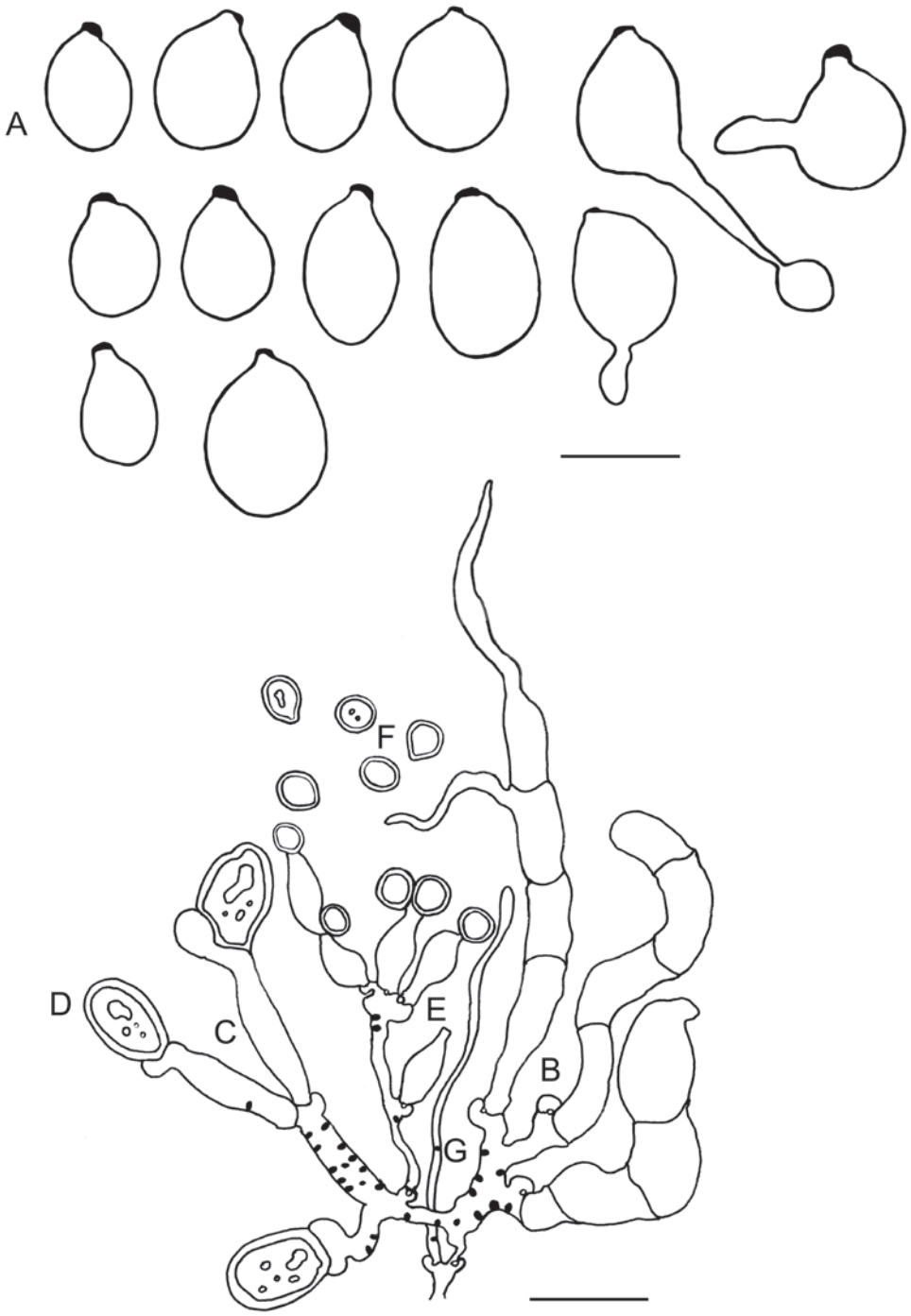

Fig. 8. *Colacogloea biconidiata sp. nov.* (VS 12415) line drawings. **A.** Basidiospores and germinating basidiospores by hyphae and secondary spores. **B.** Cluster of basidia and basidioles. **C.** Type-1 conidiophores. **D.** Type-1 conidia with basal clamps. **E.** Type-2 conidiophores. **F.** Type-2 conidia. **G.** Hyphidium. Black dots represent colacosomes. Scale bars = 10 µm.

Habitat and distribution: Currently only known from the type location in Norway, where it was collected in in a subalpine grazing area, on coniferous wood.

Material examined: This species is only known from the type collection.

Notes: This is the only species in the genus currently known to produce two types of conidia, produced by two distinct types of conidiophores. The colacosomes of this species occur scattered throughout the mycoparasite hyphae, more densely arranged in the places of physical contact between host and parasite cells. Interestingly, this mycoparasite seems to induce additional branching of host hyphae, probably to increase the contact surface where colacosomes can be formed.

Colacogloea effusa (J. Schröt.) V. Malysheva *et al.*, Mycol. Prog. 20: 414. 2021. Figs 10, 11.
Basionym: *Platygloea effusa* J. Schröt. in Cohn, *Kryptogamen Flora von Schlesien* 3(1): 384. 1889.

Typus: **Denmark**, Midtjylland: Norddjurs, Løvenholm Skov, on rotten deciduous wood, 26 Aug. 2009, *J. Heilmann-Clausen* (**neotype** C JHC 09–304, **isoneotype** GENT GENTFT00145).

Synonyms: *Colacogloea peniophorae* (Bourdot & Galzin) Oberw. & Bandoni, Canad. J. Bot. 68: 2532. 1991.
Platygloea peniophorae Bourdot & Galzin, Bull. Trimestriel Soc. Mycol. France 25: 17. 1909.

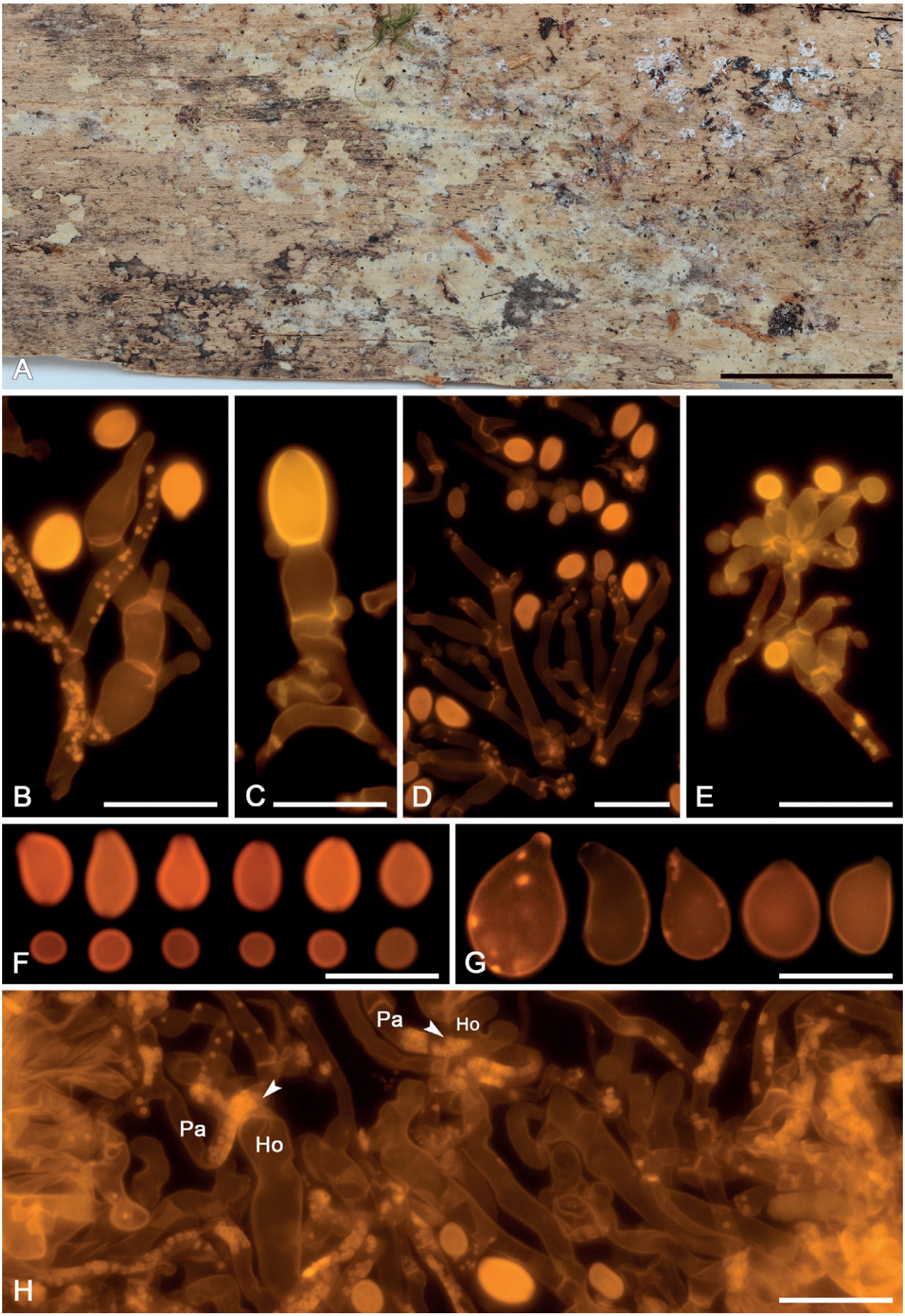

Fig. 9. *Colacogloea biconidiata sp. nov.* (VS 12415). **A.** Basidiome.. **B.** Three-septate basidium with four sterigmata, note hyphae with numerous colacosomes and three well stained conidia. **C.** Type-1 conidiophore and attached conidium with basal clamp. **D.** Cluster of type-1 conidiophores and conidia. **E.** Cluster of type-2 conidiophores. **F.** Upper row represent type-1 conidia, lower row represent type-2 conidia. **G.** Basidiospores. **H.** Host–parasite interface, Pa = parasite cell, Ho = host cell, arrowheads indicate some positions of colacosomes. Scale bars: A = 1 cm; B–G = 10 µm.

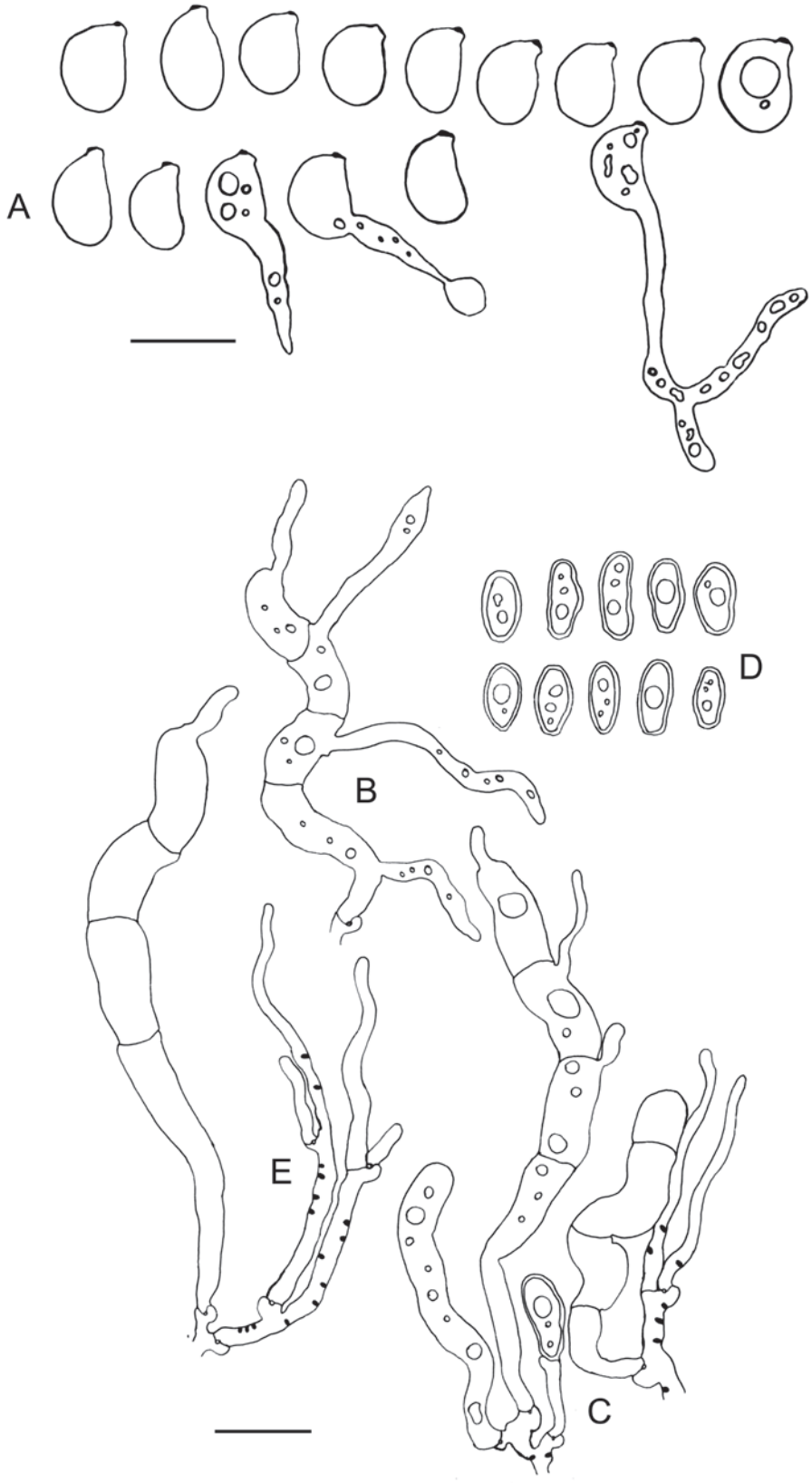

Fig. 10. *Colacogloea effusa* (NS 21-146) line drawings. **A.** Basidiospores and germinating basidiospores by hyphae and secondary spores. **B.** Basidia. **C.** Conidiophore. **D.** Conidia. **E.** Hyphidia. Black dots represent colacosomes. Scale bars = 10 µm.

Typus: **France**, Allier, Saint-Priest, 10 Aug. 1908, *H. Bourdot* (**lectotype** PC Bourdot 5945, designated here, MycoBank MBT 10013259). *Ibid.*, Saint-Bonnet de Tronçais, Forêt de Tronçais, réserve de Futaine Colbert, 16 Nov. 2021, *N. Schoutteten* (**epitype** GENT NS 21-146*°, designated here, MycoBank MBT 10013260, culture ex-epitype DSM 113583).

Description of filamentous morph: Intrahymenial, first visible as yellowish to orange, slimy patches or pustules on the host species, later fusing together and forming opalescent or yellowish, crustaceous basidiomes with tuberculate hymenial surface, darkening to reddish or brownish and remaining well-visible after drying. Monomitic; hyphae hyaline, often guttulate, thin-walled, smooth, clamped at all septa, 1.8–2.6 µm in diam. Hyphidia simple or occasionally branched, 1.2–2.5 µm in diam. Cystidia absent. Basidia narrowly tubular-clavate, straight to curved, sometimes slightly sinuous, (33.5–)42.2–64.1(–70.8) × (4.4–)4.6–5.6 µm (n = 40/2), transversally septate, four-celled when mature, clamped at the base, thin-walled, without distinct probasidium. Sterigmata

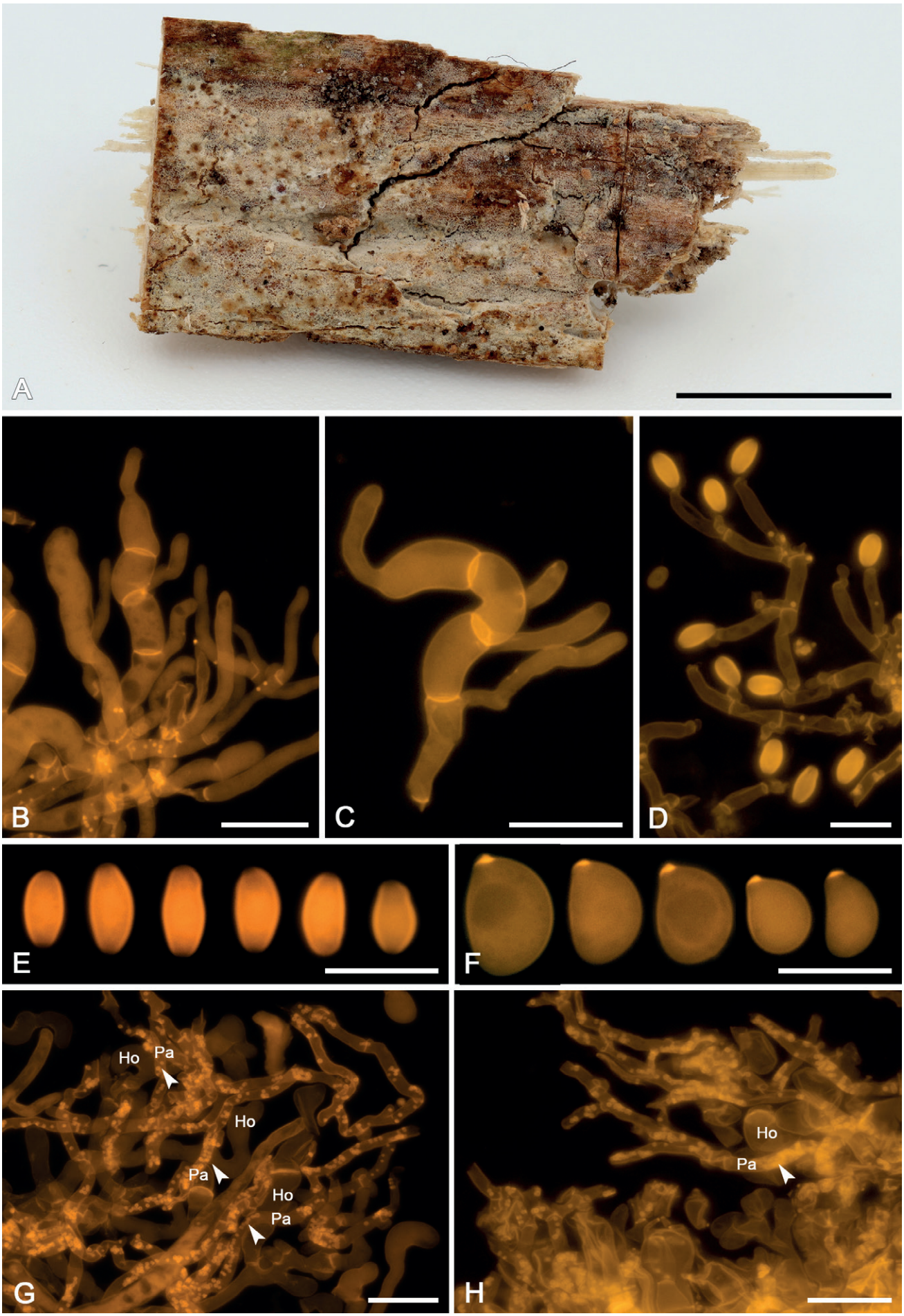

Fig. 11. *Colacogloea effusa* (NS 21-146). **A.** Basidiome. **B.** Cluster of basidium, basidiole and hyphidia. **C.** Three-septate basidium with four sterigmata. **D.** Conidiophores. **E.** Conidia. **F.** Basidiospores. **G, H.** Host–parasite interface, Pa = parasite cell, Ho = host cell, arrowheads indicate some positions of colacosomes. Scale bars: A = 1 cm; B–H = 10 µm.

up to 48 µm long. Basidiospores ellipsoid to reniform, (6.7–)6.9–10.6(–11) × (4.5–)4.7–7.3(–8) µm, L = 8.33 µm, W = 5.81 µm, Q' = (1.0–)1.2–1.7, Q = 1.4–1.7 (n = 80/2), with prominent apiculus up to 2 µm, germinating by hyphae, budding or secondary spores. Conidia ellipsoid, ovoid to subfusiform, often asymmetric, sometimes angular, mostly guttulate, thick-walled (up to 1 µm), strongly cyanophilous, basally clamped, (5.7–)6.5–8.7(–8.9) × (3.1–)3.2–4(–4.1) µm. Colacosomes scattered, no vesicular gall-like cells observed.

Description of yeast morph: After growth on YM agar plates for 1 mo at 22 °C, the streak culture is white to cream-coloured, glistening, mucoid and smooth. The margin is entire. Cells are subglobose to ovoid, occurring singly or in pairs, and proliferating by polar budding. Growth on D-glucose, D-ribose, D-arabinose, me a-D-glucoside, glycerol, ribitol, D-glucitol, D-mannitol, D-gluconate, succinate, and D-glucarate. No growth on D-galactose, L-sorbose, D-glucosamine, D-xylose, L-arabinose, L-rhamnose, sucrose, maltose, a,a-trehalose, cellobiose, salicin, melibiose, lactose, raffinose, melezitose, inulin, starch, erythritol, L-arabinitol, galactitol, myo-inositol, 5-keto-D-gluconate, D-glucuronate, D-galacturonate, DL-lactate, citrate, ethanol, L-malic acid, L-tartaric acid, and D-tartaric acid. Growth in the presence of 5 % and 8 % but not 10 % NaCl. Weak growth on MEA with 50 % and 60 % glucose. No starch-like substance is produced. Urea hydrolysis and the Diazonium blue B reaction is positive. Maximum growth temperature: 35 °C.

Habitat and distribution: *Colacogloea effusa* is presumably the most common species in the *C. effusa* species complex, with records from most European countries. Most specimens we collected, isolated and sequenced belong to this species. On a global scale, this species has been reported from various continents: Africa, Asia, Europe, North America, and South America (most of them under the name *Colacogloea peniophorae*). However, since most of these observations have been identified based on micromorphological characteristics only, it may well be that a substantial part of them belongs to other species within this species complex. It is also possible that previous reports of *C. effusa* actually comprise yet undescribed species, which may be especially true for specimens reported outside our sampling area. All our *C. effusa* collections come from deciduous wood substrates in temperate forests in Europe.

Materials examined: **Finland**, Varsinaissuomi, Raasepori, Framnäs, on an unidentified deciduous tree, growing in the basidiome of *Peniophorella praetermissa s.l.*, 21 Nov. 2019, *J. Pennanen*, JN 4226* (H). **France**, Departement Allier, St. Bonnet de Tronçais, Tour de l'étang, on an unidentified deciduous tree, growing in the basidiome of *Peniophorella praetermissa s.l.*, 15 Nov. 2021, *N. Schoutteten*, NS 21-138* (GENT); Departement Allier, St. Bonnet de Tronçais, Réserve de Nantigny, on an unidentified deciduous tree, growing in the basidiome of *Peniophorella praetermissa s.l.*, 14 Nov. 2021, *N. Schoutteten*, NS 21-128* (GENT). **Italy**, Piedmont: Alessandria, Voltaggio, Capanne di Marcarolo Nat. Regional Park, on a fallen branch of an unidentified tree, growing in the basidiome of *Peniophorella praetermissa s.l.*, 16 Oct. 2019, *N. Schoutteten*, NS 19-279* (GENT). **Netherlands**, Prov. Utrecht, Zeist, Beerschoten, on decorticated piece of deciduous wood, growing in the basidiome of *Peniophorella praetermissa s.l.*, 10 Oct. 2019, *I. Nannenga-Bruggeman*, ID 6351* (GENT); *ibid.* ID 6343* (GENT); Prov. Utrecht, Nieuw Wulven, Iepenbos, on fallen branch of a deciduous tree, growing in the basidiome of *Peniophorella praetermissa s.l.*, 13 Oct. 2020, *I. Nannenga-Bruggeman*, ID 7117* (GENT); Prov. Utrecht, Zeist, Overrijnwijck, on a fallen branch of an unidentified deciduous tree, growing in the basidiome of *Peniophorella praetermissa s.l.*, 5 Nov. 2020, *I. Nannenga-Bruggeman*, ID 7149* (GENT); Prov. Utrecht, De Bilt, Sandwijck, on a fallen branch of an unidentified deciduous tree, growing in the basidiome of *Peniophorella praetermissa s.l.*, 10 Dec. 2020, *I. Nannenga-Bruggeman*, ID 7323* (GENT); Prov. Gelderland, Barchem, Beekvliet, on fallen branch of *Alnus*, growing in the basidiome of *Peniophorella praetermissa s.l.*, 11 Jul. 2020, *M. Gotink*, MG 445* (GENT); Prov. Groningen, Kolham, Uiterdijken, paddenstoelenreservaat, on fallen branch of *Picea*, growing in the basidiome of *Peniophorella praetermissa s.l.*, 23 Nov. 2019, *R. Enzlin*, ENZ 19-092* (GENT); Prov. Groningen, Weende, Lieftinghsbroek, on a fallen branch of an unidentified deciduous tree, growing in the basidiome of *Peniophorella praetermissa s.l.*, 30 Oct. 2020, *R. Enzlin*, ENZ 20-051* (GENT); Prov. Drenthe, Gasteren, Gasterensche Holt, on a fallen branch of an unidentified deciduous tree, growing in the basidiome of *Peniophorella praetermissa s.l.*, 5 Sep. 2020, *R. Enzlin*, ENZ 20-042* (GENT). Prov. Zeeland, Oosterland, De Maire, on a fallen branch of an unidentified deciduous tree, growing in the basidiome of *Peniophorella praetermissa s.l.*, 6 Nov. 2021, *N. Schoutteten*, NS 21-110* (GENT).

Notes: The colacosomes of this species occur scattered in the mycoparasite hyphae, more densely arranged in the places of physical contact between host and parasite cells. No proliferation of host hyphae has been observed.

Colacogloea fennica Schoutteten & Miettinen, ***sp. nov.*** MycoBank MB 848657. Figs 12, 13.

Etymology: Referring to the country where the holotype of this species was collected.

Typus: **Finland**, Helsinki, Koskela, on fallen log of *Pinus sylvestris*, growing in the hymenium of *Peniophorella praetermissa s.l.*, 3 Dec. 2020, *O. Miettinen* (**holotype** GENT OM 24483*°, **isotype** H 6014790, culture ex-type DSM 112417).

Description of filamentous morph: Intrahymenial, producing yellow to orange, slimy layer on the host species, remaining visible as yellow to orange warts when dried. Monomitic; hyphae hyaline, thin-walled, smooth, clamped at all septa, 2.2–4.2 µm in diam. Hyphidia present, simple or occasionally branched, 1–2 µm in diam. Cystidia absent. Basidia narrowly tubular-clavate, straight to curved or sinuous, (50.7–)52.1–73.0(–73.2) × (4.7–)5.3–6.9(–7.0) µm (n = 20/1), transversally septate, four-celled when mature, clamped at the base, thin-walled. Sterigmata up to 46 µm long. Basidiospores ellipsoid to broadly ellipsoid, more rarely subglobose, guttulate, (6.7–)6.8–10.5 × (5.2–)5.3–8.2(–8.8) µm, L = 8.56 µm, W = 6.91 µm, Q' = (1.0–)1.1–1.5(–1.6), Q = 1.27 (n = 81/3), with prominent apiculus up to 1.2 × 1 µm, germinating by hyphae, budding or secondary spores. Conidia fusiform to amygdaliform, rarely oblong or asymmetric, mostly guttulate, thick-walled (walls up to 1 µm), strongly cyanophilous, basally clamped, 7.2–10.8(–13) × 3.5–5.0(–5.2) µm. Colacosomes scattered, no vesicular gall-like cells observed.

Description of yeast morph: After growth on YM agar plates for 1 mo at 22 °C, the streak culture is white to cream-coloured, glistening, mucoid and smooth. The margin is entire. Cells are subglobose to ovoid, occurring singly or in pairs, and proliferating by polar budding. Growth on D-glucose, D-glucosamine, D-ribose, D-arabinose, me a-D-glucoside, glycerol, D-mannitol, D-glucitol, and D-gluconate. Weak growth on erythritol, galactitol, and D-tartaric acid. No growth on D-galactose, L-sorbose, sucrose, maltose, cellobiose, a,a-trehalose, melibiose, raffinose, melezitose, inulin, starch, D-xylose, L-arabinose, L-rhamnose, ribitol, salicin, lactose, L-arabinitol, myo-inositol, 5-keto-D-gluconate, D-glucuronate, D-galacturonate, DL-

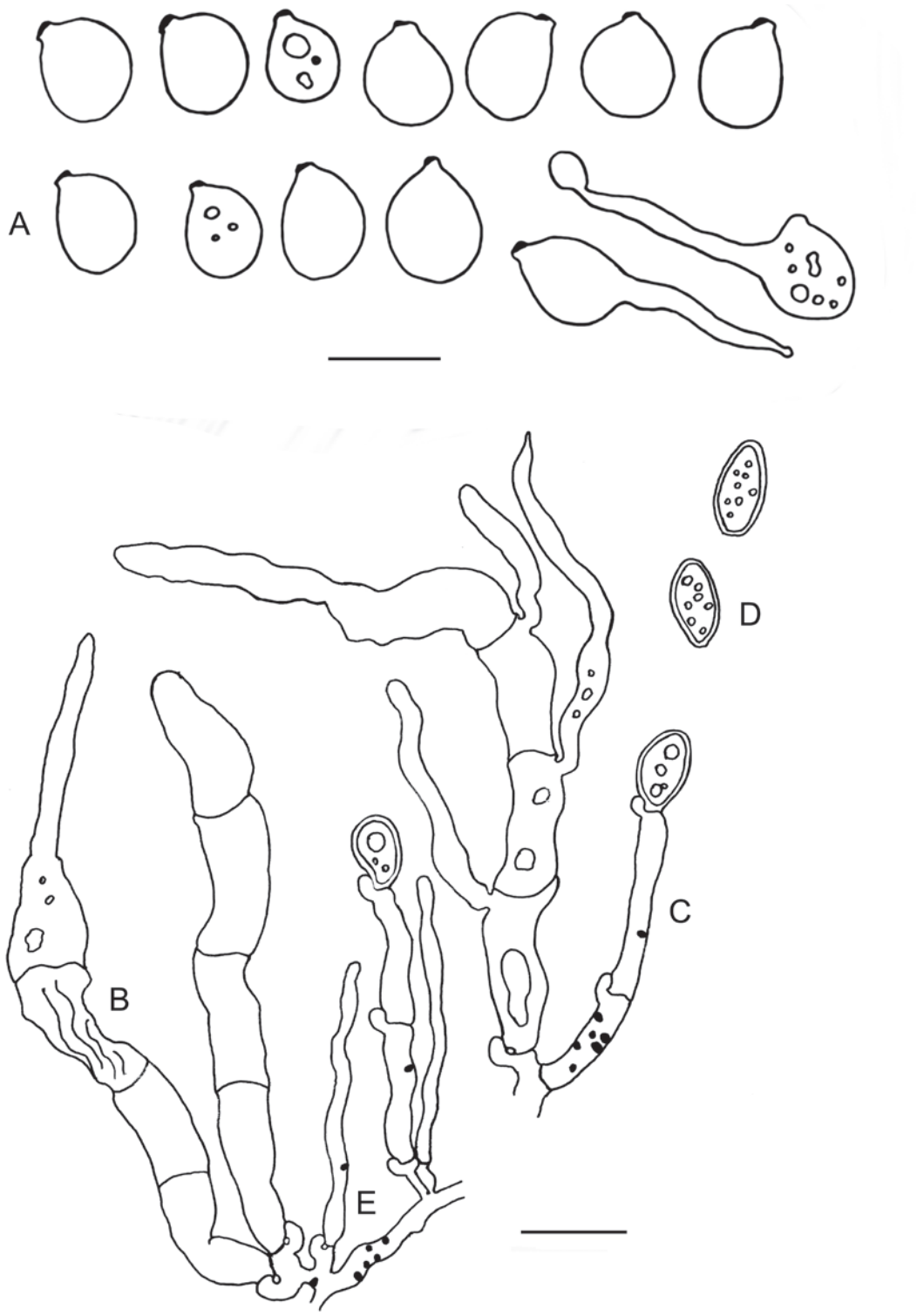

Fig. 12. *Colacogloea fennica sp. nov.* (OM 22483) line drawings. **A.** Basidiospores and germinating basidiospores by secondary spores. **B.** Basidium and basidiole. **C.** Conidiophore and basidium. **D.** Conidia, note the clamp at the base of conidia. **E.** Hyphidium. Black dots represent colacosomes. Scale bar = 10 µm.

lactate, succinate, citrate, ethanol, D-glucarate, L-tartaric acid, and L-malic acid. Growth in the presence of 5 % but not 8 % and 10 % NaCl. Growth on MEA with 50 % but not 60 % glucose. No starch-like substance is produced. Urea hydrolysis and the Diazonium blue B reaction is positive. Maximum growth temperature: 35 °C.

Habitat and distribution: Growing on coniferous wood, currently found only on *Pinus sylvestris*. Up to now only known from Finland, where it was collected in mixed forests and parks.

Materials examined: **Finland**, Helsinki, Koskela, on fallen log of *Pinus sylvestris*, growing in the hymenium of *Peniophorella praetermissa s.l.*, 26 May 2020, *O. Miettinen*, OM 23714 (= H 6200175); *ibid*. 1 Sep. 2021, *N. Schoutteten*, NS 21-014* (GENT); Helsinki, Lehtisaari, on fallen branch of *Pinus sylvestris*, growing in the hymenium of *Peniophorella praetermissa s.l.*, 15 Oct. 2008, *H. Kotiranta*, Kotiranta 22473 (= H 6073961).

Notes: The colacosomes occur scattered in the mycoparasite hyphae, more densely arranged in the places of physical contact between host and parasite cells. No proliferation of host hyphae has been observed.

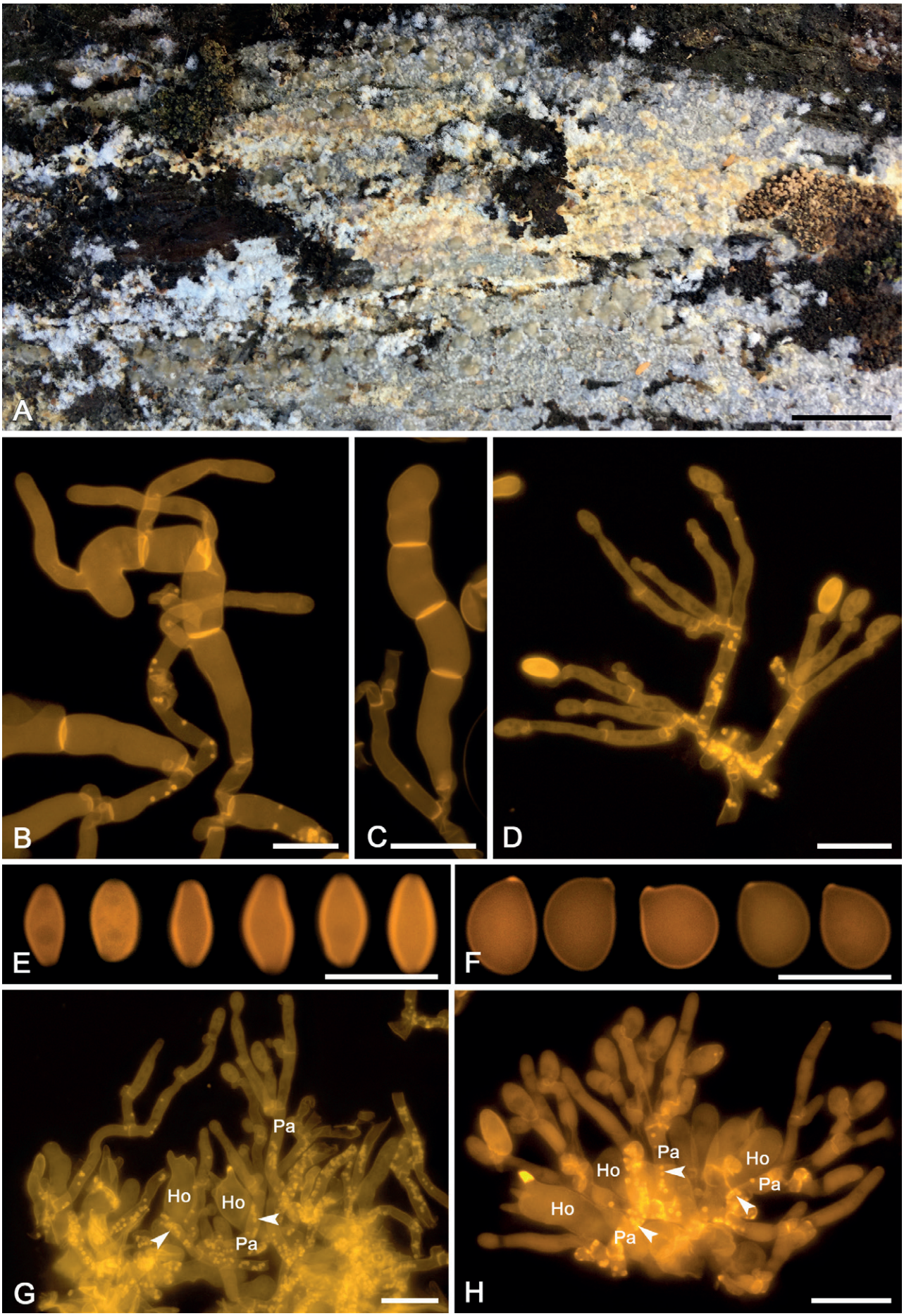

Fig. 13. *Colacogloea fennica sp. nov.* (OM 22483). **A.** Basidiome. **B.** Three-septate basidium with four sterigmata, note colacosomes in hyphae bearing the basidium but not in the basidium. **C.** Basidiole. **D.** Cluster of conidiophores and conidia, note colacosomes in hyphae but not in conidiophores. **E.** Conidia. **F.** Basidiospores. **G, H.** Host–parasite interface, Pa = parasite cell, Ho = host cell, arrowheads indicate some positions of colacosomes. Scale bars: A = 1 cm; B–G = 10 µm.

Colacogloea microspora Schoutteten, ***sp. nov.*** MycoBank MB 848658. Figs 14, 15.

Etymology: Referring to the small size of the basidiospores of this species compared to other representatives of the *Colacogloea effusa* species complex.

Typus: **Belgium**, Flanders, Vlaams-Brabant, Asse, domain of Hoeve Heierveld, on fallen branch of a deciduous tree (probably *Corylus avellana*), growing in the hymenium of *Peniophorella praetermissa s.l.*, 27 Oct. 2020, *N. Schoutteten* (**holotype** GENT NS 20-141*°, culture ex-type DSM 112413).

Description of filamentous morph: Intrahymenial, producing a yellow to orange, slimy to arid layer on the host species, remaining visible as yellow to orange warts after drying. Monomitic; hyphae hyaline, thin-walled, smooth, clamped at all septa, 2.4–3.9 µm in diam. Hyphidia absent. Cystidia absent. Basidia tubular-clavate, straight to sinuous to curved, (26.0–)27.6–43.7(–44.3) × (3.3–)4.2–5.4(–5.5) µm (n=18/1), transversally septate, four-celled when mature, clamped at the base, thin-walled, often arranged in clusters of 3–5 and appearing as scattered groups, quickly collapsing after reaching maturity. Sterigmata up to 22 µm long. Basidiospores ellipsoid to broadly ellipsoid to subglobose, (5.1–)5.2–8.0(–8.2) × (3.0–)3.8–5.3 µm, L = 6.66 µm, W = 4.53 µm, Q' = 1.1–1.8(2.1), Q = 1.48 (n = 48/1), germinating by hyphae, budding or secondary spores; apiculus occasionally eccentric, up to 1 µm. Conidia variable, fusiform to angular, often widened in the middle, sometimes oblong, slightly curved or slightly asymmetric, occasionally with a small basal outgrowth, mostly guttulate, thick-walled (walls up to 1.2 µm), strongly cyanophilous, basally clamped, (6.9–)7.2–11.1(–12.7) × (3.1–)3.6–4.8(–5.3) µm. Colacosomes scattered, no vesicular gall-like cells observed.

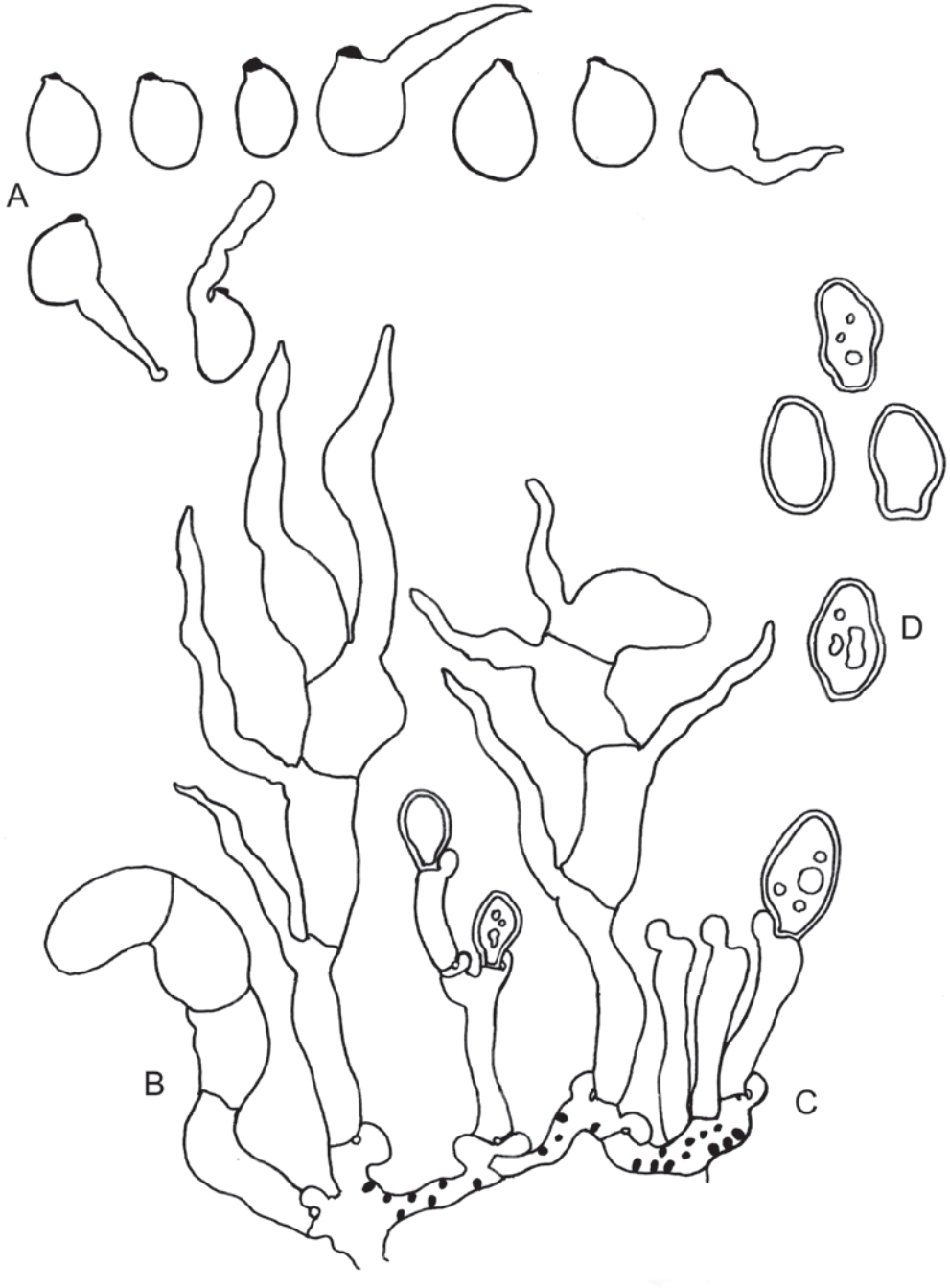

Fig. 14. *Colacogloea microspora sp. nov.* (NS 20-141) line drawings. **A.** Basidiospores and germinating basidiospores by hyphae and secondary spores. **B.** Two basidia and basidiole. **C.** Conidiophore. **D.** Conidia. Black dots represent colacosomes. Scale bar = 10 µm.

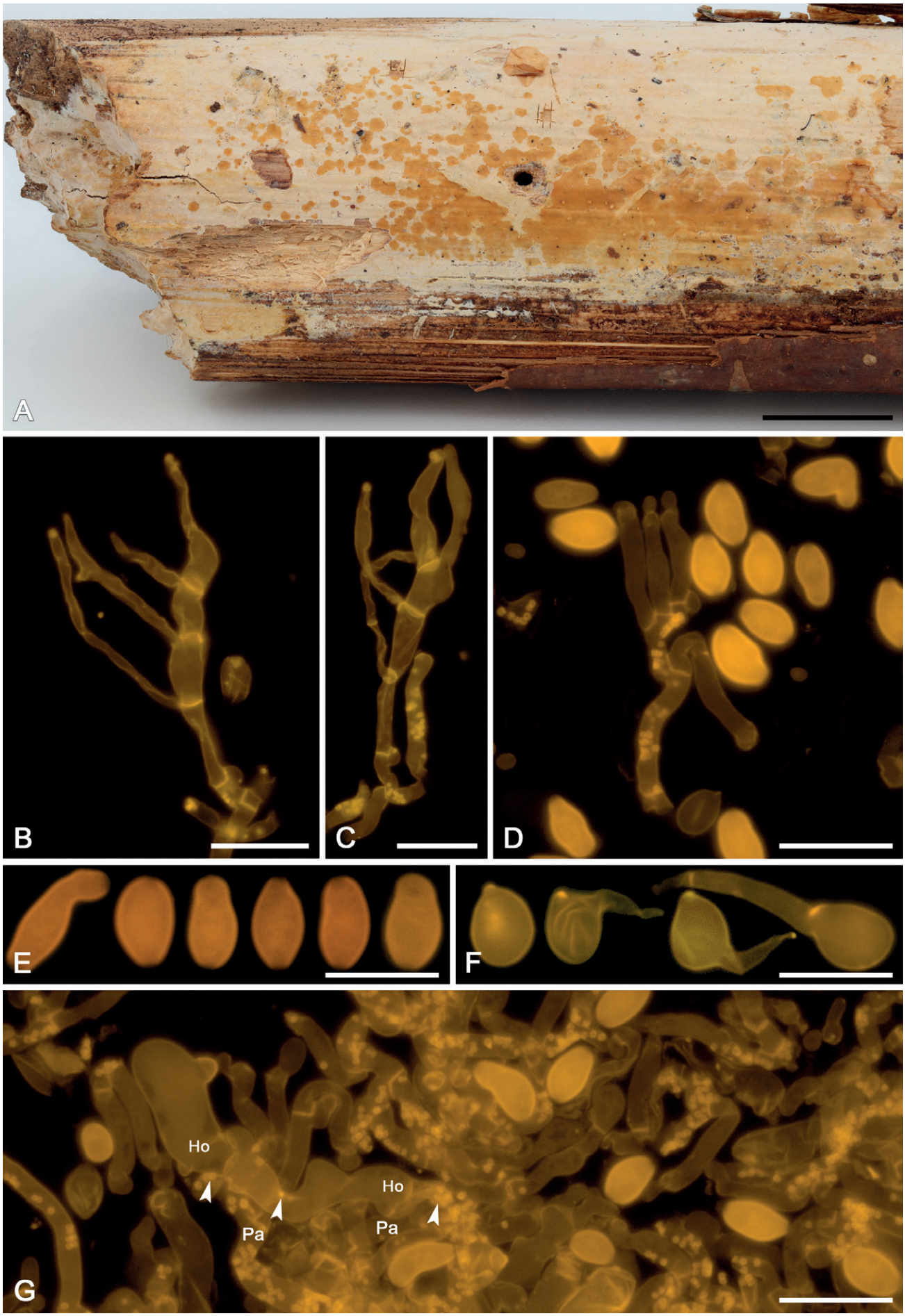

Fig. 15. *Colacogloea microspora sp. nov.* (NS 20-141). **A.** Basidiome. **B, C.** Three-septate basidia with sterigmata, note colacosomes in hyphae. **D.** Cluster of conidiophores and conidia, note colacosomes in hyphae. **E.** Conidia. **F.** Basidiospores. **G.** Host–parasite interface, Pa = parasite cell, Ho = host cell, arrowheads indicate some positions of colacosomes. Scale bars: A = 1 cm; B–G = 10 µm.

Description of yeast morph: After growth on YM agar plates for 1 mo at 22 °C, the streak culture is white to cream-coloured, glistening, mucoid and smooth. The margin is entire. Cells are subglobose to ovoid, occurring singly or in pairs, and proliferating by polar budding. Growth on D-glucose, D-glucosamine, D-ribose, D-arabinose, me a-D-glucoside, melezitose, glycerol, ribitol, D-glucitol, D-mannitol, galactitol, D-gluconate, D-glucarate, and L-tartaric acid. Weak growth on L-sorbose, sucrose, erythritol, and D-tartaric acid. No growth on D-galactose, D-xylose, L-arabinose, L-rhamnose, maltose, a,a-trehalose, cellobiose, salicin, melibiose, lactose, raffinose, inulin, starch, L-arabinitol, myo-inositol, 5-keto-D-gluconate, D-glucuronate, D-galacturonate, DL-lactate, succinate, citrate, ethanol, and L-malic acid. Growth in the presence of 5 % but not 8 % and 10 % NaCl. Growth on MEA with 50 % but not 60 % glucose. No starch-like substance is produced. Urea hydrolysis and the Diazonium blue B reaction is positive. Maximum growth temperature: 35 °C.

Habitat and distribution: Up to now only found in Belgium, in a private forest-like garden, growing on a fallen, partly decorticated branch of a deciduous tree species, probably *Coryllus avellana*.

Material examined: This species is only known from the type collection.

Notes: The yellow patches on the host hymenium mostly comprise conidial tissue. Basidia and basidiospores are to be found in adjacent regions which macroscopically do not seem to be infected. The colacosomes of this species occur scattered in the mycoparasite hyphae, more densely arranged in the places of physical contact between host and parasite cells. No proliferation of host hyphae has been observed.

Colacogloea philyla (Van der Walt *et al.*) Q.M. Wang *et al.*, Stud. Mycol. 81: 183. 2015. Figs 16, 17.
Basionym: *Torulopsis philyla* Van der Walt *et al.*, Antonie van Leeuwenhoek 37: 464. 1971.

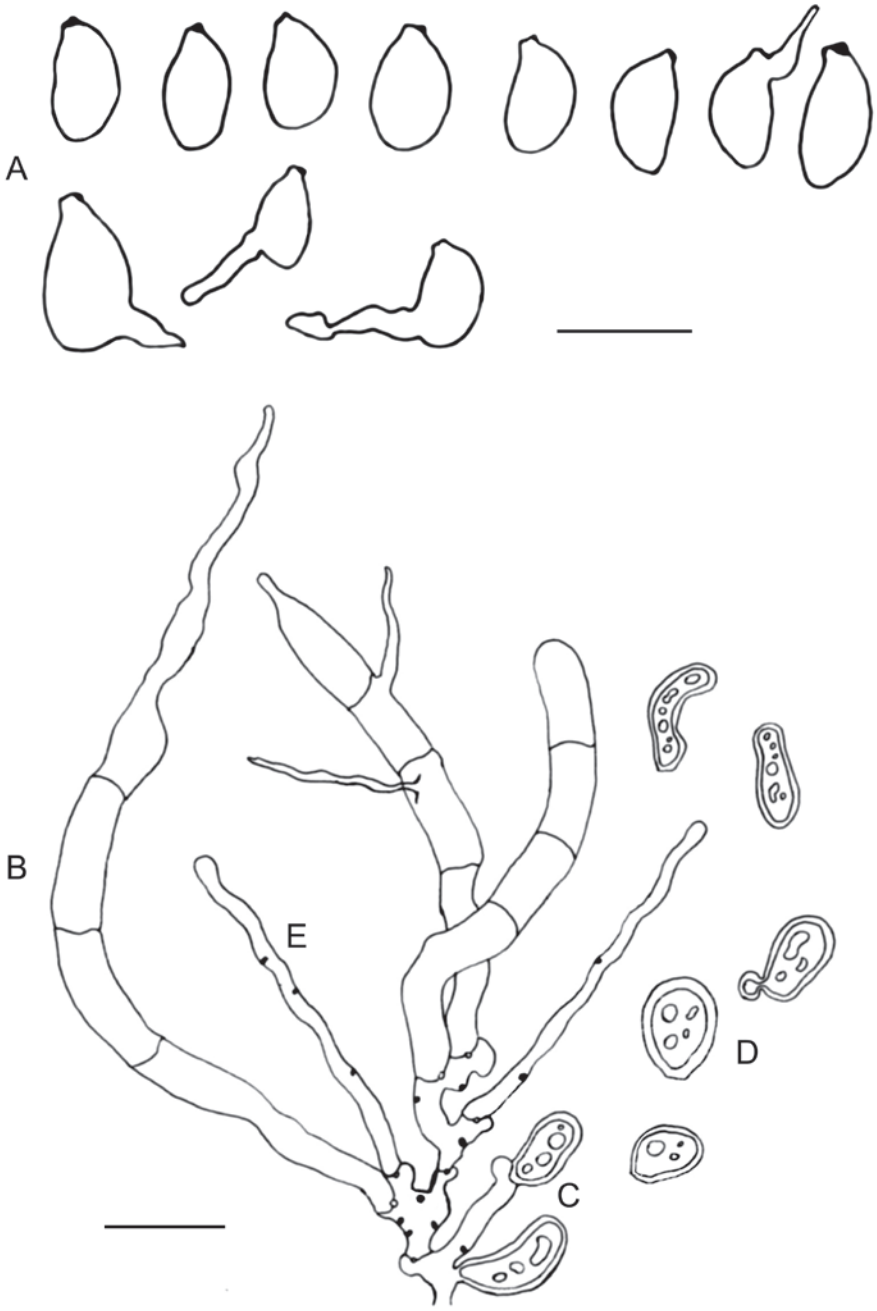

Fig. 16. *Colacogloea philyla* (MG 438) line drawings. **A.** Basidiospores and germinating basidiospores by hyphae and secondary spores. **B.** Basidium. **C.** Conidiophore. **D.** Conidia. **E.** Hyphidium. Black dots represent colacosomes. Scale bars = 10 µm.

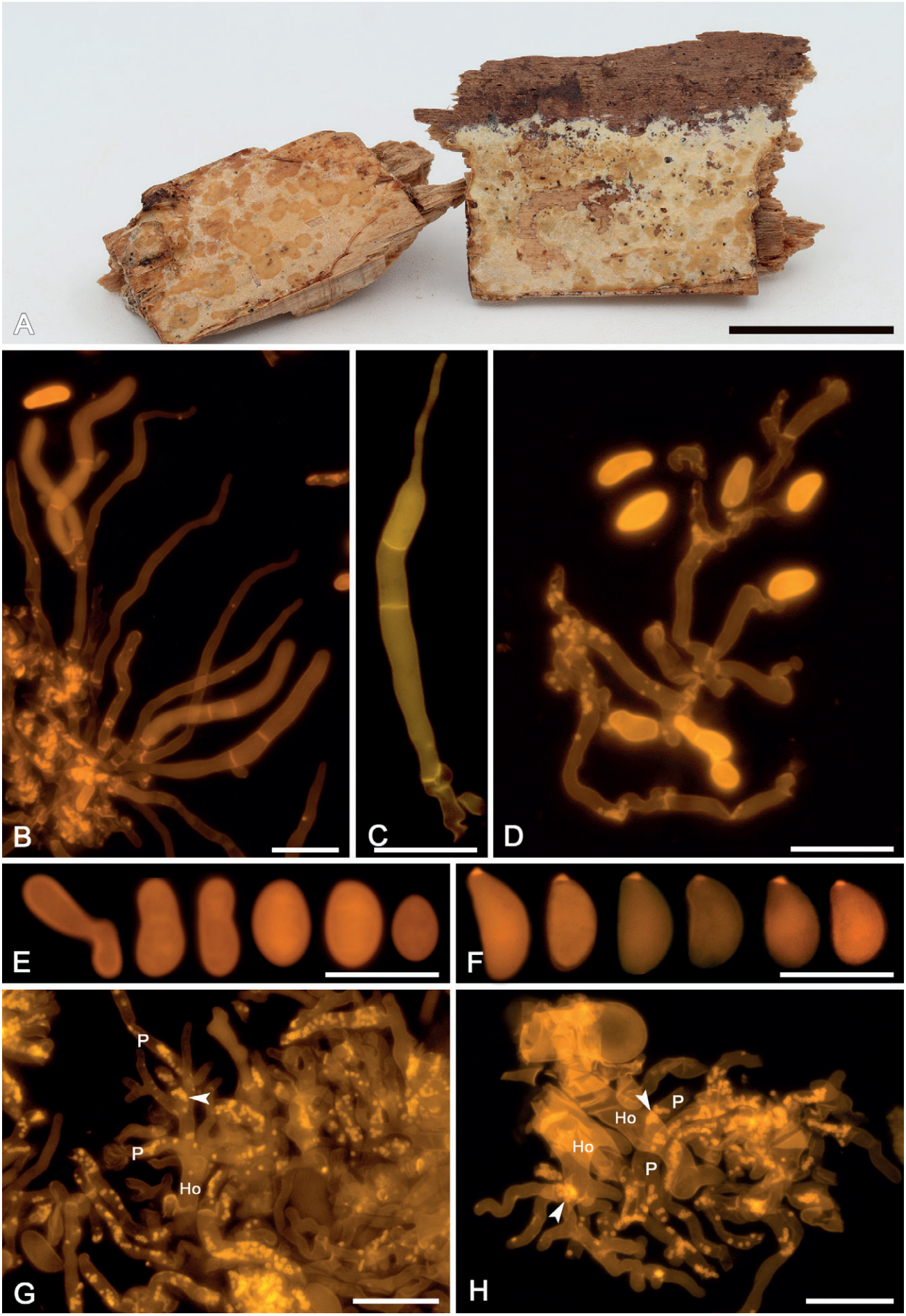

Fig. 17. *Colacogloea philyla* (MG 438). **A.** Basidiome. **B.** Cluster of three-septate basidia, basidioles and hyphidia. **C.** Two-septate basidium with apical sterigma. **D.** Cluster of conidiophores and conidia, note the colacosomes in the hyphae but not in the conidiophores. **E.** Conidia. **F.** Basidiospores. **G, H.** Host–parasite interface, Pa = parasite cell, Ho = host cell, arrowheads indicate some positions of colacosomes. Scale bars: A = 1 cm; B–H = 10 µm.

Description of filamentous morph: Intrahymenial, producing a yellow to orange slimy layer on the host species, remaining visible as yellow to orange warts after drying. Monomitic; hyphae hyaline, thin-walled, smooth, clamped at all septa, 1.8–2.5 µm in diam. Hyphidia present, simple or occasionally branched, 1–2 µm in diam. Cystidia absent. Basidia narrowly tubular-clavate, straight to curved, (31.0–)39.0–56.2(–65.0) × (3.0–)3.2–4.5 µm (n = 20/1), transversally septate, four-celled when mature, clamped at the base, thin-walled. Sterigmata up to 39 µm long. Basidiospores subfusiform, often somewhat curved, guttulate, (6.8–)6.9–9.5(–10.2) × (3.3–)3.4–5.1 µm, L = 8.31 µm, W = 4.27 µm, Q' = (1.6–)1.7–2.4(–2.7), Q = 1.96 (n = 30/1), with prominent apiculus up to 2 µm, germinating by hyphae, budding or secondary spores. Conidia highly variable in shape, ellipsoid, ovoid, subfusiform, elongated, angular, often asymmetric with variable outgrowths, mostly guttulate, thick-walled (wall up to 1 µm), strongly cyanophilous, basally clamped, (6.3–)6.6–9.8(–10.6) × 3–4.9(–5.1) µm. Colacosomes scattered, no vesicular gall-like cells observed.

Habitat and distribution: Currently, the filamentous morph of *Colacogloea philyla* has only been observed in one collection from a conifer forest in the Netherlands, and is described and illustrated in this study. The ex-type strain of *C. philyla* was isolated as a yeast obtained from beetle galleries in *Harpephyllum caffru* (*Anacardiaceae*) in South Africa. Other yeast strains of this species were isolated from decaying wood in South Africa and Portugal (Sampaio 2011). Since the host *Peniophorella pubera* is a geographically widespread species, it is likely that the dikaryotic mycoparasitic stage can also be found around the localities where *C. philyla* was isolated as a yeast. Blast results of the ITS region in GenBank indicate this species was also isolated from mangrove sediments in India.

Material examined: **Netherlands**, Prov. Flevoland, Zeewolde, Horsterwold, Stille Kern, on a decorticated *Picea* branch, growing in the hymenium of *Peniophorella pubera*, 3 Oct. 2020, *M. Gotink*, MG 438*° (GENT).

Notes: This is one of two species recovered from the host *Peniophorella pubera*. The colacosomes of this species occur scattered in the mycoparasite hyphae, more densely arranged in the places of physical contact between host and parasite cells. Similar to observations in *C. biconidiata sp. nov.*, this mycoparasite seems to induce additional branching of host hyphae, increasing the availability of contact surface where colacosomes can be formed.

Colacogloea universitatis-gandavensis Schoutteten & Verbeken, ***sp. nov.*** MycoBank MB 848659. Figs 2, 18, 19.

Etymology: The holotype is found on one of the campuses of Ghent University and we name the species after the university to acknowledge and stimulate the efforts for the Biodiversity plan, which is an official policy plan approved by the Board of Governors in 2020 and aims to realize a net gain in biodiversity on UGent campuses by 2030.

Typus: **Belgium**, Prov. Oost-Vlaanderen, Gontrode, Aelmoeseneiebos, on a log of an unidentified deciduous tree, growing in the hymenium of *Peniophorella praetermissa s.l.,* 18 Sep. 2021, *N. Schoutteten* (**holotype** GENT NS 21-013°).

Description of filamentous morph: Intrahymenial, producing a yellow to orange, slimy to arid layer on the host species, rarely making small emergences (< 0.5 mm long) on the host hymenium. Monomitic; hyphae hyaline, thin-walled, smooth, clamped at all septa, 1.8–4.8 µm in diam. Hyphidia absent. Cystidia absent. Basidia tubular-clavate, straight to curved or sinuous, (25.5–)26–36(–37.5) × 5–6.5(–7) µm (n = 17/1), transversally septate and, often somewhat constricted at each septum, four-celled when mature, clamped at the base, thin-walled, often arranged in clusters of 2–5. Sterigmata up to 38 µm long. Basidiospores ellipsoid to broadly ellipsoid, (6.7–)6.8–9.8(–10.8) × (4.2–)4.5–7.2(–7.5) µm, L = 7.83 µm, W = 5.22 µm, Q' = 1.2–1.8, Q = 1.51 (n = 34/1), with prominent apiculus up to 1 µm, germinating by hyphae or secondary spores, budding by secondary spores. Conidiophores are comprised of two cells being separated by a septum, each cell apically giving rise to a conidium, basally clamped, often arranged in clusters, intermixed with basidia, 11.5–28.5 × 3–5 µm. Mature conidia ellipsoid to ovoid, more rarely subfusiform, sometimes asymmetrical or becoming oblong, rarely with a small side outgrowth, mature conidia bearing an appendage (cell wall remnant of the smaller twin-conidium), thick-walled (walls up to 1 µm), cyanophilous, dikaryotic, (5.0–)5.2–7.9(–8.8) × (3.2–)3.3–4.9(–5.1). Colacosomes arranged both scattered in parasite hyphae and in gall-like cells produced by this species.

Habitat and distribution: Collections of this species have been found in deciduous and mixed forests in Western, Central and Northern Europe (Belgium, Finland, Switzerland and The Netherlands). This species may also be present in North America, as morphologically similar collections have been reported by Martin (1940) and Bandoni (1973). Whether these North-American collections are truly conspecific with *C. universitatis-gandavensis sp. nov.* or rather represents a closely related species remains to be investigated.

Materials examined: **Belgium**, Prov. Oost-Vlaanderen, Aalst, Osbroek, on fallen branch of an unidentified deciduous tree species, growing in the hymenium of *Peniophorella praetermissa s.l.*, 05 Sep. 2020, *N. Schoutteten*, NS 20-022*° (GENT). **Finland**, Varsinaissuomi, Turku, Ruissalo, on fallen branch of *Quercus robur*, growing in the hymenium of *Peniophorella praetermissa s.l.*, 9 Sep. 1937, *M. Laurila*, H 6086094. **Netherlands**, Zeeland, Schelphoek, on a decorticated branch of an unidentified deciduous tree, growing in the hymenium of *Peniophorella praetermissa s.l.*, 5 Nov. 2021, *B. Miedema*, Miedema 2021014 (GENT); Zeeland, nature reserve De Schotsman, on a decorticated branch of an unidentified deciduous tree, growing in the hymenium of *Peniophorella praetermissa s.l.*, 7 Nov. 2021, *H. Wassink*, NS 21-112 (GENT). **Switzerland**, Ticino region, Sementina, Boschetti, on a decorticated branch of an unidentified tree, growing in the hymenium of *Peniophorella praetermissa s.l.*, 13 Oct. 2019, *N. Schoutteten*, NS 19-119 (GENT).

Notes: This is the second species that we propose which is similar to the morphotype illustrated by Martin (1940) (see also *C. bettinae sp. nov.* and discussion). Basidia have only been observed in three out of six investigated specimens. The conidial state is always the most prominent, with basidia occurring in clusters with conidiophores. Unfortunately, no cultures could be obtained of this species.

Conidiogenesis in this species is a remarkable process with conidiophores consisting of two distinct cells (Fig. 17D). These two cells are separated by a septum, which is characterised by a simple septal pore (Greschner-Aschenbrenner 1997). One of these cells comprises the 'stalk' of the conidiophore and an apical abscission site where the conidium is produced (conidiophore cell 1). The second cell is much smaller and has a similar apical abscission site (conidiophore cell 2). Each cell of the conidiophore produces a conidium at the apical abscission site. The conidium produced

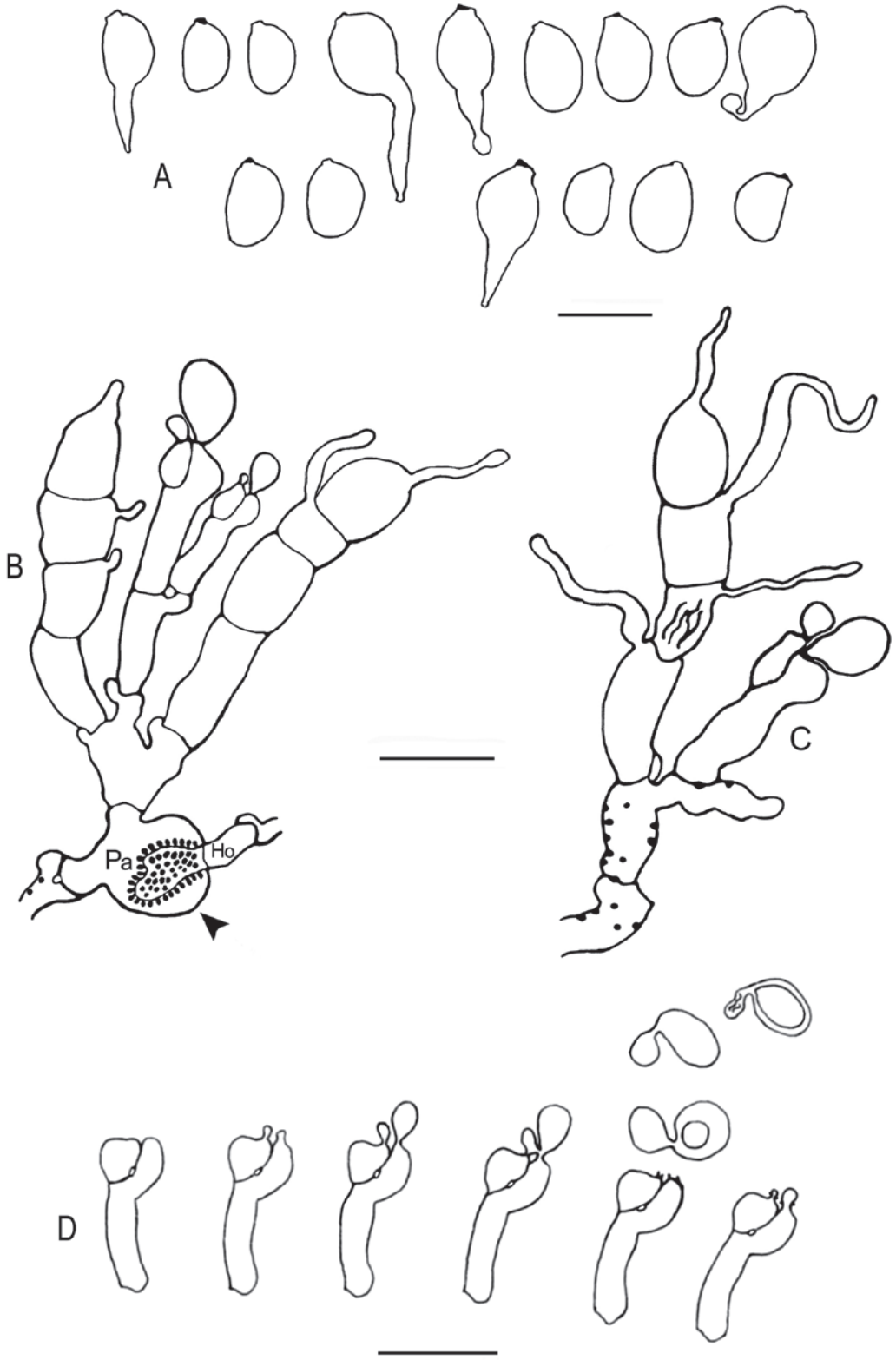

Fig. 18. *Colacogloea universitatis-gandavensis sp. nov.* (H6086094) line drawings. **A.** Basidiospores and germinating basidiospores by secondary spores. **B.** Cluster of basidia and conidiophores. **C.** Conidiophore. **D.** Conidiophores showing subsequent stages of conidiogenesis and conidia. **E.** Gall-like cell of the parasite (Pa) enveloping a host hyphae (Ho). Black dots represent colacosomes. Scale bars = 10 µm.

by conidiophore cell 1 grows remarkably larger than the conidium produced by conidiophore cell 2. At this stage, each daughter conidium is monokaryotic. At a certain moment, the two daughter conidia fuse forming a zygoconidium. Greschner-Aschenbrenner (1997) showed that the zygoconidium is abscised shortly after formation, leaving a scar at the conidiophore which can only be seen by TEM. During the short-lived zygoconidium stage, the cytoplasm (including the nucleus) of the smaller conidium is transferred to the larger conidium. Following this transfer the larger conidium becomes dikaryotic. The remnants of the smaller conidium, *i.e.*, the empty, collapsed cell wall remains attached to the cell wall of the larger conidium. The same type of conidiogenesis occurs in *C. bettinae sp. nov.*

Colacosomes are mainly arranged in vesicular gall-like cells produced by the mycoparasite. To a lesser extent, colacosomes also scattered in mycoparasite hyphae. The cell wall of these gall-

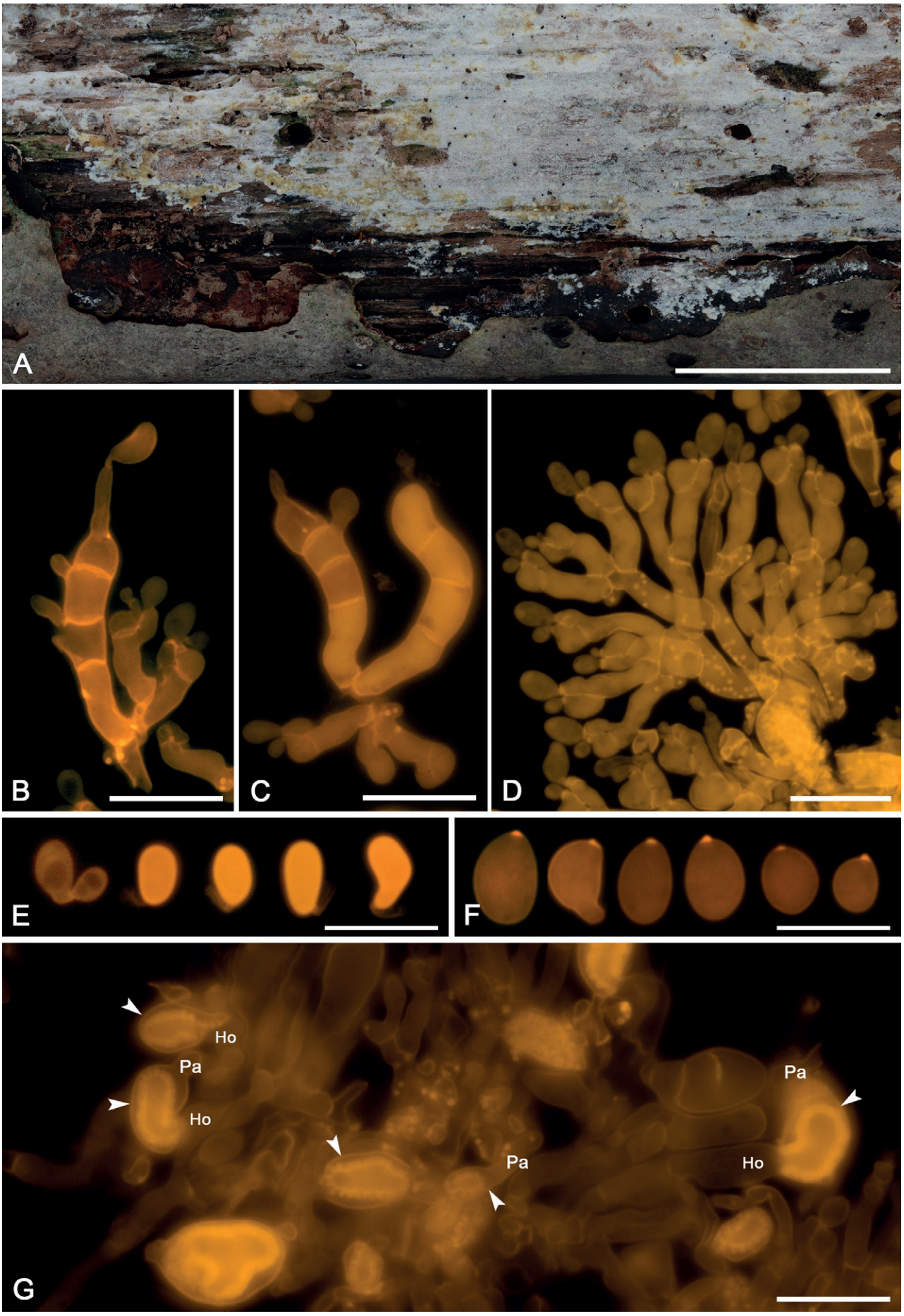

Fig. 19. *Colacogloea universitatis-gandavensis sp. nov.* (NS 21-013). **A.** Basidiome. **B.** Cluster of three-septate basidium with four sterigmata and conidiophores, note one attached basidiospore. **C.** Cluster of basidium, basidiole and conidiophores. **D.** Cluster of conidiophores, note the colacosomes in hyphae. **E.** Conidia. **F.** Basidiospores. **G.** Host–parasite interface, Pa = parasite cell, Ho = host cell, arrowheads indicate some gall-like cells of the parasite enveloping host hyphae, colacosomes are formed along the contact interface within these galls. Scale bars: A = 1 cm; B–G = 10 µm.

like structures invaginates at places where a host hypha makes physical contact. The latter continues to grow into the invagination where it becomes surrounded by the cell wall of the mycoparasite. Colacosomes are formed at regular distances along the contact surface within these galls.

Identification key based on filamentous morphs to the species within the *Colacogloea effusa* species complex

1a Growing on *Peniophorella pubera* 2
1b Growing on *Peniophorella praetermissa s.l.* 3

2a Conidia of the mycoparasite of irregular shape, no appendage present. Basidiospores subfusiform. Colacosomes scattered ..... *Colacogloea philyla*
2b Conidia of the mycoparasite of type of regular shape, generally with appendage of remaining cell wall. Ventral side of basidiospores flattened to concave. Colacosomes arranged in gall-like cells ..... *Colacogloea bettinae*

3a Conidia of the mycoparasite of regular shape, generally with appendage of the remaining cell wall. Basidiospores (broadly) ellipsoid. Colacosomes arranged in gall-like cells ..... *Colacogloea universitatis-gandavensis*
3b Conidia without appendage. Colacosomes scattered 4

4a Two types of conidia and conidiophores present. Basidiospores large, up to 12.5 µm in length ..... *Colacogloea biconidiata*
4b Only one type of conidia. Basidiospores not exceeding 11 µm in length 5

5a Basidiospores small, most spores ≤ 8µm in length, (5.1–)5.2–8.0(–8.2) × (3.0–)3.8–5.3 µm ..... *Colacogloea microspora*
5b Basidiospores larger, often ≥ 8 µm in length, up to 11 µm 6

6a Basidiospores ellipsoid to reniform, Q > 1.4 ..... *Colacogloea effusa*
6b Basidiospores ellipsoid to broadly ellipsoid, Q < 1.4 ..... *Colacogloea fennica*

Family *Mycogloiocolacaceae* Schoutteten & Yurkov, ***fam. nov.*** MycoBank MB 848661.

Description: Member of *Microbotryomycetes*. This family is mainly circumscribed by the phylogenetic analysis based on seven loci, in which it forms a well-supported lineage. The family includes species with a dimorphic life cycle. Filamentous morphs are mycoparasitic, only develop in presence of the host, and are characterised by transversally septate basidia and the presence of colacosomes. The diagnosis and nomenclature of the family *Mycogloiocolacaceae* are based on the genus *Mycogloiocolax gen. nov*.

Type genus: *Mycogloiocolax* Schoutteten & Rödel

Mycogloiocolax Schoutteten & Rödel, ***gen. nov.*** MycoBank MB 848662.

Etymology: The name is based on a similar etymology used for other genera of colacosome-interacting mycoparasites. Gloios refers to the slimy layer produced by the mycoparasite *Mycogloiocolax gerardii* when growing in its host. Colax refers to the parasitic nature of this species.

Type: *Mycogloiocolax gerardii* Schoutteten & Rödel

Generic description: Genus of dimorphic fungi. Basidiomata absent. Filamentous morph develops intrahymenial in the host, visible in fresh condition as a hyaline gelatinous, slimy layer overgrowing the host basidiome, turning to a thin, almost invisible, gelatinous layer in dry condition. Monomitic; hyphae hyaline, thin-walled, smooth, clamped at all septa. Hyphidia absent. Cystidia absent. Basidia cylindrical to tubular-clavate, often curved, sinuous or winding, transversally septate, mature basidia two-, rarely three- or four-celled, basally clamped, thin-walled. Basidiospores fusiform to amygdaliform, with suprahilar depression, asymmetric, smooth, hyaline, inamyloid, with a prominent apiculus, germinating by hyphae, budding or secondary spores. Conidia ellipsoid to subfusiform, thin-walled. Colacosomes scattered, no vesicular gall-like cells observed.

Mycogloiocolax gerardii Schoutteten & Rödel, ***sp. nov.*** MycoBank MB 848663. Figs 20, 21.

Etymology: Named after the French amateur mycologist Gérard Trichies, who has made large efforts in documenting and illustrating the diversity of heterobasidiomycetes in France.

Typus: **Germany**, Saxony, near Mölbis (51°11'16.2"N 12°30'28.9"E), growing in the basidiome of *Xenasmatella tulasnelloidea* (Höhn. & Litsch.) Oberw., 22 Oct. 2020, *T. Rödel* (**holotype** GENT TR 04096*°, culture ex-type DSM 112426).

Description of filamentous morph: Intrahymenial, visible in fresh condition as a hyaline gelatinous, slimy layer overgrowing the host basidiome, turning to a thin, almost invisible, gelatinous layer in dry condition. Monomitic; hyphae hyaline, thin-walled, smooth, clamped at all septa, 1.2–3.3 µm in diam. Hyphidia absent. Cystidia absent. Basidia cylindrical to tubular-clavate, often curved, sinuous or winding, (28.3–)31.8–34.9(–37.8) × (3.0-)3.2-4.7(4.9) µm (n = 20/2), transversally septate, mature basidia two-, rarely three- or four-celled, basally clamped, thin-walled. Sterigmata up to 27 µm long. Basidiospores fusiform to amygdaliform, with suprahilar depression, asymmetric, smooth, hyaline, inamyloid, (5.8–)6.0–10.1(–10.2) × (2.4–)3.6–5.8(–6.0) µm, L = 8.20, W =4.72, Q' = (1.2–)1.3–2.1(–4.1), Q = 1.79 (n = 31/1), with a prominent apiculus, germinating by hyphae, budding or secondary spores. Conidia ellipsoid to subfusiform, thin-walled, (3.6–)4.0–5.2(–5.8) × 2.0–2.6(–2.8) µm. Colacosomes scattered, no vesicular gall-like cells observed.

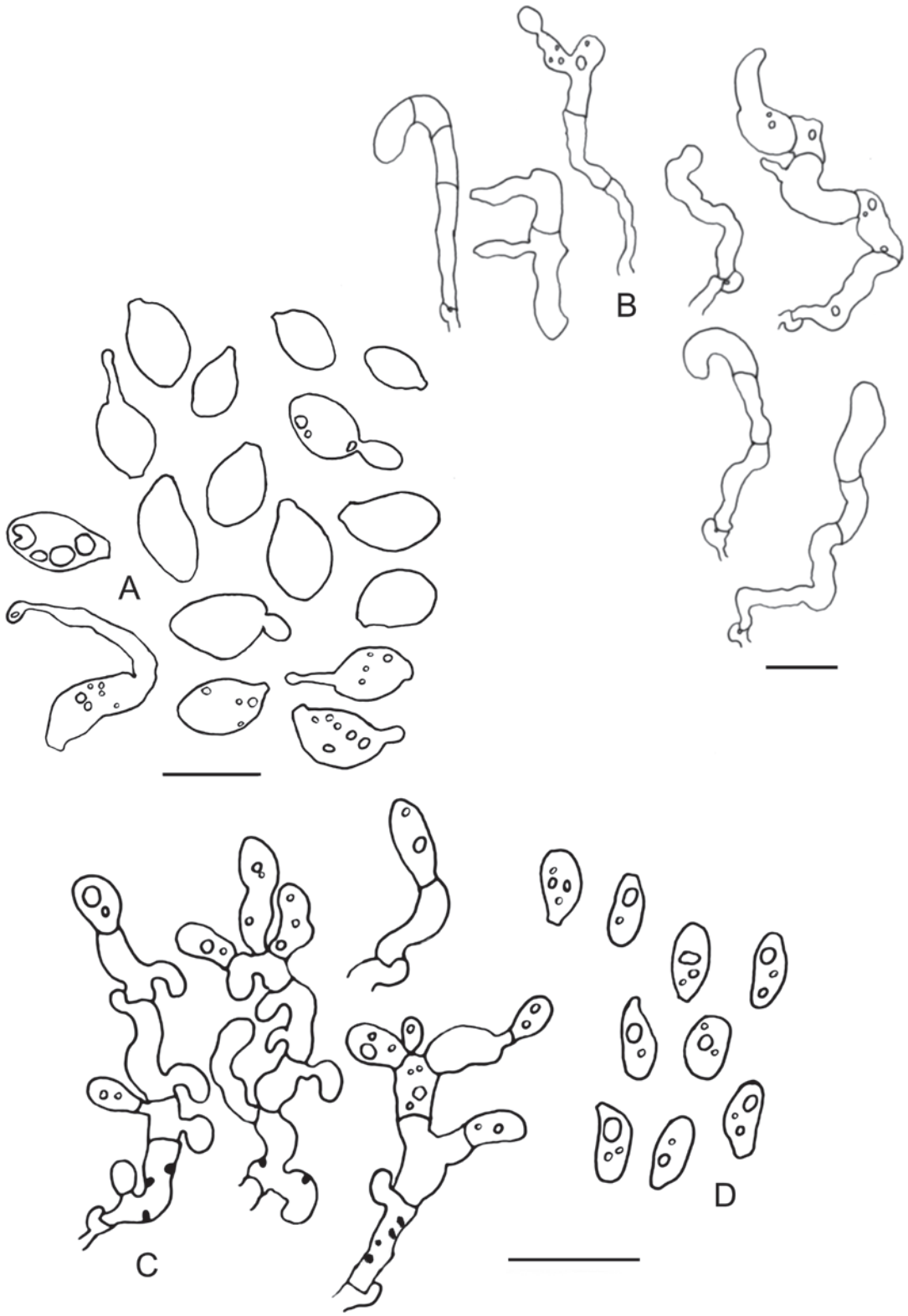

Fig. 20. *Mycogloiocolax gerardii sp. nov.* (TR 04096) line drawings. **A.** Basidiospores and germinating basidiospores by budding, hyphae and secondary spores. **B.** Basidia and basidioles. **C.** Conidiophores. **D.** Conidia. Black dots represent colacosomes. Scale bars = 10 µm.

Description of yeast morph: After growth on YM agar plates for 1 mo at 22 °C, the streak culture is white to cream-coloured, glistening, mucoid and smooth. The margin is entire. Cells are subglobose to ovoid, occurring singly or in pairs, and proliferating by polar budding. Good growth on D-glucose, D-arabinose, cellobiose, inulin, starch, glycerol, ribitol, D-glucitol, D-mannitol, galactitol, D-glucarate, D-tartaric acid, and L-malic acid. Weak growth on L-sorbose, D-glucosamine, D-ribose, L-arabinose, L-rhamnose, me a-D-glucoside, salicin, raffinose, erythritol, D-gluconate, and succinate. No growth on D-xylose, sucrose, maltose, a,a-trehalose, melibiose, lactose, melezitose, L-arabinitol, myo-inositol, 5-keto-D-gluconate, D-glucuronate, D-galacturonate, DL-lactate, citrate, ethanol, and L-tartaric acid. Weak growth in the presence of 5 % and 8 % but not 10 % NaCl. Growth on MEA with 50 % but not with 60 % glucose. No starch-like substance is produced. Urea hydrolysis and the Diazonium blue B reaction is positive. Maximum growth temperature: 35 °C.

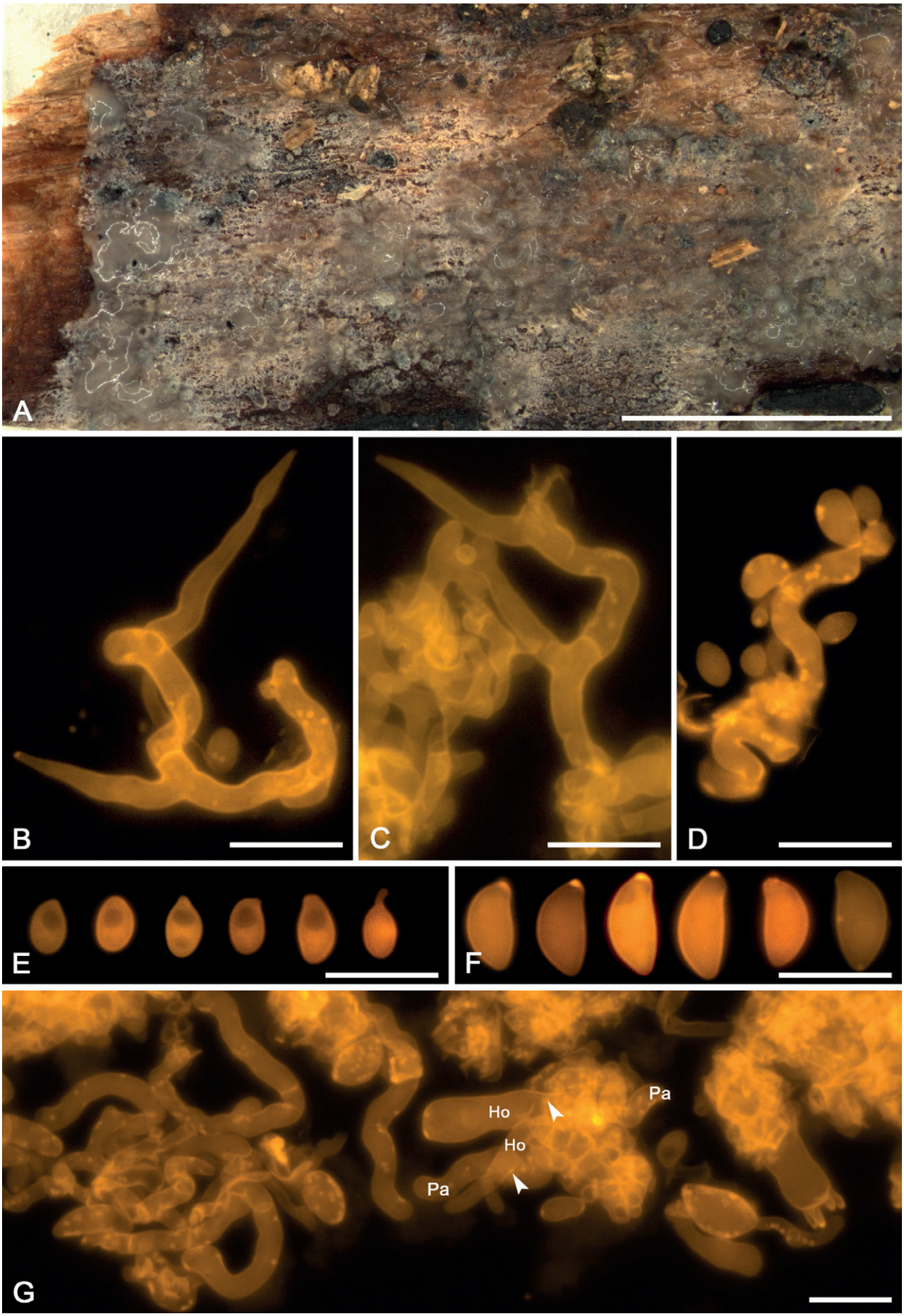

Fig. 21. *Mycogloiocolax gerardii sp. nov.* (TR 04096). **A.** Basidiome. **B, C.** One-septate basidia with two sterigmata. **D.** Conidiophore and conidia. **E.** Conidia. **F.** Basidiospores. **G.** Host–parasite interface, Pa = parasite hyphae, Ho = host hyphae, arrowheads indicate some positions of colacosomes. Scale bar: A = 1 cm; B–G = 10 µm.

Habitat and distribution: This species is an intrahymenial mycoparasite of the corticioid fungus *Xenasmatella tulasnelloidea*. Only three collections of this mycoparasite have currently been reported, from Denmark, France, and Germany. Based on the distribution of the host fungus, it is likely that this mycoparasite has a wider distribution than currently known and may be expected in various other (European) countries.

Materials examined: **Denmark**, Tadre Mølle, growing on the basidiome of *Xenasmatella tulasnelloidea*, 05 Jan. 2013, *T. Læssøe*, DMS-495673° = GENTFT00154 (GENT). **France**, Moselle, Neufchef, growing on the basidiome of *Xenasmatella tulasnelloidea* (as *Phlebiella tulasnelloidea*), 25 Jun. 2004, *G. Trichies*, GT 04098° (LIP).

Notes: This species has been reported and illustrated for the first time by Gerard Trichiès (2006), based on a collection from 2004 growing on *Xenasmatella tulasnelloidea*. Although the author realised that the specimen most likely represented an undescribed species, he decided not to describe it due to the limited set of micromorphological characters available for species delimitation. So far, it is the only mycoparasite reported from this host species. Colacosomes of *Mycogloiocolax gerardii sp. nov.* are formed in mycoparasite hyphae in places where physical contact with other hyphae occurs. Colacosomes can also be found in conidiophores, basidia and (germinating) basidiospores (Fig. 21D, G).

Updated classification of *Microbotryomycetes*

Below we provide an updated classification of the currently described genera in Microbotryomycetes, including colacosome-forming species.

Genera accepted in *Curvibasidiales*:
Curvibasidium Samp. & Golubev
Pseudoleucosporidium V. de García *et al.*

Genus accepted in *Heitmaniales*:
Heitmania X.Z. Liu *et al.*

Genera accepted in *Heterogastridiales*:
Atractocolax R. Kirschner *et al.*
Hyalopycnis Höhn (syn. *Heterogastridium* Oberw. & R. Bauer)
Pycnopulvinus Toome & Aime
Slooffia Q.M. Wang *et al.*

Genera accepted in *Kriegeriales*:
Kriegeria Bres.
Yamadamyces Q.M. Wang *et al.*
Meredithblackwellia Toome & Aime
Phenoliferia Q.M. Wang *et al.*
Libkindia Mašínová, A. Pontes *et al.*

Genera accepted in *Leucosporidiales*:
Leucosporidium Fell *et al.*
Sampaiozyma Q.M. Wang *et al.*

Genera accepted in *Sporidiobolales*:
Sporobolomyces Kluyver & C.B. Niel
Rhodosporidiobolus Q.M. Wang *et al.*
Rhodotorula F.C. Harrison

Genus accepted in *Rosettozymales*:
Rosettozyma Q.M. Wang & F.Y. Bai

Genera accepted in *Camptobasidiaceae*:
Camptobasidium Marvanová & Suberkr.
Glaciozyma Turchetti *et al.*
Cryolevonia A. Pontes *et al.*
Psychromyces L. Perini & Zalar

Genera accepted in *Chrysozymaceae*:
Chrysozyma Q.M. Wang *et al.*
Bannozyma Q.M. Wang *et al.*
Fellozyma Q.M. Wang *et al.*
Hamamotoa Q.M. Wang *et al.*
Yurkovia Mašínová *et al.*

Genera accepted in *Colacogloeaceae*:
Colacogloea Oberw. & Bandoni
Udeniozyma Q.M. Wang *et al.*

Genus accepted in *Mycogloiocolacaceae fam. nov.*:
Mycogloiocolax Schoutteten & Rödel *gen. nov.*

Microbotryomycetes incertae sedis:
Oberwinklerozyma Q.M. Wang *et al.*
Pseudohyphozyma Q.M. Wang *et al.*
Reniforma Pore & Sorenson
Spencerozyma Q.M. Wang *et al.*
Trigonosporomyces Q.M. Wang *et al.*
Vonarxula Q.M. Wang *et al.*
Yunzhangia Q.M. Wang *et al.*

DISCUSSION

In order to formulate an evolutionary hypothesis on colacosome-interacting mycoparasites in *Microbotryomycetes*, we organised the discussion in three major sections. In the first section, we focus on the proposed method for epifluorescence-based colacosome visualisation. The second section deals with three different aspects of the phylogenetic reconstruction, discussing (A) general aspects of the *Microbotryomycetes* phylogenetic reconstruction, (B) specific clades comprising colacosome-forming species and clades for which we sequenced additional loci, and (C) the phylogenetic distribution of colacosome-forming species. In the third section we discuss our results on the diversity, ecology and morphology of the four mycoparasitic genera investigated in this study: *Atractocolax*, *Colacogloea*, *Mycogloiocolax gen. nov.* and *Slooffia*.

Epifluorescence-based colacosome visualisation

The detection of colacosomes in fungi is an indispensable step in order to understand the species diversity that form these structures, as well as the evolution of the colacosome-interaction. Most previous reports of colacosomes were solely based on TEM imaging of fungal samples, derived either from (co-)cultures or directly from fresh basidiomata (Table 1). We describe an epifluorescence-based method to easily detect colacosomes and infer their organisation. This is in contrast to Oberwinkler & Bauer (2018) who stressed the necessity of TEM for the detection of colacosomes. The sample preparation encompasses conventional Congo red staining of whole-mount preparations (Clémençon

2009). We showed that epifluorescence microscopy is a more suitable method to detect colacosomes because it provides more contrast compared to traditional brightfield imaging. Colacosomes are clearly visible as they emit intense fluorescent signals in the red part of the spectrum upon illumination with green fluorescent light. Congo red strongly stains the secondary cell wall surrounding the colacosomes (Fig. 2C), which was shown by Kreger-van Rij & Veenhuis (1971b) to be a chitin-rich structure. Congo red has a strong affinity for chitin and polysaccharides (Matsuoka *et al.* 1995). Additionally, host- and parasite cell walls emit fluorescence signals that are strong enough to discriminate host and parasite hyphae and to determine the organisation of colacosomes. If nuclei need to be visualised, DAPI can be added to the Congo red staining solution, and DAPI emission can be observed using an appropriate UV filter set (Fig. 2B). In contrast to TEM, fluorescence microscopy is more accessible to researchers. Our approach requires a TRITC filter, which is one of the standard filter sets in most epifluorescence microscopes. Combined with the easy sample preparation, this method will allow more researchers to easily screen for the presence of colacosomes in fungal samples, and enlarge the list of species known to be capable of forming these structures.

Phylogenetic reconstruction

A. General *Microbotryomycetes* phylogeny

Our analysis of *Microbotryomycetes* included 33 isolates derived from colacosome-interacting mycoparasites belonging to the genera *Atractocolax*, *Colacogloea*, *Mycogloiocolax gen. nov.* and *Slooffia*. To obtain a better phylogenetic resolution, newly generated DNA sequences of ribosomal and/or protein-coding loci of *Colacogloea demeterae*, *Glaciozyma litorale*, *Hamamotoa cerberi*, *Hamamotoa telluris*, *Libkindia masarykiana*, *Slooffia velesii*, and *Yurkovia mendeliana* were analysed in the current study.

Our seven-locus ML phylogenetic reconstruction of the class *Microbotryomycetes* (Fig. 3) follows previous studies (Wang *et al.* 2015a, Li *et al.* 2020, Perini *et al.* 2021) and includes almost all currently described species from this group, except for the order *Microbotryales*, that is represented by ten isolates from four genera, similar to Wang *et al.* (2015a, b) and Li *et al.* (2020). Most previously described higher taxa within *Microbotryomycetes* are resolved as strongly supported monophyletic clades in our analysis (Table 5).

Our analysis reveals five distinct clades that were not yet assigned to higher taxa: 1) the lineage of the genus *Oberwinklerozyma*; 2) the lineage of the genera *Reniforma* and *Yunzhangia*, along with presently unclassified yeast isolates KBP Y-5457, KBP Y-4635 and KBP Y-4912; 3) the genus *Pseudohyphozyma*; 4) the genus *Slooffia*; and 5) the genus *Atractocolax*. The supported clustering of *Reniforma* and *Yunzhangia* as sister to *Microbotryales* was also observed in the seven-locus phylogenetic reconstruction of Li *et al.* (2020), whereas Wang *et al.* (2015a, b) found these two genera in a cluster with *Heterogastridium*. As in Li *et al.* (2020), the order *Rosettozymales* is found here to be sister to all other *Microbotryomycetes*, although with low support in both analyses. As observed in various previous studies, the phylogenetic relationships of the monotypic genera *Reniforma*, *Spencerozyma*, *Trigonosporomyces*, and *Vonarxula* remain unresolved, and these representatives are generally placed on long branches in phylogenetic ML analyses (Wang *et al.* 2015b, Li *et al.* 2020). Long branches can be the result of fast-evolving genetic regions and/or taxon sampling error (Prasanna *et al.* 2019, Galindo *et al.* 2021). Improved sampling will potentially lead to a more robust phylogenetic placement for these taxa.

Our phylogenetic analysis (Fig. 3) includes the recently described genera *Cryolevonia* and *Psychromyces* and revises the placement of the genera *Libkindia*, and *Yurkovia*, and the composition of the order *Kriegeriales*. The order *Kriegeriales* was erected by Toome & Aime (2013) based on phylogenetic analyses incorporating the three nuclear ribosomal loci SSU, ITS and LSU to accommodate the families *Camptobasidiaceae* and *Kriegeriaceae*. In our analysis, *Kriegeriales* is monophyletic and strongly supported, but only accommodates the family *Kriegeriaceae*, with the genera *Kriegeria*, *Libkindia*, *Meredithblackwellia*, *Phenolipheria* and *Yamadamyces*. Similar to findings by Wang *et al.* (2015a), Mašínová *et al.* (2017), de Garcia *et al.* (2020), Li *et al.* (2020) and Perini *et al.* (2021), our analysis reveals *Camptobasidiaceae* as a separate monophyletic, strongly supported lineage including the genera *Camptobasidium*, *Glaciozyma*, *Cryolevonia*, and *Psychromyces*. The inclusion of *Camptobasidiaceae* in *Kriegeriales* seems to be an artefact retrieved in analyses based on phylogenetic reconstructions that only incorporate ribosomal DNA sequence data (Toome & Aime 2013, Wang *et al.* 2015a, Li *et al.* 2020). When nuclear (and mitochondrial) protein coding genes are incorporated in the analyses, both families are retrieved as separate monophyletic lineages (Li *et al.* 2020, Perini *et al.* 2021). However, due to the lack of support for deeper nodes, a possible sister relationship of the families cannot be ruled out.

Interestingly, the family *Kriegeriaceae* has not always been recovered as monophyletic by several authors (Wang *et al.* 2015b, Li *et al.* 2020, Pontes *et al.* 2020, Perini *et al.* 2021). On one hand, these analyses were sensitive to taxon sampling. On the other hand, we found that the published DNA sequences of the protein-coding genes *RPB1, RPB2, TEF-1α* and mitochondrial *CYT-B* for the type strains of *Kriegeria eriophori* (CBS 8387) and *Libkindia masarykiana* (PYCC 6886) and *Yurkovia mendeliana* (PYCC 6884) were in fact derived from *Candida* (*Ascomycota*) contaminations. Furthermore, for the ex-type strain of *Meredithblackwellia eburnea* only SSU, ITS and LSU rDNA sequences are available in public databases. It may be expected that accurate DNA sequences of the aforementioned protein-coding genes of these species will lead to more consistent phylogenetic reconstructions of *Microbotryomycetes*, and the family *Kriegeriaceae* and order *Kriegeriales* in particular. In our analyses, the genus *Yamadamyces* is polyphyletic (Fig. 3), and it could be argued that both *Yamadamyces* species should be placed in *Meredithblackwellia*. A more robust dataset could also reveal whether the two yeast genera *Meredithblackwellia* and *Yamadamyces* should be merged with the dimorphic genus *Kriegeria*. These genera share a unique morphology of budding yeast morphs, forming rosettes (Oberwinkler 2017). However, due to the lack of protein-coding DNA sequence data for multiple loci, we refrain from such taxonomic conclusions here.

B. Discussion of specific clades

Chrysozymaceae — This family was proposed by Wang *et al.* (2015b), to accommodate the genera *Bannozyma*, *Chrysozyma*, *Fellozyma*, and *Hamamotoa* which formed a strongly supported clade in seven-locus phylogenetic reconstructions (Wang *et al.* 2015a, b). In our phylogenetic reconstruction, this family is recovered as monophyletic, with an ultrafast bootstrap (UFB) support value of 92 (Fig. 3). Interestingly, in the analysis of Li *et al.* (2020), this family proved to be polyphyletic in a constrained LSU ML analyses, whereas in the seven-locus ML analysis this family was found strongly supported and monophyletic. Perini

et al. (2021) found this family to be monophyletic and strongly supported based on a seven-locus phylogenetic ML reconstruction (including SSU, 5.8S, LSU, *RPB1, RPB2, EF1-α* and *CYT-B*). In our analysis, three strongly supported clades can be recognised within this family: 1) the lineage with the genera *Bannozyma* and *Chrysozyma*, 2) the lineage comprising *Fellozyma*, *Hamamotoa cerberi* and *H. telluris*, and 3) the lineage comprising the genus *Yurkovia*, *Hamamotoa lignophila* and *H. singularis*. Our analyses indicate the genus *Hamamotoa* to be polyphyletic, based on which we propose *Fellozyma cerberi comb. nov.* and *Fellozyma telluris comb. nov.* These two species were described by Yurkov *et al.* (2016) using a LSU-based analysis. Even though the statistical support for the placement was low in their analysis (NJ: 53 %), the authors justified their placement to *Hamamotoa* by their high sequence similarity (99 %) to *H. singularis* (Yurkov *et al.* 2016). The polyphyly of *Hamamotoa* was also detected by Kachalkin (2022) based on a combined ITS-LSU analysis. Our study additionally highlights the fact that LSU phylogenies have strong limitations compared to multi-locus analyses. Comparing overall distances in the type genus of the family, *Chrysozyma*, and in the genera *Fellozyma*, *Hamamotoa* and *Yurkovia* (Fig. 3), we cannot exclude merging the three latter genera into a single genus in the future.

Colacogloeaceae — This family comprises the genera *Colacogloea* and *Udeniozyma*, and is retrieved as a monophyletic clade in our phylogenetic reconstruction (Fig. 3). The monotypic genus *Udeniozyma* is recovered as sister to the genus *Colacogloea* with strong bootstrap support. The same sister relationship was also recovered by Wang *et al.* (2015a, b) and Li *et al.* (2020). Similar to the pattern observed in the LSU-based phylogenetic ML reconstruction of Wang *et al.* (2021), the genus *Colacogloea* is composed of two distinct subclades. Subclade 1 comprises species recovered as yeast morphs from soils and phylloplanes, and no conjugation or filamentous morphs have been reported for them so far. Subclade 2 mainly comprises dimorphic species of which the filamentous morph represents a mycoparasitic stage and engages in colacosome-interaction. Subclade 2 includes the genus type *Colacogloea effusa*, and a few species isolated as yeasts from plant substrates for which the filamentous morph was not yet reported. Most likely all *Colacogloea* species are dimorphic colacosome-interacting mycoparasites. However, for many species the mycoparasitic stage remains to be discovered. This is especially true for *Colacogloea retinophila* and *C. terpenoidalis*, which are nested in subclade 2 and whose closest relatives are known to have a mycoparasitic stage. *Colacogloea philyla*, another member of subclade 2, was originally isolated as a yeast from bark beetle galleries. Crossing experiments using the available strains failed to induce dikaryotisation, and a filamentous morph was until now never reported (Sampaio 2011). We discovered that the filamentous morph of *C. philyla* is a mycoparasite developing in the hymenium of *Peniophorella pubera*. Whether the genus *Colacogloea* should be split in two based on these subclades remains to be seen, but we argue that this phylogenetic pattern alone, combined with insufficient knowledge on the biology and ecology of these species provide insufficient ground to make such decision.

Heterogastridiales — This order was established by Oberwinkler *et al.* (1990) along with the family *Heterogastridiaceae* to accommodate *Hyalopycnis blepharistoma*, a filamentous fungus originally described as asexually reproducing. Oberwinkler *et al.* (1990) observed the sexual stage of this fungus, for which they proposed the name *Heterogastridium pycnidioideum*, which serves as nomenclatural basis for the family and the order. Contrary to Aime *et al.* (2018), we advocate for the protection of the name *Heterogastridium* over *Hyalopycnis*. In our analysis, this species clusters with *Pycnopulvinus aurantiacus*. These two species produce pycnidioid and stilboid structures respectively, and both are presumed mycoparasites. Various colacosome-forming fungi from the genera *Atractocolax*, *Colacogloea* and *Krieglsteinera* have been tentatively assigned to this order based on micromorphological similarities and the presence of colacosomes, but these relationships have never been tested for phylogenetic support. We show that the genera *Atractocolax* and *Slooffia* can be assigned to *Heterogastridiales* (Fig. 3). On the contrary, the genus *Colacogloea* forms a well-supported and distinct clade in our analysis. It is possible that other, yet to be sequenced, *Colacogloea* species or *Krieglsteinera lasiosphaeriae* belong to *Heterogastridiales*. For the time being, we prefer to treat those species for which no genetic data is available as *Microbotryomycetes incertae sedis*.

C. Phylogenetic distribution of colacosome-forming species

Prior to this study, the presence of colacosomes was reported from 17 species from nine genera in *Microbotryomycetes* (Table 1). We provide evidence for the presence of colacosomes in eight more species belonging to three genera in this class, resulting in at least 25 species and 11 genera of *Microbotryomycetes* from which colacosomes are reported. Phylogenetically, colacosome-forming species are widely distributed within this class, and are currently reported from six lineages: the families *Chrysozymaceae*, *Colacogloeaceae*, and *Mycogloiocolacaceae fam. nov.*, and orders *Heterogastridiales*, *Leucosporidiales*, and *Sporidiobolales*. The clade with most colacosome-forming taxa is *Colacogloeaceae* (eight species), followed by *Sporidiobolales* (five species) and *Leucosporidiales* (four species). Within *Colacogloeaceae*, colacosome-forming species are restricted to the so-called subclade 2 of the genus *Colacogloea* (*sensu* Wang *et al.* 2021), which contains all currently known mycoparasites within the genus. As outlined below, reconstructing the evolution of the capability of colacosome formation in *Microbotryomycetes* remains difficult for two major reasons, being firstly, an insufficient screening for these structures, and secondly, a poor phylogenetic resolution of the deeper nodes of this class.

As shown in Fig. 3, only few species of *Microbotryomycetes* have been subjected to adequate screening for the presence of colacosomes. We believe that the vast majority of Microbotryomycetes are dimorphic fungi, although for many species only the haploid stage or yeast morph is known. It should be considered that colacosomes are generally produced only in the dikaryotic stage of the lifecycle of these organisms, which requires conjugation of cells from compatible strains and it might be complicated to obtain in culture under laboratory conditions due to the lack of a compatible strain. Since only one or a few strains are available for the majority of *Microbotryomycetes*, compatible strains for crossing experiments are rarely available. Also, for some species, colacosome forming may require the presence of a suitable host. Consequently, the situation in which for a certain species the dikaryotic stage was not observed, or colacosomes have not been observed, should not be interpreted as the proved inability of that respective species to produce colacosomes. Due to these reasons, proving the inability of a species to produce colacosomes is very difficult, and a certain degree of ambiguity will often remain. As a good example, Sampaio *et al.* (2003) applied such crossing experiments in a number of *Microbotryomycetes*.

The authors assessed the presence of colacosomes based on TEM investigation of yeast- and filamentous morphs, and reported four species which were devoid of colacosomes, *i.e.*, *Camptobasidium hydrophylum*, *Kriegeria eriophori*, *Glaciozyma antarctica*, and *Pseudoleucosporidium fasciculatum*.

The second reason is that the absence of strongly supported deeper nodes in phylogenetic reconstructions of *Microbotryomycetes* does not allow to infer relationships between the different clades and, thus, predict the presence of colacosomes in ancestors and any random species within *Microbotryomycetes*. One distinct pattern that was already reported is the absence of colacosomes in the two phytoparasitic lineages within *Microbotryomycetes*, namely the genus *Kriegeria* and the order comprising anther smuts, *Microbotryales* (Sampaio *et al.* 2003, Bauer 2004, Bauer *et al.* 2006). Weiß *et al.* (2004) already suggested that phytoparasitic lineages in *Microbotryomycetes*, *i.e.*, *Microbotryales* and *Kriegeria*, most likely evolved from colacosome-interacting mycoparasitic ancestors. This hypothesis is strongly supported by our data, given the wide phylogenetic distribution of the colacosome-interaction and mycoparasitic taxa in our reconstruction of *Microbotryomycetes*.

Mycoparasitic genera in *Microbotryomycetes*

The genus *Colacogloea*

The genus *Platygloea* comprises a heterogenous group of fungi that only shares the character of transversally septate basidia (Schröter 1887, Bandoni 1956). Bourdot & Galzin (1909) described *Platygloea peniophorae* as a mycoparasite of the corticioid fungi *Peniophorella praetermissa* and *Peniophorella pubera*. Following the discovery of colacosomes in *Platygloea peniophorae* by Bauer and Oberwinkler (1991), the genus *Colacogloea* was introduced for this species (Oberwinkler *et al.* 1990a). The authors argued that the combined occurrence of simple septal pores, colacosomes, and yeast budding of basidiospores is sufficient to separate *Pl. peniophorae* from *Platygloea disciformis*, which is considered the type species of the genus *Platygloea* (syn. *Achroomyces*). Following the introduction of the genus *Colacogloea*, three more filamentous mycoparasites were assigned to the genus, based on the presence of colacosomes: *C. allantospora*, *C. bispora*, and *C. papilionacea* (Oberwinkler *et al.* 1999, Kirschner & Oberwinkler 2000, Bandoni *et al.* 2002). More recently, Wang *et al.* (2015a, b) assigned several yeast species from the genera *Rhodotorula* and *Sporobolomyces* to the genus *Colacogloea* based on phylogenetic reconstructions. These species were isolated as yeasts from various substrates, mostly plants and soils, but little is known about their ecology. Although it may be assumed these species have dimorphic lifecycles, only the yeast morph was observed for these species, and the presence of colacosomes has not been assessed (Wang *et al.* 2015b, Yurkov *et al.* 2016, Li *et al.* 2021, Wang *et al.* 2021).

The instatement of the genus *Colacogloea* to accommodate the mycoparasite *Platygloea peniophorae* resulted in the name *Colacogloea peniophorae*, which was assigned as generic type (Oberwinkler *et al.* 1990a). Recently, Malysheva *et al.* (2021) provided evidence for the synonymy of *Platygloea effusa* and *C. peniophorae*, and proposed the name *Colacogloea effusa* as valid name for this taxon. *Platygloea effusa* was originally interpreted as a resupinate saprobic species with transversally septate basidia growing on rotten stumps, and was not recognised as a mycoparasite at that time (Schröter 1887). Malysheva *et al.* (2021) assigned a neotype for *Platygloea effusa*, but the authors did not provide typification of *Platygloea peniophorae*. Here, we selected a lectotype from the herbarium of Bourdot (PC) which was used for the original description of *Platygloea peniophorae*, and assigned an epitype to support the lectotype. The selected epitype was recently collected in the same area of the lectotype, and its yeast morph was isolated in pure culture allowing molecular characterisation.

Literature research shows that the mycoparasite *Pl. peniophorae* has been reported and documented from Europe and North America (Bourdot & Maire 1920, Bourdot & Galzin 1928, Pilat 1957, Bandoni 1973). As outlined below, a certain degree of morphological variation has been observed, and two distinct morphotypes can be recognised.

In their seminal work *Hyménomycètes de France*, Bourdot & Galzin (1928) mentioned some degree of variation in macro- and micromorphological characters between studied collections of *Platygloea peniophorae* and assigned them to different forms of the same species (see also Bourdot & Maire 1920, Bourdot 1932). The authors also reported two different host species for this mycoparasite, but never suggested this taxon may comprise different species. The morphotype illustrated by Bourdot & Galzin (1928) is here referred to as the 'non-gall-like morphotype'.

Martin (1940) reported a strongly deviating collection from this typical *Platygloea peniophorae*. He illustrated an American collection of *Pl. peniophorae* (fig. 5 in Martin 1940), which produced vesicular gall-like cells and thick-walled oval conidia with attached remnants – here referred to as the 'gall-like morphotype' (Martin 1940). These characters described from Martins' collection are highly reminiscent of those that we observed in *Colacogloea bettinae sp. nov.* and *C. universitatis-gandavensis sp. nov.* (see Figs 6 and 18). Interestingly, Martin (1940) noted that these gall-like cells become filled with 'oval bodies' in some cases 'surrounding a central columella-like stalk'. These oval bodies can now be interpreted as colacosomes, surrounding an invaginating host hyphae in the gall-like cell of the mycoparasite. As such, Martin (1940) was the first to provide an illustrated report of colacosomes. Based on morphological studies of Canadian and European collections, Bandoni (1973) illustrated these two distinct morphotypes of *Pl. peniophorae* and argued they may constitute two different species, though he neither mentioned nor illustrated the gall-like cells. According to his insights, specimens of the gall-like morphotype are restricted to North America, whereas those of the non-gall-like morphotype occurred in both Europe and North-America. When Oberwinkler *et al.* (1990) proposed the genus *Colacogloea*, the authors investigated and illustrated the typical non-gall-like morphotype of *Pl. peniophorae*. They briefly mentioned the existence of the gall-like morphotype illustrated by Martin (1940) and suggested the two forms may comprise two different species. This idea was later supported by Greschner-Aschenbrenner (1997) based on detailed comparison of micromorphological and ultrastructural characters. However, her taxonomic conclusions were never formally published. We name one of our species after her, since she made the most in-depth comparative study of these two aforementioned morphotypes (see *C. bettinae sp. nov.*).

For our study of the *Colacogloea effusa* species complex, we studied freshly sampled European collections from Belgium, France, The Netherlands, Finland and Norway. Our collections were found on two different host species: *Peniophorella praetermissa* and *Pe. pubera*. Among our collections, we not only found the typical non-gall-like morphotype, but also the gall-like morphotype as illustrated by Martin (1940), which until now was believed to be restricted to North America (Bandoni 1973). A polyphasic approach combining micromorphological analyses, yeast morph characterisation, and a multilocus phylogenetic

reconstruction allow us to recognise seven different species within the *Colacogloea effusa* species complex. Most of our sequenced collections are assigned to *C. effusa* (syn. *Platygloea peniophorae*), which is a parasite of *Pe. praetermissa*. On the same host species, four other colacosome-forming mycoparasites can be recognised. Of them, *C. biconidiata sp. nov.*, *C. fennica sp. nov.*, and *C. microspora sp. nov.* resemble the non-gall-like morphotype, whereas *C. universitatis-gandavensis sp. nov.* resembles the gall-like morphotype. On the host *Pe. pubera*, two distinct mycoparasitic species were found. The first, *C. philyla*, constitutes the non-gall-like morphotype, whereas *C. bettinae sp. nov.* constitutes the gall-like morphotype. These seven species within the *C. effusa* complex can be separated based on a combination of characteristics such as yeast morph physiology, host species, shape and dimensions of spores, basidia, and conidia. Hallenberg *et al.* (2007) showed that *Pe. praetermissa*, one the two host species of the *C. effusa* species complex, constitutes a species complex itself. It is possible that the mycoparasites might be strictly host specific, although there currently is not enough data available to test this hypothesis.

Two major differences can be recognised between species of the gall-like (*Colacogloea bettinae sp. nov.* and *C. universitatis-gandavensis sp. nov.*) and the non-gall-like morphotypes (*C. biconidiata sp. nov., C. effusa*, *C. fennica sp. nov.*, *C. microspora sp. nov.*, and *C. philyla*).

The first difference concerns the conidiogenesis and the shape of conidia. In the gall-like morphotype, conidia are born on distinct, stalked conidiophores which consist of two apical lids, each giving rise to a daughter conidium (Figs 6C, 18D). In a later stage, these two daughter conidia merge, forming a zygoconidium. The content, incl. the nucleus, of one daughter conidium is transferred to the other daughter conidium. In the non-gall-like morphotype, conidia are born singly, with a basal clamp connection, and formed on conidiophores which can be interpreted as terminal hyphae (Figs 8C, 10C, 12C, 14C, 16C). In the gall-like morphotype, conidia are characterised by a regular, oval shape and the presence of an appendage (= cell wall remnants of the second daughter conidium of which the content was transferred) (Figs 6D, 18D). In species of the non-gall-like morphotype, conidia have a more irregular shape, and do not have such an appendage (Figs 8D, 10D, 12D, 14D, 16D). To date, zygoconidia have been reported from three different *Colacogloea* species: *C. bettinae sp. nov.*, *C. papilionacea* and *C. universitatis-gandavensis sp. nov.* (Kirschner & Oberwinkler 2000). This character is considered rare among *Basidiomycota*, with only few other genera sharing this character: *Papiliotrema*, *Trimorphomyces*, *Syzygospora* (*Tremellomycetes*), and *Zygogloea* (*Basidiomycota incertae sedis*) (Oberwinkler & Bandoni 1983, Roberts 1994, Weiß *et al.* 2014).

The second difference is the organisation of colacosomes in the hyphae of the mycoparasite. In the gall-like morphotype, most colacosomes are positioned at regular distances in vesicular gall-like cells along the host–parasite interface (Figs 6E, 18E). To a lesser extent, colacosomes also occur scattered in hyphae, conidiophores, or rarely, other elements of the mycoparasite. In the non-gall-like morphotype, no vesicular gall-like cells are present and colacosomes occur scattered in hyphae of the mycoparasite, with highest concentrations at those places where physical contact with host hyphae is established. In all the species that have been investigated by TEM, colacosomes were also observed in mycoparasite hyphae making contact with other hyphae of the same individual. This phenomenon was also observed in other colacosome-forming species and self-parasitism was put forward as an explanation for this phenomenon (Greschner-Aschenbrenner 1997, van der Klei *et al.* 2011). Both the scattered colacosome organisation and the organisation of colacosomes in vesicular gall-like cells have been observed in other mycoparasites in *Microbotryomycetes* and *Cryptomycocolacomycetes* (Table 1). Regarding the vesicular gall-like cells, an interesting question on whether the mycoparasite attracts a host hypha to grow into the invagination of the gall-like cell, or the gall-like cell actively overgrows a host hypha after which colacosomes are formed at the contact interface, remains unanswered.

The genus *Mycogloiocolax gen. nov.*

In this study, we erect the genus *Mycogloiocolax gen. nov.* and family *Mycogloiocolacaceae fam. nov.* for a clade comprising isolates of two distinct species. The first isolate represents *Mycogloiocolax gerardii sp. nov.*, a dimorphic fungus, of which the filamentous morph represents a colacosome-interacting mycoparasitic stage. This stage develops intrahymenially in the basidiome of the corticioid fungus *Xenasmatella tulasnelloidea* and is visible as a gelatinous, hyaline layer overgrowing the host in humid conditions. Its yeast morph was isolated in pure culture. Currently, this is the only known mycoparasite of *Xenasmatella* species. This species was reported for the first time by Trichies (2006), who illustrated his collection with drawings and a description, but did not decide to formally publish it as a new species. Due to the limited set of available morphological characteristics, he assigned his collection tentatively to the genus *Achroomyces*, which is a heterogenous gathering of *Basidiomycota* with transversally septate basidia. In his description, he mentions the basidia as strictly bisporic. We observed only bisporic basidia with sterigmata, although we also observed some basidioles with two and three septa, but never with outgrowing sterigmata in these cases.

The second isolate in this clade represents the yeast strain KBP Y-6479 (DSM 110867), representing a currently undescribed species. It was derived as an endophyte from a lichen thallus of *Cladonia rangiferina*, collected near Pokachi town, Tyumen region, Russia. We know this species only from this single strain, and its ecology and distribution patterns remain largely unknown (Dr. Aleksey Kachalkin, pers. comm.). Physiologically, strain KBP Y-6479 differs very markedly from *Mycogloiocolax gerardii sp. nov.*, and has a maximum growth temperature below 30 °C (Supplementary Table 1).

The genus *Slooffia*

The genus *Slooffia* was erected by Wang *et al.* (2015b) to accommodate yeast species comprising the *Sporobolomyces tsugae* clade. All these species were isolated as yeasts from different natural environments and substrates, including phylloplanes, dead organic material and soils. Only one or a few number of isolates are available for the currently known *Slooffia* species, and no filamentous morphs were reported in literature so far. The yeast morphs are considered to be saprobic (Sampaio 2011, Wang *et al.* 2015b, Begerow *et al.* 2018). *Slooffia micra comb. nov.* represents the first species in the genus for which the filamentous morph is observed in natural conditions, representing a colacosome-interacting mycoparasitic stage. It can be assumed that filamentous morphs of other *Slooffia* species exist, and it is possible that they also engage in mycoparasitism, although this remains to be investigated. As outlined below, the filamentous morph of *S. micra* has previously been illustrated and formally described under two names by different authors.

Bourdot & Galzin (1924) described *Platygloea micra* as a heterobasidiomycete with transversally septate basidia, growing on

rotten *Populus* wood. The authors did not mention the presence of a second fungal species or a possible mycoparasitic interaction in the description of their collection. Reinvestigation of the only specimen of this species in the herbarium of Bourdot (PC), showed the presence of hyphae, longitudinally septate basidia and basidiospores of the host species *Myxarium podlachicium*, although the state of these structures was degraded. The gelatinous context of the host basidiome was probably misinterpreted by Bourdot & Galzin (1924, 1928) as being part of *Pl. micra*. We easily detected the presence of colasosomes in hyphae of the mycoparasite by epifluorescence microscopy (result not shown). Hauerslev (1993) described *Achroomyces insignis* as an intrahymenial mycoparasite of *Myxarium podlachicium*, although he did not observe interaction structures. However, investigation of the holotype by epifluorescence microscopy clearly demonstrated the presence of colacosomes (Fig. 5). Interestingly, Hauerslev (1993) interpreted the conidia as chlamydospores (= thick-walled spores which are formed directly on hyphae), and did not mention the presence of the typical conidiophores (Fig. 5B). Comparing the type specimens of both species for their ecological and micromorphological characteristics, we conclude that *Platygloea micra* and *A. insignis* are conspecific. We select epitypes for both names and ex-type cultures are available for both types. The host–parasite interface of *Slooffia micra comb. nov.* is characterised by hyphae of the mycoparasite coiling around host hyphae. This results in rosette-like structures when imaged with epifluorescence microscopy (Fig. 5F, G). At the contact interface, colacosomes are densely arranged. To a lesser extent, colacosomes also occur scattered in hyphae of this species. The coiling of mycoparasite hyphae around host hyphae is also known from *Colacogloea papilionacea* (compare fig. 1 in Kirschner & Oberwinkler (2000) with Fig. 5F, G in this publication).

We investigated two other presumed mycoparasitic species of *Myxarium* spp. which have been published previously. *Platygloea abdita* Bandoni was described from the USA (Bandoni 1959), and *Cystobasidium sebaceum* G.W. Martin was described from Colombia (Martin 1939). Since no recent collections or cultures of these species are available, DNA sequence data is not available. Epifluorescence microscopy imaging of *Pl. abdita* and *Cystobasidium sebaceum* showed that both species are colacosome-interacting mycoparasites of *Myxarium* spp. (N. Schoutteten, results not shown). Differences in micromorphological characters suggest that these species are not conspecific with *Slooffia micra comb. nov.* (results not shown). Since both mycoparasites share the colacosome-interaction, the same type of conidiophores, and the same host genus as *S. micra*, it is possible that they belong to the genus *Slooffia*. However, such conclusions can only be made when DNA sequences are available and support is provided by phylogenetic reconstructions.

The genus *Atractocolax*

The genus *Atractocolax* was erected by Kirschner *et al.* (2001) to accommodate *A. pulvinatus*, a peculiar dimorphic mycoparasite, isolated from bark beetle galleries in decaying logs of coniferous tree species in Germany and Switzerland. This species develops pulvinate basidiomes and has transversally septate basidia. Passively released spores accumulate in slimy droplets extruding from the basidiome, which may be an adaptation to insect dispersal (Kirschner *et al.* 1999). Although the authors succeeded in isolating the species in axenic culture, DNA sequence data was never generated and its classification in *Microbotryomycetes* was tentative. In our seven-locus ML phylogenetic reconstruction (Fig. 3), *A. pulvinatus* is recovered as sister lineage to the clade of *Hyalopycnis* and *Pycnopulvinus*, and thus we propose to include this species in the order *Heterogastridiales*.

It is unclear whether the samples for TEM were derived from mixed or axenic cultures, but the published pictures only show colacosomes interacting with hyphae of the mycoparasite itself (Kirschner 1999, Oberwinkler & Bauer 2018). The host range of *A. pulvinatus* is not known, but it is assumed that the host is an ophiostomatoid ascomycete, a group of fungi frequently co-occurring on the same substrate (Kirschner *et al.* 1999). To our knowledge, the species was never recollected in its sexual morph after the original publication. A search for similar sequences in public sequence databases revealed three yeasts from a study screening for xylose-fermenting yeasts in the gut microbiome of the wood-feeding termite *Reticulitermes chinensis* (Ali *et al.* 2017). These isolates were originally identified as *Hamamotoa lignophila*. Our results show that these three isolates are conspecific with *A. pulvinatus*. By extrapolating physiological results of Ali *et al.* (2017), we conclude that *A. pulvinatus* is capable of fermenting D-xylose and producing ethanol. Anaerobic conversion of carbohydrates, fermentation, is rare among *Basidiomycota* species, and is limited to slow glucose fermentation by, *e.g.*, *Rhynchogastrema glucofermentans*, *Filobasidium capsuligenum*, and species of the genera *Mrakia* and *Phaffia* (*Tremellomycetes*) (Fell 2011, Fell & Johnson 2011, Kwon-Chung 2011). Touchette *et al.* (2022) recently reported fermentation of glucose for one other species in *Microbotryomycetes*, *i.e.*, *Rhodotorula frigidialcoholis*, suggesting that production of ethanol could be a yet little studied adaptation to life at low temperatures. This character should be carefully studied in the future for other representatives of this class, especially those isolated from cold habitats.

CONCLUSIONS

The present study demonstrates the diversity of colacosome-forming fungi in *Microbotryomycetes* and shows the utility of Congo red staining combined with epifluorescence microscopy for easy colacosome detection. Freshly collected and cultivated colacosome-forming mycoparasites allowed analyses of micromorphology, yeast morph characterisation, and generation of nucleotide sequence data. Based on our results, the total number of fungi in which colacosomes have been detected increases to 27. We reveal three distinct types of colacosome organisation in *Microbotryomycetes*, being a scattered occurrence, hyphae of the mycoparasite coiled around host hyphae, and vesicular gall-like cells of the mycoparasite surrounding host hyphae. We show that the colacosome-forming fungus *Atractocolax pulvinatus* is a member of *Microbotryomycetes*, related to *Slooffia* and other members of *Heterogastridiales*. *Platygloea micra* is identified as a colacosome-interacting mycoparasite of *Myxarium podlachicum*. This species is combined in the genus *Slooffia*, hitherto only known from yeast morphs, and thus it represents the first species for which a filamentous morph is reported, representing a mycoparasitic stage. In the genus *Colacogloea*, five new species are described in the *C. effusa* species complex, and the first report of the filamentous morph of *C. philyla* is presented as a colacosome-interacting mycoparasite. The family *Mycogloiocolacaceae fam. nov.* is proposed for the newly described *Mycogloiocolax gerardii sp. nov.*, a colacosome-interacting mycoparasite of *Xenasmatella tulasnelloidea*. Sequences obtained from these mycoparasites, derived from yeast cultures and filamentous morphs, allowed us to produce a robust phylogeny of *Microbotryomycetes*, resolving

several problematic taxa. Within *Microbotryomycetes*, colacosomes occur in the families *Chrysozymaceae*, *Colacogloeaceae*, and *Mycogloiocolacaceae fam. nov.* and the orders *Heterogastridiales*, *Leucosporidiales*, and *Sporidiobolales*. A mycoparasitic strategy is likely for species that were found to only produce colacosomes in pure culture, although their host range remains to be determined. These combined results improve our understanding of the diversity and ecology of *Microbotryomycetes*. Further field sampling and careful analyses of mycoparasites and lichenicolous fungi, including their cultivation, will be key to further resolving evolutionary relationships in this class of fungi.

ACKNOWLEDGEMENTS

Research Foundation Flanders (FWO) supported this study through a PhD Fellowship Fundamental Research to Nathan Schoutteten (11E0420N) and a Junior Postdoctoral Fellowship to Danny Haelewaters (1206620N). The work of Otto Miettinen was supported by a project grant from the Academy of Finland (grant No. 315927). We are grateful to Myriam Claeys of the TEM Expertise Centrum of Ghent University. Dr Aleksey Kachalkin and Dr Vera Malysheva are gratefully acknowledged for providing DNA sequences and metadata of specific isolates, as well as providing comments on the manuscript. Dr Viacheslav Spirin is gratefully acknowledged for providing specimens, aid in microscopic examination of specimens, outlining the species descriptions, and advise on nomenclatural aspects. Sincere acknowledgements go to the Belgian and Dutch contributors of the Phragmoproject (https://www.mycologen.nl/onderzoek/systematiek-taxonomie/phragmo-project/): Roeland Enzlin, Martin Gotink, Ida Nannenga-Bruggeman, Hermien Wassink†, Inge Somhorst, Greet Van Autgaerden, Marc Detollenaere, and Bregtje Miedema; and to Thomas Rödel, who provided valuable collections for this research. Peter Roberts is gratefully acknowledged for providing comments on the group of *Platygloea micra*. Juliana Leshchenko is greatfully acknowledged for editing figure 1. We are grateful to Geoffrey Kibby for editing drawings and proofreading of the manuscript. Ruben De Lange is gratefully acknowledged for proofreading the manuscript. We acknowledge the fungaria of C, H, LIP, and PC for providing loans or access to specimens for investigation. Nadine Masuch (DSMZ) is acknowledged for assistance in the lab.

DECLARATION ON CONFLICT OF INTEREST

The authors declare that there is no conflict of interest.

REFERENCES

Aime MC, Castlebury LA, Abbasi M, *et al.* (2018). Competing sexual and asexual generic names in *Pucciniomycotina* and *Ustilaginomycotina* (*Basidiomycota*) and recommendations for use. *IMA Fungus* **9**: 75–89.

Aime MC, Matheny PB, Henk DA, *et al.* (2006). An overview of the higher-level classification of *Pucciniomycotina* based on combined analyses of nuclear large and small subunit rDNA sequences. *Mycologia* **98**: 896–905.

Aime MC, Toome M, McLaughlin DJ (2014). *Pucciniomycotina*. In: *The Mycota VII. Systematics and evolution. Part A.* (McLaughlin DJ, Spatafora JW eds). Springer, Germany: 271–294.

Ali SS, Wu J, Xie R, *et al.* (2017). Screening and characterizing of xylanolytic and xylose-fermenting yeasts isolated from the wood-feeding termite, *Reticulitermes chinensis*. *PLoS One* **12**: e0181141.

Bandoni RJ (1956). A preliminary survey of the genus *Platygloea*. *Mycologia* **48**: 821–840.

Bandoni RJ (1959). An undescribed species of *Platygloea* from Iowa. *Mycologia* **51**: 94–96.

Bandoni RJ (1973). Epistolae mycologicae II. Species of *Platygloea* from British Columbia. *Syesis* **6**: 229–232.

Bandoni RJ (1995). Dimorphic *Heterobasidiomycetes*: taxonomy and parasitism. *Studies in Mycology* **38**: 13–28.

Bandoni RJ, Krug J, Ginns J (2002). On some *Colacogloea* species from Canada. *Czech Mycology* **54**: 31–43.

Bauer R (2004). Basidiomycetous interfungal cellular interactions–a synopsis. In: *Frontiers in basidiomycote mycology*. (Agerer R, Piepenbring M, Blanz P, eds). IHW-Verlag, Germany**:** 325–337.

Bauer R, Begerow D, Sampaio JP, *et al.* (2006). The simple-septate basidiomycetes: a synopsis. *Mycological Progress* **5**: 41–66.

Bauer R, Lutz M, Oberwinkler F (2004). *Tuberculina*-rusts: a unique basidiomycetous interfungal cellular interaction with horizontal nuclear transfer. *Mycologia* **96**: 960–967.

Bauer R, Oberwinkler F (1991). The Colacosomes: New Structures at the Host-parasite Interface of a Mycoparasitic Basidiomycete. *Botanica Acta* **104**: 53–57.

Bauer R, Oberwinkler F, Vánky K (1997). Ultrastructural markers and systematics in smut fungi and allied taxa. *Canadian Journal of Botany* **75**: 1273–1314.

Begerow D, Kemler M, Feige A, *et al.* (2017). Parasitism in yeasts. In: *Yeasts in natural ecosystems: Ecology*. (Buzzini P, Lachance MA, Yurkov A, eds). Springer Cham, Switserland: 179–210.

Begerow D, McTaggart A, Agerer R (2018). 1/3 *Basidiomycota* and *Entorrhizomycota* In: *A. Engler's Syllabus der Pflanzenfamilien* (Frey W, ed). Bontraeger Science Publishers, Germany.

Beguin H (2010). *Tritirachium egenum*, a thiamine-and siderophore-auxotrophic fungal species isolated from a *Penicillium rugulosum*. *FEMS Microbiology Ecology* **74**: 165–173.

Bezerra JDP, Santos MGS, Barbosa RN, *et al.* (2013). Fungal endophytes from cactus Cereus jamacaru in Brazilian tropical dry forest: a first study. *Symbiosis* **60**: 53–63.

Biswas SK, Yokoyama K, Nishimura K, *et al.* (2001). Molecular phylogenetics of the genus *Rhodotorula* and related basidiomycetous yeasts inferred from the mitochondrial cytochrome b gene. *International Journal of Systematic and Evolutionary Microbiology* **51**: 1191–1199.

Boekhout T, Fonseca A, Sampaio JP, *et al.* (2011). Discussion of teleomorphic and anamorphic basidiomycetous yeasts. In: *The yeasts* (Kurtzman CP, Fell JW, Boekhout T, eds). Elsevier, Germany: 1339–1372.

Boekhout T, Yamada Y, Weijman A, *et al.* (1992). The significance of coenzyme Q, carbohydrate composition and septal ultrastructure for the taxonomy of ballistoconidia-forming yeasts and fungi. *Systematic and Applied Microbiology* **15**: 1–10.

Bourdot H (1932). Hyménomycètes nouveaux ou peu connus. *Bulletin Trimestriel de la Société Mycologique de France* **48**: 204–232.

Bourdot H, Galzin A (1909). Hyménomycètes de France. I Hetérobasidiés. *Bulletin Trimestriel de la Société Mycologique de France* **25**: 14–36.

Bourdot H, Galzin A (1924). Heterobasidiae nondum descriptae. *Bulletin Trimestriel de la Société Mycologique de France* **39**: 261–266.

Bourdot H, Galzin A (1928). *Hyménomycètes de France. Hétérobasidiés — homobasidiés gymnocarpes*. P. Lechevalier, published under the auspices of the Société Mycologique de France, France.

Bourdot H, Maire L (1920). Notes critiques sur quelques Hymenomycètes nouveaux ou peu connus. *Bulletin Trimestriel de la Société Mycologique de France* **36**: 69–85.

Brefeld O (1888). *Basidiomyceten II. Protobasidiomyceten. Untersuchungen aus den Gesammtgebiet der Mykologie 7*. Arthur Felix Verlag, Germany.

Buzzini P, Lachance MA, Yurkov A (Eds). (2017). *Yeasts in natural ecosystems: diversity*. Springer Cham, Switserland.

Buzzini P, Turchetti B, Yurkov A (2018). Extremophilic yeasts: the toughest yeasts around? *Yeast* **35**: 487–497.

Caiafa MV, Smith ME (2022). Polyphyly, asexual reproduction and dual trophic mode in *Buchwaldoboletus*. *Fungal Ecology* **56**: 101141.

Capella-Gutiérrez S, Silla-Martínez JM, Gabaldón T (2009). trimAl: a tool for automated alignment trimming in large-scale phylogenetic analyses. *Bioinformatics* **25**: 1972–1973.

Chernomor O, Von Haeseler A, Minh BQ (2016). Terrace aware data structure for phylogenomic inference from supermatrices. *Systematic Biology* **65**: 997–1008.

Clémençon H (2009). *Methods for Working with Macrofungi. Laboratory Cultivation and Preparation of Larger Fungi for Light Microscopy.* IHW-Verlag, Germany.

Cubeta MA, Echandi E, Abernethy T, *et al.* (1991). Characterization of anastomosis groups of binucleate *Rhizoctonia* species using restriction analysis of an amplified ribosomal RNA gene. *Phytopathology* **81**: 1395–1400.

De Garcia V, Trochine A, Uetake J, *et al.* (2020). Novel yeast taxa from the cold: description of *Cryolevonia giraudoae sp. nov.* and *Camptobasidium gelus sp. nov. International Journal of Systematic and Evolutionary Microbiology* **70**: 3711–3717.

De Hoog GS, Boekhout T (1982). Teliospores, teliospore-mimics and chlamydospores. *Studies in Mycology* **22**: 15–22.

Doweld A (2001). *Prosyllabus Tracheophytorum: Tentamen Systematis Plantarum Vascularium Tracheophy*. Geos, Russian Federation.

Doweld A (2014). Nomenclatural novelties. *Index Fungorum* **95**.

Fell JW (2011). *Mrakia* Y. Yamada & Komagata (1987). In: *The Yeasts* (Kurtzman CP, Fell JW, Boekhout T, eds). Elsevier, Germany: 1503–1510.

Fell JW, Johnson EA (2011). *Phaffia* MW Miller, Yoneyama & Soneda (1976). In: *The Yeasts* (Kurtzman CP, Fell JW, Boekhout T, eds). Elsevier, Germany: 1853–1855.

Gardes M, Bruns TD (1993). ITS primers with enhanced specificity for basidiomycetes - application to the identification of mycorrhizae and rusts. *Molecular Ecology* **2**: 113–118.

Galindo LJ, López-García P, Torruella G, *et al.* (2021). Phylogenomics of a new fungal phylum reveals multiple waves of reductive evolution across *Holomycota*. *Nature communications* **12**: 1–14.

Greschner-Aschenbrenner B (1997). *Vergleichende morphologische und ultrastrukturelle Untersuchungen an Colacogloea–Arten*. Diplomarbeit, Lehrstühl Spezieller Botanik und Mykologie, Universität Tübingen, Germany.

Hallenberg N, Nilsson RH, Antonelli A, *et al.* (2007). The *Peniophorella praetermissa* species complex (*Basidiomycota*). *Mycological Research* **111**: 1366–1376.

Hamamoto M, Boekhout T, Nakase T (2011). *Sporobolomyces* Kluyver & van Niel (1924). In: *The yeasts* (Kurtzman CP, Fell JW, Boekhout T, eds). Elsevier, Germany: 1929–1990.

Hauerslev K (1993). New tremellaceous fungi from Denmark. *Mycotaxon* **49**: 217–233.

Hass H, Taylor TN, Remy W (1994). Fungi from the Lower Devonian Rhynie chert: Mycoparasitism. *American Journal of Botany* **81**: 29–37.

He MQ, Zhao RL, Hyde KD, *et al.* (2019). Notes, outline and divergence times of *Basidiomycota*. *Fungal Diversity* **99**: 105–367.

Hoang DT, Chernomor O, von Haeseler A, *et al.* (2018). UFBoot2: Improving the ultrafast bootstrap approximation. *Molecular Biology and Evolution* **35**: 518–522.

Kachalkin AV (2014). Yeasts of the White Sea intertidal zone and description of *Glaciozyma litorale sp. nov. Antonie van Leeuwenhoek* **105**: 1073–1083.

Kachalkin AV (2022). Phylogeny of *Rhodotorula pinalis* and its reclassification as *Fellozyma pinalis comb. nov. Microbiology* **91**: 417–420.

Kachalkin AV, Turchetti B, Inácio J, *et al.* (2019). Rare and undersampled dimorphic basidiomycetes. *Mycological Progress* **18**: 945–971.

Kalyaanamoorthy S, Minh BQ, Wong TKF, *et al.* (2017). ModelFinder: Fast Model Selection for Accurate Phylogenetic Estimates. *Nature Methods* **14**: 587–589.

Katoh K, Rozewicki J, Yamada KD (2019). MAFFT online service: multiple sequence alignment, interactive sequence choice and visualization. *Briefings in Bioinformatics* **20**: 1160–1166.

Kirk PM, Cannon PF, Minter DW, *et al.* (2008). *Dictionary of the Fungi.* 10th ed. CABI Europe, UK.

Kirschner R, Bauer R, Oberwinkler F (1999). *Atractocolax*, a new heterobasidiomycetous genus based on a species vectored by conifericolous bark beetles. *Mycologia* **91**: 538–543.

Kirschner R, Bauer R, Oberwinkler F (2001). *Colacosiphon*: a new genus described for a mycoparasitic fungus. *Mycologia* **93**: 634–644.

Kirschner R, Oberwinkler F (2000). A new species of *Colacogloea* with zygoconidia. *Sydowia* **52**: 195–203.

Kreger-van Rij NJW, Veenhuis M (1971a). A comparative study of the cell wall structure of basidiomycetous and related yeasts. *Microbiology* **68**: 87–95.

Kreger-van Rij NJW, Veenhuis M (1971b). Some features of yeasts of the genus *Sporidiobolus* observed by electron microscopy. *Antonie van Leeuwenhoek* **37**: 253–255.

Koch RA, Herr JR (2021). Transcriptomics Reveals the Putative Mycoparasitic Strategy of the Mushroom *Entoloma abortivum* on Species of the Mushroom Genus *Armillaria*. *Msystems* **6**: e00544-21.

Kumar S, Stecher G, Tamura K (2016). MEGA7: molecular evolutionary genetics analysis version 7.0 for bigger datasets. *Molecular Biology and Evolution* **33**: 1870–1874.

Kurtzman CP, Fell JW, Boekhout T, *et al.* (2011). Methods for isolation, phenotypic characterization and maintenance of yeasts. In: *The Yeasts* (Kurtzman CP, Fell JW, Boekhout T, eds). Elsevier, Germany: 87–110.

Kwon-Chung KJ (2011). *Filobasidium* Olive (1968). In: *The Yeasts* (Kurtzman CP, Fell JW, Boekhout T, eds). Elsevier, Germany: 1457–1465.

Li AH, Yuan FX, Groenewald M, *et al.* (2020). Diversity and phylogeny of basidiomycetous yeasts from plant leaves and soil: proposal of two new orders, three new families, eight new genera and one hundred and seven new species. *Studies in Mycology* **96**: 17–140.

Liu YJ, Whelen S, Hall BD (1999). Phylogenetic relationships among ascomycetes: evidence from an RNA polymerse II subunit. *Molecular Biology and Evolution* **16**: 1799–1808.

Lutz M, Bauer R, Begerow D, *et al.* (2004). *Tuberculina*: rust relatives attack rusts. *Mycologia* **96**: 614–626.

Malysheva V, Schoutteten N, Verbeken A, *et al.* (2021). Identity and typification of *Achroomyces effusus* (*Pucciniomycotina*, *Basidiomycota*). *Mycological Progress* **20**: 413–417.

Martin GW (1939). New or noteworthy fungi from Panama and Colombia. *Mycologia* **31**: 507–518.

Martin GW (1940). Some heterobasidiomycetes from eastern Canada. *Mycologia* **32**: 683–695.

Mašínová T, Pontes A, Carvalho C, *et al.* (2017). *Libkindia masarykiana gen. et sp. nov.*, *Yurkovia mendeliana gen. et sp. nov.* and *Leucosporidium krtinense fa sp. nov.*, isolated from temperate forest soils. *International Journal of Systematic and Evolutionary Microbiology* **67**: 902–908.

Matheny PB (2005). Improving phylogenetic inference of mushrooms with RPB1 and RPB2 nucleotide sequences. *Inocybe*; *Agaricales*. *Molecular Phylogenetics and Evolution* **35**: 1–20.

Matheny PB, Liu YJ, Ammirati JF, *et al.* (2002). Using RPB1 sequences to improve phylogenetic inference among mushrooms. *Inocybe*, *Agaricales*. *American Journal of Botany* **89**: 688–698.

Matsuoka H, Yang HC, Homma T, *et al.* (1995). Use of Congo red as a microscopic fluorescence indicator of hyphal growth. *Applied Microbiology and Biotechnology* **43**: 102–108.

Menolli N Jr, Sánchez-García M (2020). Brazilian fungal diversity represented by DNA markers generated over 20 years. *Brazilian Journal of Microbiology* **51**: 729–749.

Moore RT (1972). *Ustomycota*, a new division of higher fungi. *Antonie van Leeuwenhoek* **38**: 567–584.

Moore RT (1996). An inventory of the phylum *Ustomycota*. *Mycotaxon* **59**: 1–31.

Naranjo-Ortiz MA, Gabaldón T (2019). Fungal evolution: major ecological adaptations and evolutionary transitions. *Biological Reviews* **94**: 1443–1476.

Nguyen LT, Schmidt HA, von Haeseler A, *et al.* (2015) IQ-TREE: A fast and effective stochastic algorithm for estimating maximum likelihood phylogenies. *Molecular Biology and Evolution* **32**: 268–274.

Oberwinkler F (1964). Intrahymeniale Heterobasidiomyceten. Fruchtkörperlose *Sebacina*-Sippen und ihre systematische Stellung. *Nova Hedwigia* **7**: 489–499.

Oberwinkler F (2012). Evolutionary trends in *Basidiomycota*. *Stapfia* **96**: 45–104.

Oberwinkler F (2017). Yeasts in *Pucciniomycotina*. *Mycological Progress* **16**: 831–856.

Oberwinkler F, Bandoni RJ (1983). *Trimorphomyces*: a new genus in the *Tremellaceae*. *Systematic and Applied Microbiology* **4**: 105–113.

Oberwinkler F, Bauer R (1990). *Cryptomycocolax*: a new mycoparasitic heterobasidiomycete. *Mycologia* **82**: 671–692.

Oberwinkler F, Bauer R (2018). Ultrastructure in basidiomycetes–requirement for function. In: *Biodiversity and Ecology of Fungi, Lichens, and Mosses*. (Blanz P, ed). Austrian Academy of Sciences Press, Austria: 381–418.

Oberwinkler F, Bauer R, Bandoni RJ (1990a). *Colacogloea* - A new genus in the auricularioid *Heterobasidiomycetes*. *Canadian Journal of Botany* **68**: 2531–2536.

Oberwinkler F, Bauer R, Bandoni RJ (1990b). *Heterogastridiales*: a new order of *Basidiomycetes*. *Mycologia* **82**: 48–58.

Oberwinkler F, Bauer R, Tschen J (1999). The mycoparasitism of *Platygloea bispora*. *Kew Bulletin* **54**: 763–769.

Oberwinkler F, Cruz D, Suárez JP (2017). Biogeography and ecology of *Tulasnellaceae*. In: *Biogeography of mycorrhizal symbiosis*. (Tederso L, ed). Springer International Publishing AG, Switserland: 237–271.

O'donnell K (1993). *Fusarium* and its near relatives. In: *The fungal holomorph: mitotic, meiotic and pleomorphic speciation in fungal systematics* (Reynolds DR, Taylor JW, eds). CAB International, Great Britain: 225–233.

Parmasto E, Parmasto I (1987). Variation in basidiospores in the Hymenomycetes and its significance to their taxonomy. *Bibliotheca Mycologica* **115**: 1–168.

Passer AR, Coelho MA, Billmyre RB, *et al.* (2019). Genetic and genomic analyses reveal boundaries between species closely related to *Cryptococcus* pathogens. *Mbio* **10**(3)e00764-19.

Perini L, Andrejašič K, Gostinčar C, *et al.* (2021). Greenland and Svalbard glaciers host unknown basidiomycetes: the yeast *Camptobasidium arcticum sp. nov.* and the dimorphic *Psychromyces glacialis gen*. and *sp. nov. International Journal of Systematic and Evolutionary Microbiology* **71**: 004655.

Pilat A (1957). Übersicht der europäischen *Auriculariales* und *Tremellales* unter besonderer Berücksichtigung der Tschechoslowakischen Arten. *Acta Musei Nationalis Pragae* **13**: 115–210.

Pontes A, Ruethi J, Frey B, *et al.* (2020). *Cryolevonia* gen. *nov.* and *Cryolevonia schafbergensis sp. nov.*, a cryophilic yeast from ancient permafrost and melted sea ice. *International Journal of Systematic and Evolutionary Microbiology* **70**: 2334–2338.

Prasanna AN, Gerber D, Kijpornyongpan T, *et al.* (2019). Model choice, missing data, and taxon sampling impact phylogenomic inference of deep *Basidiomycota* relationships. *Systematic Biology* **69**: 17–37.

Redhead SA, Ammirati JF, Walker GR, *et al.* (1994). *Squamanita contortipes*, the Rosetta Stone of a mycoparasitic agaric genus. *Canadian Journal of Botany* **72**: 1812–1824.

Rehner SA, Buckley E (2005). A *Beauveria* phylogeny inferred from nuclear ITS and EF1-α sequences: evidence for cryptic diversification and links to *Cordyceps* teleomorphs. *Mycologia* **97**: 84–98.

Roberts P (1994). *Zygogloea gemellipara*: an auricularioid parasite of *Myxarium nucleatum*. *Mycotaxon* **52**: 241–246.

Sampaio JP (2011). *Rhodotorula* Harrison (1928). In: *The yeasts* (Kurtzman CP, Fell JW, Boekhout T, eds). Elsevier, Germany: 1873–1927.

Sampaio JP, Gadanho M, Bauer R, *et al.* (2003). Taxonomic studies in the *Microbotryomycetidae*: *Leucosporidium golubevii sp. nov.*, *Leucosporidiella gen. nov.* and the new orders *Leucosporidiales* and *Sporidiobolales*. *Mycological Progress* **2**: 53–68.

Sampaio JP, Kirschner R, Oberwinkler F (2011). *Colacogloea* Oberwinkler & Bandoni (1990). In: *The yeasts* (Kurtzman CP, Fell JW, Boekhout T, eds). Elsevier, Germany: 1403–1408.

Savchenko A, Zamora JC, Shirouzu T, *et al.* (2021). Revision of *Cerinomyces* (*Dacrymycetes*, *Basidiomycota*) with notes on morphologically and historically related taxa. *Studies in Mycology* **99**: 1–72.

Schröter J (1887). Die Pilze Schlesiens. In: *Kryptogamen Flora von Schlesien 3*. (Cohn, FJ ed). J. V. Kern's Verlag, Germany: 1–814.

Selosse MA, Schneider-Maunoury L, Martos F (2018). Time to re-think fungal ecology? Fungal ecological niches are often prejudged. *New Phytologist* **217**: 968–972.

Spirin V, Malysheva V, Roberts P, *et al.* (2019). A convolute diversity of the *Auriculariales* (*Agaricomycetes, Basidiomycota*) with sphaeropedunculate basidia. *Nordic Journal of Botany* **37**: 1–26.

Spirin V, Malysheva V, Trichies G, *et al.* (2018). A preliminary overview of the corticioid *Atractiellomycetes* (*Pucciniomycotina*, *Basidiomycetes*). *Fungal Systematics & Evolution* **2**: 311–340.

Thiers B (2022). *Index Herbariorum: A global directory of public herbaria and associated staff*. New York Botanical Garden's Virtual Herbarium. Accessed on 01 October 2022.

Toome M, Aime MC (2014). *Pycnopulvinus aurantiacus gen. et sp. nov.*, a new sporocarp-forming member of *Pucciniomycotina*. *MycoKeys* **8**: 43–50.

Toome M, Roberson RW, Aime MC (2013). *Meredithblackwellia eburnea gen. et sp. nov.*, *Kriegeriaceae fam. nov.* and *Kriegeriales ord. nov.* – toward resolving higher-level classification in *Microbotryomycetes*. *Mycologia* **105**: 486–495.

Touchette D, Altshuler I, Gostinčar C, *et al.* (2022). Novel Antarctic yeast adapts to cold by switching energy metabolism and increasing small RNA synthesis. *The ISME Journal* **16**: 221–232.

Trichies G (2006). Hétérobasidiomycètes inusuels ou nouveaux découverts en France. *Bulletin de la Société Mycologique de France* **122**: 29–60.

Van Der Klei I, Veenhuis M, Brul S, *et al.* (2011). Cytology, cell walls and septa: a summary of yeast cell biology from a phylogenetic perspective. In: *The yeasts – A taxonomic study,* Vol. 1, 5th edition (Kurtzman CP, Fell JW, Boekhout T, eds). Elsevier, Germany: 111–128.

Vilgalys R, Hester M (1990). Rapid genetic identification and mapping of enzymatically amplified DNA from several *Cryptococcus* species. *Journal of Bacteriology* **172**: 4238–4246.

Wang GS, Sun Y, Wang QM (2021). *Colacogloea armeniacae sp. nov.,* a novel pucciniomycetous yeast species isolated from apricots. *Mycoscience* **62**: 42–46.

Wang QM, Groenewald M, Takashima M, *et al.* (2015a). Phylogeny of yeasts and related filamentous fungi within *Pucciniomycotina* determined from multigene sequence analyses. *Studies in Mycology*, **81**: 27–53.

Wang QM, Yurkov AM, Göker M, *et al.* (2015b). Phylogenetic classification of yeasts and related taxa within *Pucciniomycotina*. *Studies in Mycology* **81**: 149–189.

Weiß M, Bauer R, Begerow D (2004). Spotlights on *heterobasidiomycetes*. In: *Frontiers in basidiomycote mycology*. (Agerer R, Piepenbring M, Blanz P, eds). IHW-Verlag, Germany: 7–48.

Weiß M, Bauer R, Sampaio JP, *et al.* (2014). *Tremellomycetes* and Related Groups. In: *The Mycota VII. Systematics and evolution. Part A.* (McLaughlin DJ, Spatafora JW, eds). Springer, Germany: 331–355.

Weiß M, Waller F, Zuccaro A, *et al.* (2016). *Sebacinales* – one thousand and one interactions with land plants. *New Phytologist* **211**: 20–40.

White TJ, Bruns T, Lee SJWT, *et al.* (1990). Amplification and direct sequencing of fungal ribosomal RNA genes for phylogenetics. In: *PCR protocols: a guide to methods and applications*. (Innis MA, Gelfand DH, Sninsky JJ, White TJ, eds). Academic Press Inc., USA: 315–322.

Willis KJ (ed.) (2018). *State of the Worlds Fungi 2018*. Report. Royal Botanic Gardens, Kew, Great Britain: 1–92.

Yurkov AM, Wehde T, Federici J, *et al.* (2016). Yeast diversity and species recovery rates from beech forest soils. *Mycological Progress* **15**: 845–859.

Zhao RL, Li GJ, Sánchez-Ramírez S, *et al.* (2017). A six-gene phylogenetic overview of *Basidiomycota* and allied phyla with estimated divergence times of higher taxa and a phyloproteomics perspective. *Fungal Diversity* **84**: 43–74.

Supplementary Material: https://studiesinmycology.org/

Table S1. Physiological and biochemical characteristics of *Atractocolax*, *Colacogloea*, *Mycogloiocolax* and *Slooffia* species.